Cosmological constraints on Primordial Black Holes

Master's thesis
Jyväskylä, 24.06.2019

Author:

Antonino Cangialosi

Supervisor:

Prof. Sami Nurmi

UNIVERSITY OF JYVÄSKYLÄ
DEPARTMENT OF PHYSICS

Abstract

Primordial Black Holes(PBH) may have formed from collapse of high-density primordial fluctuations in the early Universe. Interest for PBH has been stirred anew by the LIGO detection of gravitational waves from massive black hole mergers which might be of primordial origin.
In this thesis, we discuss how primordial fluctuations are produced from vacuum fluctuations, which get stretched out of causal contact by an early inflationary epoch. Later, we discuss the thresholds above which these perturbations could end up in forming black holes once re-entered in causal contact.
PBHs are distinct from those black holes of stellar origin precisely because the formation proceed through a top-down accretion of structure. PBHs are expected to form before the recombination era—the moment in the cosmic history when atoms came into being for the first time—thus, defying the mass bounds from the nuclear processes due to the exotic state of primordial matter. Finally, we present current observational constraints on the abundance and mass spectrum of PBHs.

Cangialosi, Antonino
Cosmological constraints on Primordial Black Holes
Master's thesis
Department of Physics, University of Jyväskylä, 2019, 107 pages.

Keywords: Thesis, black hole, primordial

Contents

Chapter 1

Introduction

Which came first, the chicken or the egg?

Plutarch, "The Symposiacs"

It was 1915 when Albert Einstein published the theory of General Relativity [1], a geometrical theory of gravity which reduces to the Newtonian theory in the weak field limit. It was only a handful of months later when Karl Schwarzschild, bedridden at warfront in Russia, attained an exact solution to a asymptotically flat, static, spherically symmetric, point-like mass distribution of Einstein's equation [2], which he promptly sent to Einstein. Much to his surprise, Einstein was positively impressed by the results, which he admittedly thought would not held an exact solution.

Probably the biggest realizations of this work was the emergence of a characteristic length scale related to the mass of the object being the source of the gravitational field, the so-called Schwarzschild radius. There, the solution presents a singularity, which puzzled physicists for a long time, especially because it was not clear whether its nature was mathematical or physical. The value of the radius was already clear to physics, already in the 19^{th} century, Laplace derived the same radius using energy consideration, as the minimum radius for which not even light could escape the gravitational pull of an homogeneous spherical body. In 1924 Eddington evinced that the singularity can disappear [3] by a suitable choice of coordinates. Still the behavior of null geodesics around the solution has remained ununderstood for about 40 years, when Finkelstein pointed out that the surface with Schwarzschild's radius must act as an event horizon. His results were already been found by Kruskal, albeit unpublished, and impelled him to publish a maximally extended solution of Schwarzschild metric. Because of the presence of an event horizon, acting as a unilateral membrane, Black holes were considered to be eternal, until Hawking proved [4] that taking quantum effects into account then black holes should also radiate; hence lose mass and have a finite lifetime.

Along the history of research on black holes the main mechanism for their formation was considered to be the gravitational collapse: as stars run out of fuel to sustain the nuclear reactions in their core, they undergo a series of subsequent stages, of which the Black Hole represents the ultimate phase. The physics of collapse of a star is still an active field of research; however, for neutron stars it exist an upper limit above which they collapse to black holes, the Tolman-Oppenheimer-Volkoff limit, currently estimated around 1.5-3.0 solar masses [5], yet for black holes formed by the collapse of a single star there is an upper mass theoretical limit around 10 solar masses, due to the successive expulsions of material during the evolution [6].

Another kind of black holes was studied by Hawking [7], who indicated that the formation mechanism could take place within the radiation dominated era in the early phases of the universe, although such kind of objects had been already independently proposed by Zel'dovich and Novikov in 1966 [8]. As opposed to stellar black holes, the latter would arise from overdense regions in the thermal phase of the universe, in other words fluctuations of the homogeneous primordial soup of particles, and as such would be older than any other star or structure actually known to astrophysics. This class of black holes, now referred in the literature as Primordial Black Holes(PBHs), have recently found renewed interest— following the detection of Gravitational Waves by LIGO collaboration [9]— due to the fact that most of the masses in the systems of coalescing black holes are typically one order of magnitude above stellar mass. As a consequence, several groups [10][11][12] independently proposed that these objects might be due to PBHs.

Primordial black holes are distinct from black holes of stellar origin in several ways. First among all, primordial black holes form high density fluctuations in the early Universe, in a era where the matter was still in the form of primordial plasma and atoms or even nuclei still had not formed. For this reason, they are insensitive to the chain of reactions taking place in the core of the stars, which matters for the formation of astrophysical black holes. In this sense, the formation of PBHs could only happen directly from high-density spacetime perturbation unable to resist the gravitational interaction that ultimately leads to their collapse. The earlier the process takes place in cosmic time, the smaller was the radius of causality and the mass enclosed inside it; as a result, primordial black holes are expected to span a huge range of masses.

There are several compelling reasons to study PBHs: they might act as seed for the formation of galactic structures in later phases, they are ideal candidate for Massive Astrophysical Compact Halo Objects(MACHOs) which are a type of Dark Matter and they might account for inhomogeneities in the Cosmic Microwave Background [13]. In addition, the observation of a superMassive black hole(SMBH) at early cosmic epoch [14] and the observation of a swarm of X-ray binaries in the Galactic Center [15], provided some support to the possibility that PBHs might accrete into SMBH; thus providing a possible solution to the problem of formation of these be-

hemoths.

This thesis is structured as follows:

- in Chapter 2, we introduce the basics of General Relativity, and the Friedman-Lemaitre-Robertson-Walker(FRLW) cosmology describing the expansion of the universe in its largest scales.
- in Chapter 3, we introduce cosmological perturbation theory to investigate the growth of structures on top of the homogeneous and isotropic background. We discuss the formation of primordial perturbations during inflation and present an alternative approach to perturbation theory based on gradient expansion on large scales and its first order truncation, also known as separate universe approach.
- in Chapter 4, we investigate the collapse of primordial perturbations into black holes and quantify the collapse threshold in several different settings.
- in Chapter 5, we make a link between mass and abundance of PBHs to details of inflationary physics and discuss the cosmological constraints on PBHs.

Notations

In the rest of this manuscript, unless explicitly stated, we will adopt the natural units convention with $\hbar = c = k_{\rm B} = 1$, and define the reduced Planck mass as $M_P = (8\pi G)^{-1/2}$. We denote partial derivatives as $\partial_\mu(\#) = \#_{,\mu}$, and covariant derivatives as $\nabla_\mu(\#) = \#_{;\mu}$, and repeated indices are summed over. We use ∇ to indicate the covariant derivative with respect to metric restricted to spatial coordinates. A dot indicates derivative with respect to time and an apostrophe with respect conformal time, e.g $\dot{a} = \frac{\partial a}{\partial t}$ and $a' = \frac{\partial a}{\partial \eta}$. The metric signature is taken to be mostly plus, so that $\eta_{\mu\nu} = \text{diag}(-1, 1, 1, 1)$.

Chapter 2

Fundamentals of General Relativity and Cosmology

> Spacetime tells matter how to move;
> matter tells spacetime how to curve.
>
> John Archibald Wheeler

The aim of this chapter is to briefly introduce some essential features of the nonperturbed cosmology and how the chronology of the universe can be divided in different epochs.

Modern cosmology is based on two elements: the "Cosmological Principle"— stating that our location in the universe is not special and the universe looks the same in all the directions [16] —supported by the observations of the Cosmic Microwave Background(CMB), and the empirical observation that the incoming light from far galaxies appears redshifted the further they are from us; hence, galaxies are receding from us and so the universe is undergoing an expansion. These two elements justified the Big Bang Theory, which traced back the evolution of the universe toward a series of high-density and -temperature phases to a phase of hot dense plasma, and it resulted in specific prediction of Big Bang Nucleosynthesis(BBN). However, from spectrum of CMB, it can be deduced that only a tiny percentage of the matter content of the universe is known. In order to justify the growth of structure and accelerating expansion of the universe, Dark Matter(DM) and Dark Energy(Λ) had to be taken into account in the ΛCDM model, the prevailing paradigm of the universe today.

The theory of General Relativity is the main framework on which Cosmology is based. This theory describes how spacetime, a set of 4 dimensional points $\{x^\mu\}$, is affected by its matter and energy content, characterized by the energy-momentum tensor $T^\mu_{\ \nu}$. To do so, we need to specify a metric $g_{\mu\nu} = g_{\mu\nu}(x)$ a $(0,2)-$tensor which gives the interval between two points: $\mathrm{d}\, s^2 = g_{\mu\nu}\, \mathrm{d}\, x^\mu\, \mathrm{d}\, x^\nu$. The metric of spacetime

is determined by Einstein field equation [17]:

$$G_{\mu\nu} + \Lambda g_{\mu\nu} = 8\pi G T_{\mu\nu}, \tag{2.1}$$

where G and Λ are the gravitational and cosmological constants and $G_{\mu\nu} = G_{\mu\nu}(g_{\mu\nu}; g_{\mu\nu,\rho})$ is a non-linear, second-order differential operator of the metric. The Einstein tensor can be written as:

$$\begin{aligned} G_{\mu\nu} &= R_{\mu\nu} - \frac{1}{2} R g_{\mu\nu} \\ R_{\mu\nu} &= R^{\alpha}{}_{\mu\alpha\nu}, \qquad\qquad R = g^{\mu\nu} R_{\mu\nu} \\ R^{\alpha}{}_{\beta\mu\nu} &= \Gamma^{\alpha}{}_{\beta\nu,\mu} - \Gamma^{\alpha}{}_{\beta\mu,\nu} + \Gamma^{\alpha}{}_{\mu\rho}\Gamma^{\rho}{}_{\beta\nu} - \Gamma^{\alpha}{}_{\nu\rho}\Gamma^{\rho}{}_{\beta\mu} \\ \Gamma^{\alpha}{}_{\mu\nu} &= \frac{1}{2} g^{\alpha\beta}(g_{\beta\nu,\mu} + g_{\mu\beta,\nu} - g_{\mu\nu,\beta}) \end{aligned} \tag{2.2}$$

where the second line contains respectively the Ricci Tensor and Ricci Scalar, the third line the Riemman tensor, and the last line the Christoffel Symbol. The Christoffel symbol is used to assemble the covariant derivative of tensorial objects: for instance the covariant derivative of a $(1,1)$-tensor, such as T^{μ}_{ν}, is given by $T^{\mu}_{\nu;\alpha} = T^{\mu}_{\nu,\alpha} + \Gamma^{\mu}{}_{\alpha\beta} T^{\beta}_{\nu} - \Gamma^{\beta}{}_{\alpha\nu} T^{\mu}_{\beta}$, and can be trivially generalized for an arbitrary (p,q)-tensor [18]. Once the metric is obtained, free falling particles move along geodesics(6), which is equivalent to say that in General Relativity the gravitational effects are only induced by the curvature of spacetime and not by a force.

Expanding Universe

The Cosmological Principle, its earlier forms date as back as nearly Copernicus. Isaac Newton already postulated a similar principle, but in his view he reached different conclusions from nowadays cosmology. As a matter of fact, in his view the universe was roughly uniform, with stars scattered in all the directions, static and infinite, as it would collapse under its own gravity otherwise.

A counter argument was presented by a German astronomer H.W. Olbers in 1826, which is known as Olbers' Paradox [19]: assuming a static, infinitely old and large, and uniform universe, then no matter which direction one chooses, in its line of sight will find a star eventually. Thence every point of the sky should be lit by a star, therefore night should be as luminous as the day. Mathematically, it can be formulated as the number of stars in a thin spherical shell at distance d, increases proportionally to d^2, and their luminosity reaches Earth with a $1/d^2$ intensity, thus leading to a constant brightness. He used this argument to yield that one or more of the assumptions he made must be wrong.

Based on numerous observations, the modern interpretation is that the universe is expanding under the effect of gravity, and this is inferred through the behaviour of light we receive from distant sources. The wavelength of a light signal emitted from a source moving at constant speed with respect to an observer is stretched or

contracted according to whether the emitter is receding from or progressing towards the observer; this is the relativistic Doppler effect. The effect can be summed up in a single observable, called redshift z:

$$z = \frac{\lambda_{\text{observer}} - \lambda_{\text{emitter}}}{\lambda_{\text{emitter}}}, \tag{2.3}$$

where λ is the wavelength as measured by either the observer or the emitter, this relation is often more conveniently written as $1 + z = \lambda_{\text{obs}}/\lambda_{\text{em}}$ [20]. When the Doppler effect was applied to the study of the luminosity of Cepheids, Hubble found a rough proportionality between the velocity and the distance, far galaxies were moving further at an higher speed (this is intended as average speed, i.e. after their velocity with respect their local cluster was singled out). The actual observables are the redshift and the brightness of the stars; the former being related to the speed, and the latter can be used as standard candle and gives in turn an estimation of the distance. This result is known as Hubble's law which takes the form:

$$z \simeq H_0 d, \tag{2.4}$$

where d is the distance, and H_0 is the Hubble constant or rate [21]. There are other ways to derive the Hubble rate, and it needs to be stressed that, although the misleading name, it does not need to be a constant. In fact, along the last century the measured value of the Hubble rate has given different results for different methods. To keep track of the uncertainties it might be useful to redefine the Hubble's constant in term of a dimensionless Hubble parameter h:

$$H_0 = h \cdot 100 \text{km}\,\text{s}^{-1}\text{Mpc}^{-1}. \tag{2.5}$$

The value of H_0 obtained by measurements from local sources, i.e. low redshift, returns $h = 0.7324 \pm 0.0174$ [22]. However, since we are interested in the physics from early universe, we will make use of the result from the Planck experiment [23] which sets $h = 0.674 \pm 0.005$, obtained through the observation of CMB. The tension between the two values is still an open field of research and would deserve a more detailed discussion.

Friedman-LeMaître-Robertson-Walker models

We will now derive the metric for an expanding universe starting from the Cosmological Principle. Since different observers, described by different coordinate systems x^μ and x'^μ, must give an equivalent description of the history of the universe; consequently, cosmic fields must be form-invariant [24], meaning that at any coordinate point y, $g_{\mu\nu}(y) = g'_{\mu\nu}(y)$, $T^\mu_{\ \nu}(y) = T'^\mu_{\ \nu}(y)$. The statement that universe look the same in all the directions, is equivalent to require the spatial part of the metric to be isotropic; in other words, the metric must contain no dependence on the angular components[1]. Requiring spatial isotropy at every point yields that the universe must

[1] In mathematical terms, a metric space filled with a congruence of timelike curves is spatially isotropic about a point p if given a timelike vector u^μ tangent to the curve at p and any two unit spatial vectors s_1^μ and s_2^μ— i.e. orthogonal to u^μ—there exists an isometry φ that leaves the point invariant, $\varphi(p) = p$, and turns one vector into the other, $\varphi_*(s_1^\mu) = s_2^\mu$ [25].

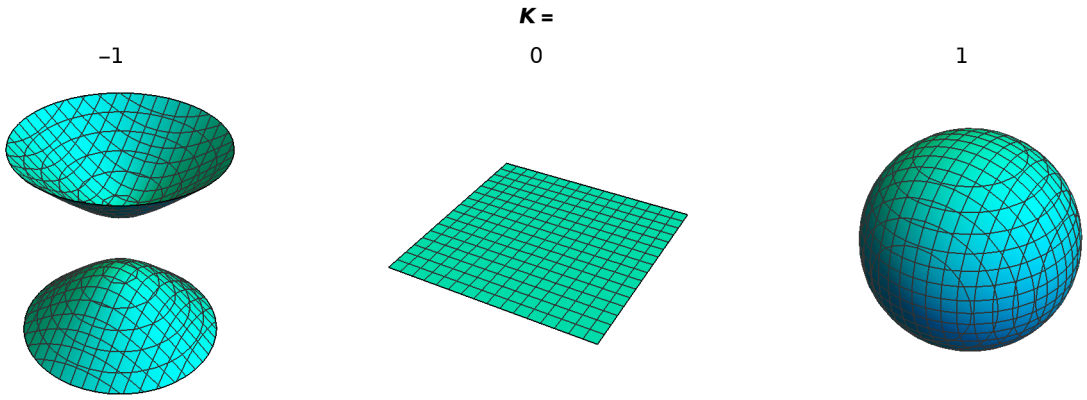

Figure 2.1. In the figure are shown different 2-dimensional spaces embedded in a higher 3-dimensional space. From left to right, we have an embedding of spaces as hypersurfaces given by the constraints $x^2 + y^2 - h^2 = -1$, $x^2 + y^2$ at $h = const$ and $x^2 + y^2 + h^2 = +1^2$; where h is the additional dimension of the ambient space and K is the extrinsic curvature.

be spatially homogeneous. Loosely speaking, at any arbitrary instant of time, any point of space is undistinguishable from any other point[2].To define an absolute time we can use any cosmic scalar quantity: by the fact that the universe is expanding, this is going to be monotonically decreasing everywhere, and so cosmic time can be parametrized in terms of it.

Both homogeneity and isometry of the universe are to be intended as a coarse-grained characteristic: they do not hold on a small scale, as if they were then the existence of structures and different physical phenomena would be hindered. Nonetheless, they are not mere simplifications, our universe does appear homogeneous and isotropic on scales larger than $\sim$ 100Mpc [26], this is often called unperturbed cosmology. Therefore deviations from these characteristics are allowed on smaller scales and, as such, treated as perturbations. The study of how inhomogeneities develops into the galaxy distribution is called Large Scale Structure(LSS).

A space which is both homogeneous and isotropic by every point is maximally symmetric— it is uniquely specified by its curvature constant K and the signature of its metric— then a universe which is spatially homogeneous and isotropic by each point will admit a maximally symmetric subspace. There exist only three kinds of maximally symmetric spaces with simple topology: Lobachevski space, flat space, and 3 dimensional sphere [27]. They can be described by embedding them in a bigger 4 dimensional space, where they live on a hypersurface of constraint $h^2 + K\mathbf{x}^2 = 1$, where K is negative, zero or positive respectively.

[2]A mathematical formulation of this concept is that a metric space is spatially homogeneous if there exist a one-parameter family of spacelike hypersurfaces Σ_t that foliate the space such that any two points of a given sheet can be connected by an isometry [25].

The expansion of the universe is encoded in the scale parameter $a(t)$, and we introduce the comoving coordinates x^i with $i = 1, 2, 3$, which characterize observers at rest with respect to the expansion of space. We relate the measurable physical (primed) and the comoving (unprimed) coordinates through $x'^i = a(t)x^i$; the scaling can be extended to the extra dimension of the ambient space $h' = a(t)h$. Therefore, a purely spatial line element reads as $\mathrm{d}\, s^2 = a^2\left[\mathrm{d}\,\mathbf{x}^2 + K\,\mathrm{d}\,h^2\right]$, but the dependence on the extra dimension can be made implicit by differentiating the hypersurface constraint [28]: $h\,\mathrm{d}\,h = -K\mathbf{x}\cdot\mathrm{d}\,\mathbf{x}$. To make the symmetry explicit, we use spherical coordinates, so that $\mathrm{d}\,\mathbf{x}^2 = \mathrm{d}\,r^2 + r^2\,\mathrm{d}\,\Omega_2{}^2$ and $r\,\mathrm{d}\,r = \mathbf{x}\cdot\mathrm{d}\,\mathbf{x}$; we can write down the Friedman-Lemaître-Robertson-Walker interval as:

$$\mathrm{d}\, s^2 = \mathrm{d}\, t^2 - a(t)^2\left[\mathrm{d}\,\mathbf{x}^2 + K\frac{(\mathbf{x}\cdot\mathrm{d}\,\mathbf{x})^2}{1-K\mathbf{x}^2}\right] = \mathrm{d}\, t^2 - a(t)^2\left[\frac{\mathrm{d}\, r^2}{1-Kr^2} + r^2\,\mathrm{d}\,\Omega_2{}^2\right], \quad (2.6)$$

where $\Omega_2{}^2 = \mathrm{d}\,\theta^2 + \sin^2(\theta)\,\mathrm{d}\,\phi$. In order to avoid the singularity at $r^2 = K^{-1}$, it is convenient to define the metric distance coordinate χ such that $\mathrm{d}\,\chi = \mathrm{d}\, r/\sqrt{1-Kr^2}$, and it is convenient to define the conformal time through $\mathrm{d}\,\eta = \mathrm{d}\, t/a$. Thus, we have:

$$\mathrm{d}\, s^2 = a(\eta)^2[-\mathrm{d}\,\eta + \mathrm{d}\,\chi^2 + S_k(\chi)^2\,\mathrm{d}\,\Omega_2{}^2], \quad (2.7)$$

$$\text{with} \quad S_k(\chi) = r = \begin{cases} \sin(\sqrt{K}\chi)/\sqrt{K} & \text{if } K > 0 \\ \chi & \text{if } K = 0\,. \\ \sinh(\sqrt{-K}\chi)/\sqrt{-K} & \text{if } K < 0 \end{cases} \quad (2.8)$$

The metric distance and the comoving coordinates coincide for a flat spacetime, $K = 0$; in point of observations of CMB and Baryonic Acustic Oscillations(BAO), this seems to be the case for our universe within 1σ accuracy of 0.2% [23].

Now if we consider the physical motion of an object at distance d in our coordinates, we see that:

$$\frac{\mathrm{d}}{\mathrm{d}t}\mathbf{d}(t) = \dot{a}(t)\boldsymbol{\chi} + a(t)\dot{\boldsymbol{\chi}} = H(t)\mathbf{d}(t) + \mathbf{u}_{\text{peculiar}}, \quad (2.9)$$

where the $\mathbf{u}_{\text{peculiar}}$ is the velocity of an object measured by an observer comoving with the expansion of the universe, whereas the first term defines the Hubble flow, which is the proper expansion as seen by non-comoving observers. With regard to the Hubble flow we recognize $H(t)$ as the Hubble parameter, related to the one in Hubble's law (2.4) by the $H_0 = H(t_0)$, where t_0 is referring to the current age of the universe.

Cosmic components

The FLRW metric has been derived from first principles, we are going to make use of Einstein's field equations to attain predictions about the dynamical evolution and time dependence of the scale factor. For this purpose, we need to know the energy-momentum tensor,which by the requirement of homogeneity and isotropy, is forced

to be that of a perfect fluid, and so it is characterized uniquely by its energy density ρ, and isotropic pressure p:

$$T^{\mu}_{\ \nu} = (\rho + p)u^{\mu}u_{\nu} + p\delta^{\mu}_{\nu}, \tag{2.10}$$

where u^{μ} is the 4-velocity of the fluid in the comoving frame, where the fluid can be thought to be at rest: $u^{\mu} = (1, 0, 0, 0)$. As a matter of fact, the identification of $-T^0_0$ with the energy can be done only in this particular frame [29], and the energy-momentum vector can be defined as $J^{\mu} = T^{\mu}_{\nu}u^{\nu}$.

Once we substitute the energy-momentum tensor inside the Einstein's equations we obtain two independent equations. The first is called Friedman equation:

$$\left(\frac{\dot{a}}{a}\right)^2 = H^2 = \frac{8\pi G}{3}\rho - \frac{K}{a^2} + \frac{\Lambda}{3}, \tag{2.11}$$

it describes the dependence of Hubble parameter in terms of energy density, cosmological constant and curvature. The second Friedman equation, also referred as acceleration equation relates the expansion to pressure, density and the cosmological constant:

$$\frac{\ddot{a}}{a} = \dot{H} + H^2 = -\frac{4\pi G}{3}(\rho + 3p) + \frac{\Lambda}{3}. \tag{2.12}$$

In addition to Friedman equations, as a consequence of the conservation of energy-momentum tensor,$T^{\mu\nu}_{\ \ ;\mu} = 0$, we get a third independent equation describe the dynamic, called continuity equation:

$$u^{\nu}T^{\mu}_{\nu\ \ ;\mu} = 0 \quad \Rightarrow \quad \dot{\rho} + 3H(\rho + p) = 0, \tag{2.13}$$

where the contraction with the fluid velocity was performed for mere sake of covariance. From the first Friedman equation, setting $\Lambda = 0$, there is a critical density $\rho_c(t) = 3H^2(t)/8\pi G$ for which the universe appears flat [30]. A perfect fluid is completely specified by the equation of state which relate $p = p(\rho, T)$, but since for our purposes T is constant at each instant of the cosmic time, we write:

$$p = w\rho, \tag{2.14}$$

this will be referred as the equation of state, with w called adiabatic index. From the equation of state and continuity equation, it can be derived that the quantity $a^{3(1+w)}\rho$ is constant in time. This relation can be reverted to give:

$$\rho(t) \propto a(t)^{-3(w+1)}, \tag{2.15}$$

which, remarkably, it is valid for any fluid which respects (2.13) and (2.14) independently from the geometry of spacetime.

The density and pressure of the universe will be due to several components, for simplicity they are taken to be non-interacting so that the total energy density and

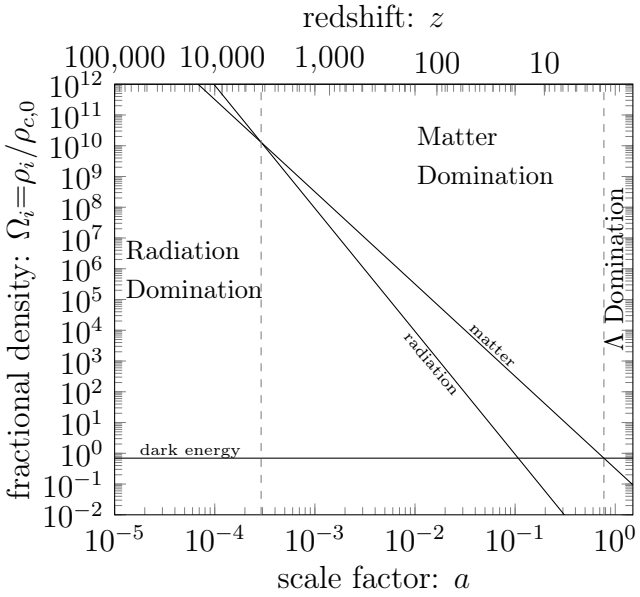

Figure 2.2. In the figure, the evolution of the scale factors of single components is plotted using the data from Planck [23]. This allows to distinguish different epochs of domination of one component over the others. In particular, the domination of matter ends at $z \simeq 0.29$, and domination of radiation at $z \simeq 3440$.

pressure are given by the sum, $\rho(t) = \sum_i \rho_i(t)$ and $p(t) = \sum_i p_i(t)$. As long as we can treat them as perfect fluids; for each of them, we can write:

$$p_i = w_i(\rho_i)\rho_i, \qquad \rho_i(t) \propto a_i(t)^{-3(1+w_i)}. \tag{2.16}$$

This allows us to describe the behavior of the density as a function of the scale parameter for each component, and few ideal cases can be distinguished:

- radiation: for ultra-relativistic matter $w = 1/3$, thus $\rho_r = \rho_{r,0}a^{-4}$,
- matter: non-relativistic matter, often called dust, is assumed as a cold pressureless gas, $p \ll \rho$, and so $w_m = 0$, giving $\rho_m = \rho_{m,0}a^{-3}$,
- vacuum or dark energy: if we consider the energy-momentum of vacuum $T^{\mu\nu}_V$, by Lorentz invariance in a locally inertial system, it must be proportional to the Minkowski metric, this requires $w = -1$, so $\rho_\Lambda = \rho_\Lambda a^0$.

Comparing this behaviours with observations from type Ia supernovae [31], we can deduce that the universe is now in a phase where the density is dominated by the a dark energy. Going back in time there was a matter dominated era, in which the galactic structures formed; earlier that this, there was a radiation dominated era, where the universe was so hot and dense that atomic structures where hindered by frequent collisions of highly energetic particles [28].

It is conventional to set the scale factor at present time equal to unity, $a(t_{\text{now}}) = 1$. Since the energy density during dark energy domination is constant, there we have

$a(t) = \exp(\sqrt{(\Lambda + 8\pi\rho)/3}(t - t_{\text{now}}))$ until the time at which dark energy equated the matter at t_Λ. In the matter epoch the scale factor, neglecting the cosmological constant, evolves with a time as $t^{2/3}$, and we have $a(t) = a(t_\Lambda)(t/t_\Lambda)^{2/3}$ during $t_{\text{eq}} \leq t \leq t_\Lambda$, where t_{eq} is the time of matter-radiation equality. For $t \leq t_{\text{eq}}$ we have that the scale factor evolves as $a(t) = a(t_{\text{eq}})(t/t_{\text{eq}})^{1/2}$.

As a matter of fact, another earlier phase of Inflation is thought to have happened. Originally, it was a solution to three problems of the Big Bang theory [30]: the Horizon Problem (the high degree of homogeneity and isotropy of CMB requires that disconnected causal patches of the universe must have been in thermal equilibrium, which can only be achieved by causality), the Flatness Problem (the fact that the density has stayed compatibly close to the critical density along the various epoch requires fine-tuned initial conditions, which is unlikely) and the problem of unwanted relics the fact the no exotic relics of the high energetic phase have been observed. The success of the inflationary paradigm lies in providing a mechanism that explains how large scale fluctuations have emerged from random quantum fluctuations, and this lead to predictions that have been successfully tested in the large-scale spectrum of CMB [32]. In between the inflationary epoch and radiation domination there could have been one or more additional phases called reheating or preheating in which the energy is transferred from the inflationary field(s) to the other fields that play a role during the Big Bang [33].

Chapter 3

Primordial Perturbations

> We cannot conceive of matter
> being formed of nothing,
> since things require
> a seed to start from.
>
> Lucretius, "De Rerum Natura"

The framework of homogeneous and isotropic cosmology developed in the previous chapter will serve us as a base for perturbation theory in the FRLW background. In order for to discuss the formation of primordial black holes one needs to understand how perturbations formed in the early phases of the Universe and how can we describe their evolution.

Cosmological Perturbation Theory

As we stated earlier, the homogeneous and isotropic metric has to be intended as a coarse-grained approximation of the metric of the universe; thanks to the observations we can assume that this idea was particularly accurate at early times. The mere existence of astrophysical objects—planets and stars ($\delta\rho/\bar{\rho} \sim 10^{30}$), galaxies ($\delta\rho/\bar{\rho} \sim 10^{5}$), clusters and voids ($\delta\rho/\bar{\rho} \sim \pm 1$) [34] —represents the most conspicuous evidence that inhomogeneities must have ripened from early universe's homogeneity, and the structures must have formed and evolved from them.

The idea is to expand the Einstein's equations around the FRLW metric as a background metric and treat the deviations from homogeneity as perturbations. The linear order was pioneered by Lifshitz in 1945 [35], and later improved by Bardeen [36] and others [37][38][39], the general metric can be split as follows:

$$g_{\mu\nu}(t, x^i) = \bar{g}_{\mu\nu}(t) + \delta g_{\mu\nu}(t, x^i), \tag{3.1}$$

where $\bar{g}_{\mu\nu}$ is the FRLW metric (2.6) and $\delta g_{\mu\nu}$ is the metric due to the perturbations. Nonetheless, this way of developing perturbation theory does not come without

repercussions: the approach of performing the splitting is not covariant; meaning that the separate parts will not, in general, change as 4-tensors under any arbitrary coordinate changes. The problem is that the perturbed part depend on the choice of the coordinates, but doing so it spoils the diffeomorphism invariance[1] of General Relativity.

To distinguish space from time we introduce an arbitrary slicing of spacetime in spatial sections at a given time Σ_t. This can be formally defined as a diffeomorphism $\phi : \mathcal{M} \to \Sigma \times I$, where $I \in \mathbb{R}$ is the set of possible values time can assume and Σ is the set of space points. Then, slices corresponds to the set of spacelike curves $\Sigma_t = \phi^{-1}(\Sigma \times \{t\})$, and threads are elements of the set of timelike curves $\phi^{-1}(\Sigma \times \{t\})$. Thanks to these curves we can introduce a Killing vector field, ∂_t, associated with the time coordinate, which can be split into components tangent to the slices Σ_t, β, and orthonormal to them, n^μ: $\partial_t = \alpha n + \boldsymbol{\beta}$ [41]. If we consider the case of the background universe, the maximal symmetry makes the $\boldsymbol{\beta}$ vector vanish; then the threads corresponds to the geodesics of comoving observers, and are orthogonal to the slices, then by setting $\alpha = 1$ we can identify the time coordinate with the proper time of these observers. The perturbed spacetime no longer possesses this property: threading cannot be orthogonal to the slices [30]. However, since coordinate points $\{x^\mu\}$ carry no physical meaning by themselves but act just a label for the points of the spacetime manifold; we can make use of an infinitesimal gauge transformation, generated by $\xi^\mu(\bar{x}^\mu)$ and introduce another set of coordinates $\hat{x}^\mu = x^\mu + \xi^\mu(x)$. By this means, we can easily see how, in a FLRW universe, spurious perturbations arise taking a look at the density in the newly introduced frame:

$$\bar{\rho}(\hat{x}) = \bar{\rho}(x) + \xi^\mu(x)\bar{\rho}_{,\mu}(x) = \bar{\rho}(t) + \xi^0(x)\,\partial_0\,\bar{\rho}(t). \tag{3.2}$$

On the RHS we made use of the fact that that unperturbed density do not depends on spatial coordinates because of the homogeneity of the metric—i.e. $\bar{\rho}(\hat{x}) = \bar{\rho}(\hat{t})$. So it should be in the other framed because of form invariance of the FLRW metric. Still, the 0^{th} component of the generator can give rise to inhomogeneities,but it is an artifact of choosing a different gauge which carries no physical meaning [42].

We can give a formal definition of the perturbation of a general tensor δQ as the difference between the quantity in the physical spacetime Q and the quantity in the background $\bar{Q}$, but in order to take the difference of two tensors they must be evaluated at the same point, but they are defined in two different manifolds. To circumvent this difficulty, we need to make use of a diffeomorphism $\mathcal{D} : \bar{\mathcal{M}} \to \mathcal{M}$, in order to relate points of the background to points of the physical space. In this sense, a gauge choice can be understood as the choice of the diffeomorphism, and then, once we pick a point p in the background, the perturbation is defined as:

$$\delta Q(p) = Q(\mathcal{D}^{-1}(p)) - \bar{Q}(p). \tag{3.3}$$

[1] Diffeomorphism invariance derives from the principle of general covariance, according to which the form of laws of physics is left unchanged under a general coordinate transformation [40]. This means that the group of diffeomorphisms is taken as the gauge group of gravitation.

The advantage of this procedure is that the change of the perturbation under an infinitesimal gauge transformation can be expressed as the Lie derivative[2] by the infinitesimal generator vector field:

$$\Delta_\xi Q = \delta\hat{Q} - \delta Q = \mathcal{L}_\xi Q, \tag{3.4}$$

this method can be used to generalize for perturbations beyond the first order [43]. Loosely speaking, perturbations are objects living on top of the background space, and once the spacetime is split into slices, we can characterize them in terms of their behaviour under spatial rotations; for the same reasons we can use the spatial part of the background metric, $\bar{\gamma}$ to raise and lower their indices. Au contraire, for tensors living on the whole spacetime, take T^μ_ν and u^μ as two instances, the full metric g is needed.

In the following sections we will endorse the background spacetime, $(\bar{\mathcal{M}}, \bar{g})$, with a coordinate system $\{x^\mu\} = \{\eta, \chi^i\}$ corresponding to the metric given by equation (2.7), and we will indicate with $\bar{\gamma}_{ij}$ the spatial metric induced on Σ. This coordinate system will define on the physical(perturbed) spacetime $(\mathcal{M}, g)$ the global $3+1$ threading and slicing. Additionally, we introduce on $\mathcal{M}$ a locally orthonormal frame (t, x_i) corresponding to the physical coordinates of the perturbed spacetime.

Classifying the metric perturbations

Now that we have established how perturbations transform under a general infinitesimal gauge transformation, we can use this tool to construct gauge invariant quantities.

Before doing it, we introduce the most general form of metric perturbation and comment on the physical meaning of its components. As the metric itself carries 10 degrees of freedom the most general perturbation will contain 10 infinitesimal parameters which, in turn, depend on the spacetime coordinates. As a first attempt, we introduce a perturbation that takes into account the $3+1$ slicing of the isotropic and homogeneous metric, and to threat all the perturbations of the same dimensional footing we switch to conformal time η; the form of the metric perturbation will then be:

$$\delta g = a^2\Big[-2A\,\mathrm{d}\,\eta^2 + 2\beta_i\,\mathrm{d}\,\eta\,\mathrm{d}\,\chi^i + (-2C\bar{\gamma}_{ij} + 2e_{ij})\,\mathrm{d}\,\chi^i\,\mathrm{d}\,\chi^j\Big], \tag{3.5}$$

where e_{ij} is taken to be traceless. The A parameter is sometimes referred in the literature as the lapse perturbation[3] [37], as its effect is to modify the redshift between two adiacent sheets of the foliation. The $\boldsymbol{\beta}$ vector is referred as the shift-vector

[2] The Lie derivative of a given (1,1)-tensor T^μ_ν by a generic vector V^μ can be written as:

$$\mathcal{L}_V = V^\rho T^\mu_{\nu,\rho} - T^\rho_\nu V^\mu_{,\rho} + T^\mu_\rho V^\rho_{,\nu},$$

where the second and third terms can be generalized to the case of an arbitrary (p,q)-tensor.

[3] This name is slightly inappropriate: the lapse function is given by the proportionality α of the proper time along the threads with the normal vector to the slices, so we have $1-2A = \alpha^2$. In this sense, the lapse function measures the coordinate time interval between two infinitesimally detached slices; A should be called linear perturbation of the lapse.

[37], in the locally orthonormal frame is the velocity with respect to the threads of the worldline orthogonal to the slices: it introduces a dragging between adjacent slices. The C parametrizes the local and isotropic modification of the scale factor, whereas e_{ij} are the components of a tensor which adds anisotropies to the metric[29]. Nonetheless, the perturbations written in this form are not completely irreducible: they can still be split in irreducible parts according to Helmholtz decomposition. This implies that the shift vector can be uniquely factorized into a solenoidal part, meaning divergence-free, and a part uniquely arising from the gradient of a scalar; similarly, the anisotropy tensor can be uniquely factorized into a scalar, solenoidal vector part and a traceless, transverse tensor(TT-tensor)[29]. In components this read as:

$$\begin{aligned} \beta_i &= S_i + \nabla_i B, \\ e_{ij} &= (\nabla_i \nabla_j - \frac{1}{3}\gamma_{ij}\nabla^2)E + \nabla_{(i} F_{j)} + h_{ij}, \end{aligned} \tag{3.6}$$

where ∇ stands for the covariant derivative of the spatial part of the metric γ_{ij}, and $\nabla^2 = \gamma^{ij}\nabla_i\nabla_j$. Therefore, we have $\nabla^i S_i = 0$, $\nabla^i F_i = 0$, $\nabla^i h_{ij} = 0$ and $h^i_i = 0$. This decomposition guarantees that perturbations of different character do not mix in linear perturbation theory,and so scalars, vectors and tensors evolve separately according to their equation of motion [39]. Sometimes in place of C another scalar parameter is introduced, called curvature perturbation $\psi = C + \frac{1}{3}\nabla^2 E$ [44]. It takes its name from the spatial perturbation of the Ricci scalar:

$$\delta^{(3)}R = \frac{4}{a^2}(\nabla^2 + K)(C + \frac{1}{3}\nabla^2 E) = \frac{4}{a^2}(\nabla^2 + K)\psi. \tag{3.7}$$

Additionally, it serves the purpose of getting rid of the double laplacian of E, greatly simplifying the Einstein tensor.

To sum up we have 4 scalar degrees of freedom given by the the A, B, C, E parameters, 4 degrees given by the vectors S, F and two in the tensor h[4]. However, we should not be too hasty in attaching physical meaning to the perturbations as they are dependent on the choice of coordinates, and since the gauge freedom takes 4 degrees of freedom, we can only build 6 physical quantities. If we consider the variation of the metric under a gauge transformation, and we perform a decomposition on the gauge vector $\xi^\mu = (\xi^0, \xi^i + \nabla^i \xi)$, where ξ^i is solenoidal, we can compare the change in the perturbed metric in the two coordinates $\delta\hat{g}_{\mu\nu} = \delta g_{\mu\nu} + \mathcal{L}_\xi g_{\mu\nu}$ to see how the parameters are affected, and we derive:

$$\begin{aligned} &\hat{A} = A + \frac{(a\xi^0)'}{a}, \quad \hat{B} = B - \xi^0 + \xi', \quad \hat{C} = C - \frac{a'}{a}\xi^0 - \frac{1}{3}\nabla^2\xi, \\ &\hat{E} = E + \xi, \quad \hat{S}_i = S_i + \xi'_i, \quad \hat{F}_i = F_i + \xi_i, \quad \hat{h}_{ij} = h_{ij} \quad \hat{\psi} = \psi - \frac{a'}{a}\xi^0. \end{aligned} \tag{3.8}$$

Interestingly, we can see that the tensor perturbations are automatically gauge invariant, and thus they represent the 2 degrees of freedom due to gravitational waves;

[4] It is important to stress that all the parameters are intended to be functions of the spacetime coordinates.

these are called radiative modes, and are generated when the spherical symmetry of the background is broken.

We can use the remaining relations to build gauge invariant quantities, but the choice is not unique. The simplest choice is due to Bardeen, who first showed how to derive such quantities [36], and are generally called Bardeen Potentials:

$$\Phi = A + \frac{1}{a}[a(B - E')]', \quad \Psi = C - \frac{a'}{a}(B - E') + \frac{1}{3}\nabla^2 E, \quad \Phi_i = S_i - F_i', \tag{3.9}$$

which carry in total 4 degrees of freedom: 2 from the scalar quantities, and 2 from the vector potential. The understanding of their physical meaning must be postponed to a later stage, till we will have derived their equations of motion.

Matter perturbations

Now, we turn to describe the perturbations of the energy-momentum tensor, the background unperturbed part takes the same form we derived in equation (2.10): $\bar{T}^{\mu}_{\ \nu} = (\bar{\rho} + \bar{p})\bar{u}^{\mu}\bar{u}_{\nu} + \bar{p}\delta^{\mu}_{\nu}$. At the level of first order perturbation theory both $\bar{\rho}$ and $\bar{p}$ behave as scalar quantities under a Lorentz transformation, because maximal symmetry guarantees invariance under rotations, and Lorentz boosts contribute to a change proportional to v^2, which is second-order and thus neglected.

The perturbed energy-momentum tensor can be written as [45]:

$$\delta T^{\mu}_{\ \nu} = (\delta\rho + \delta p)\bar{u}^{\mu}\bar{u}_{\nu} + \delta p\ \delta^{\mu}_{\ \nu} + (\bar{\rho} + \bar{p})(\bar{u}^{\mu}\delta u_{\nu} + \delta u^{\mu}\bar{u}_{\nu}) + \Sigma^{\mu}_{\ \nu}, \tag{3.10}$$

where $\Sigma^{\mu}_{\ \nu}$ is the anisotropic stress tensor which characterizes the shear stress of the perturbed fluid. This tensor is taken to be traceless, $\Sigma^{\mu}_{\ \nu} = 0$, because its trace can be reabsorbed in the isotropic pressure, p; it is also chosen to be orthogonal to the 4-velocity, $\Sigma^{\mu}_{\ \nu}u^{\nu} = 0$. The quantities $\delta\rho$, δp, δu^{ν} and $\Sigma^{\mu}_{\ \nu}$ are all taken to be first-order in perturbation, and thus the orthogonality of the stress tensor with the four-velocity guarantees that $\Sigma^{0}_{\ 0} = \Sigma^{0}_{\ i} = 0$; moreover, it can be decomposed in its scalar,vector and tensor part: $\Sigma_{ij} = (\nabla_i\nabla_j - \frac{1}{3}\bar{\gamma}_{ij}\nabla^2)\sigma + 2\nabla_{(i}\sigma_{j)} + \sigma_{ij}$.
Since indices are raised and lowered with the unperturbed metric, equations are made a little bit messier. To compute δu^{μ} and δu_{μ}, we recall that $g_{\mu\nu}u^{\mu}u^{\nu} = -1$ and $\bar{g}_{\mu\nu}\bar{u}^{\mu}\bar{u}^{\nu} = -1$, which yields $\delta u^0 = -A/a$. Since at the background level $\bar{u}^i = 0$, we have that $\delta u^i = u^i = \dot{x}^i = x^{i\prime}\frac{\mathrm{d}\eta}{\mathrm{d}\tau} = v^i/a$, where v^i is the rescaled peculiar velocity of (2.9), or better its first-order part which grants us to use the lowest-order expression for the $\tau(\eta)$, which otherwise has a non-linear dependence. Finally, we can lower the index to find:

$$u_{\mu} = g_{\mu\nu}u^{\nu} = \bar{g}_{\mu\nu}\delta u^{\nu} + \delta g_{\mu\nu}\bar{u}^{\nu} = (-a(1 + A), a(u_i + \beta_i)), \tag{3.11}$$

thus $\delta u_{\mu} = a(-A, v_i + \beta_i)$. The peculiar velocity can also be split into irreducible parts: $v_i = v_i^{\perp} + \nabla_i v$, and it is useful to introduce the so-called velocity divergence

parameter $\theta = \nabla^2 v$, which coincide with the divergence of the peculiar velocity.

In the literature it is customary to introduce a fractional dimensionless parameter instead of the perturbation of the density called density contrast [30]:

$$\delta = \frac{\rho - \bar{\rho}}{\bar{\rho}}, \tag{3.12}$$

so that the perturbation of energy density is written as: $\delta\rho = \bar{\rho}\,\delta$. For the linear perturbation theory to apply we need to have $|\delta| \ll 1$, but this condition needs not to be strictly satisfied at a general level; indeed, as δ approaches unity perturbation theory breaks down and we need to switch to the non-linear theory instead. As a matter of fact, on astrophysical scales we have $|\delta| \geq 1$ more often than not, and equations are solved by recurring to numerical simulations.

In presence of anisotropic stress we can no longer expect the pressure to be depending only on the energy density; instead we have $p = p(\rho, S)$, a dependence on the entropy. A direct consequence is that the pressure perturbation can be written in terms of perturbations of energy density and entropy:

$$\delta p = \left.\frac{\mathrm{d}p}{\mathrm{d}\rho}\right|_S \delta\rho + \left.\frac{\mathrm{d}p}{\mathrm{d}S}\right|_\rho \delta S = c_\mathrm{S}^2 \delta\rho + \sigma\delta S \tag{3.13}$$

We can identify c_S as the adiabatic speed of sound, and σ with the scalar anisotropic pressure [46]. This allows us to make an additional distinction between two classes of perturbations: adiabatic perturbations and isocurvature(or entropy) perturbations. The former are characterized by $\delta S = 0$, while the latter are given by $\delta\rho = 0$ and do not affect the intrinsic spatial curvature. To state this differently, adiabatic perturbations are local perturbations of the curvature, whereas the isocurvature perturbation are local perturbations in the equation of state and, in order to have this kind of perturbation, a multicomponent fluid is required so to have a local variation of the number density of different components. It makes sense to define the entropic perturbations in terms of the components: $S_{AB} = \frac{\delta_A}{1+w_A} - \frac{\delta_B}{1+w_B}$, where A and B label the fluid type. This implies that for a 2-components fluid $\delta\rho_A = -\delta\rho_B$, and $S_{AB} \equiv 0$ for adiabatic perturbations [47]. In the following, we will also use the quantity $\Gamma = \frac{\delta p}{\dot{\bar{p}} - \frac{\delta\rho}{\bar{\rho}}}$, so that for the total pressure we have $\delta p = c_s^2\delta\rho + \dot{p}\Gamma$, and the last term represents in the non-adiabatic pressure perturbation $\delta p_\mathrm{nad} = \dot{p}\Gamma = \sigma\delta S$.

In order to match the left side of the Einstein equation, we still need to lower one index from the energy-momentum tensor with the full metric; doing so we attain $T_{\mu\nu} = \bar{g}_{\mu\rho}\bar{T}^\rho{}_\nu + (\bar{g}_{\mu\rho}\delta T^\rho{}_\nu + \delta g_{\mu\rho}\bar{T}^\rho{}_\nu) = \bar{T}_{\mu\nu} + \delta T_{\mu\nu}$, we can explicitly read:

$$\begin{aligned}
\delta T_{00} &= \bar{\rho}a^2(\delta + 2A), \\
\delta T_{0i} &= -\bar{\rho}a^2[(1+w)v_i + \beta_i], \\
\delta T_{ij} &= a^2[(\delta p + 2C)\bar{\gamma}_{ij} + 2pe_{ij} + \Sigma_{ij}].
\end{aligned} \tag{3.14}$$

We see that lowering an index generates a mixing between matter and metric perturbations [45]. We can now consider the variation of parameters of perturbation under an infinitesimal gauge transformation. Yet first we recast continuity equation (2.13) in terms of conformal time: $\bar{\rho}' + 3\mathcal{H}(\bar{\rho} + \bar{p}) = 0$, where $\mathcal{H} = a'/a$, which we can use inside of the density contrast and the variation of pressure:

$$\begin{aligned} \hat{\Sigma}_{ij} &= \Sigma_{ij}, & \hat{v}^{\perp i} &= v^{\perp i} - \xi^{i\prime}, \\ \hat{\delta S} &= \delta S, & \hat{\delta} &= \delta + \xi^0 \frac{\bar{\rho}'}{\bar{\rho}} = \delta - 3\mathcal{H}\bar{\rho}(1+w)\xi^0, \\ \hat{v} &= v - \xi', & \hat{\delta p} &= \delta p + \xi^0 \bar{p}' = \delta p - 3\mathcal{H}\bar{\rho}c_{\mathrm{S}}^2(1+w)\xi^0, \end{aligned} \tag{3.15}$$

from which we can construct gauge-invariant quantities; again, the choice is not unique, tough.Furthermore, their construction necessarily involve mixing of matter and metric perturbations [29]. With an eye towards our next developments, we make a choice among the various gauge invariant combinations for the density contrast, we present one choice of such perturbations:

$$\begin{aligned} V &= v + E', \\ V_i &= v_{\perp i} + S_i, \\ \Delta &= \delta + \frac{\rho'}{\rho}(v + B) = \delta - 3\mathcal{H}(1+w)(v+B), \end{aligned} \tag{3.16}$$

where Δ is called comoving-gauge density contrast [20], and no expression for pressure perturbation was given as it is entirely dependent on Δ and δS.

Gauge fixing

In the study of the evolution of perturbations which is following, using a general gauge with all the perturbations parameter is superfluous. Solving the linearized Einstein equations is straightforward but tedious, and doing it in the most general gauge can be messy and hide the physical content, as well.

Another way of proceeding is attained by fixing the gauge. This means that we give some specific constraints on the form perturbation can assume so that the various perturbations reduce to the gauge-invariant quantities. In practice, one chooses a specific coordinate system and imposes the initial condition in that particular frame, but, in doing so, special care is needed in discriminating the evolution of physical modes from spurious modes due to the choice of coordinates [48]. In the following, we will perform the transition from the most arbitrary gauge to a specific one by fixing the time slicing by specifying ξ^0, the space threading by ξ, the shearing by ξ_i. There is a copious number of common gauges choices used in the literature , but we will take under analysis only a small sample, mostly suited to our purposes:

- conformal Newtonian gauge
  This gauge is chosen so that the perturbation matrix assume a diagonal form, thus $\hat{B} = 0 = \hat{\beta}_i$ [49]. This condition imposes $\xi^0 = B - E'$, $\xi_i = -\int S_i \, \mathrm{d}\, \eta +$

$\Xi_i(\boldsymbol{\chi})$ and $\xi = -E$; fixing the gauge completely for the scalar sector, but leaving a residual gauge freedom for the vector sector as expressed by $\Xi_i(\boldsymbol{\chi})$: an arbitrary function of space coordinate carrying no physical value. Furthermore, we have:

$$\hat{A} = \Phi, \quad \hat{C} = \psi = \Psi, \quad \hat{v} = V, \quad \hat{v}_i = V_i. \tag{3.17}$$

As a result, calculations done in this gauge in terms of the scalar Bardeen potentials are valid in any other gauge. In particular, using this gauge we can interpret Ψ itself as the source for the perturbation of the spatial curvature: $\delta^{(3)}R = \frac{4}{a^2}(\nabla^2 + K)\Psi$; and write the non-homogeneous scale factor as:

$$a(\eta, \boldsymbol{\chi}) = a(\eta) + \delta a(\eta, \boldsymbol{\chi}) = a(\eta)\sqrt{1 - 2\Psi(\eta, \boldsymbol{\chi})}. \tag{3.18}$$

In this gauge one can assemble a different gauge invariant density contrast from the one provided in (3.16) defined as $\delta^N = \delta + \frac{\bar{\rho}'}{\bar{\rho}}(v + B)$, but this quantity can be related to the comoving one: $\Delta = \delta^N + \frac{\bar{\rho}'}{\bar{\rho}}V$.

- comoving time-orthogonal gauge
  The choice of this gauge represents observers for which there is no net energy flux out of the slices, which translates into $T^0_{\ i} = 0$. This yields $\hat{v} = 0 = \hat{B}$ and $\hat{v}^i_\perp = -\hat{S}^i$ [37], and thus choosing $\xi^0 = B + v$, $\xi = \int v d\eta + \Xi(\boldsymbol{\chi})$ and $\xi_i = \int (v^i_\perp - S^i)\, \mathrm{d}\, \eta + \Xi_i(\boldsymbol{\chi})$, therefore leaving a residual gauge freedom expressed by a generic vector field $\boldsymbol{\Xi}(\boldsymbol{\chi})$. The nice feature of this gauge is that the slicing is comoving, meaning that the in this gauge the fluid 4-velocity appears to be orthogonal to the equal time surfaces.
  It is conventional to introduce the comoving curvature perturbation $\mathcal{R}$ in this gauge:

$$\mathcal{R} = -\hat{\psi} = -\psi + \mathcal{H}\xi^0 = -\psi + \mathcal{H}(B + v), \tag{3.19}$$

  the gauge time parameter can be expressed also as $\xi^0 = \frac{\delta\phi}{\phi'}$, where ϕ is the inflaton field and $\delta\phi$ its fluctuations, this will be useful in the discussion of initial conditions of the perturbations [50].

- uniform density gauge
  Another gauge of interest is the gauge in which the time slicing is chosen so that the density appears uniform on each slice $\hat{\delta}\rho = 0$, with the additional requirement that $\hat{E} = 0$ [51]. These two requirements completely fix the scalar gauges quantities: $\xi^0 = -\frac{\delta\rho}{\bar{\rho}'}$ and $\xi = -E$.
  As in the comoving gauge, it result convenient to define the so-called primordial curvature perturbation:

$$\zeta = -\hat{\psi} = -\psi + \mathcal{H}\xi^0 = -\psi - \mathcal{H}\frac{\delta\rho}{\bar{\rho}'}, \tag{3.20}$$

  this curvature will play an important role in generating the seeds of the collapsing matter for the PBHs.

- spatially flat gauge
  This is the most important gauge when working with quantities deriving from inflation, its name is self explanatory: it is obtained by requiring the spatial curvature to vanish $\delta^{(3)}R = 0$, this can be attained by setting $\hat{\psi} = 0 = \hat{E}$ [20], and so $\xi^0 = \mathcal{H}^{-1}\psi$ and $\xi = -E$; leaving no residual gauge freedom.

It needs to be emphasized that the fixing of the gauge presented are performed starting from the most arbitrary gauge, yet it is also possible switch between any two of these gauge by combining the gauge-fixing conditions. As an example, it can be useful to relate $\mathcal{R}$ and ζ:

$$\zeta - \mathcal{R} = \frac{\Delta}{3(1+w)}, \tag{3.21}$$

which was obtained by subtracting (3.19) from (3.20) and recalling the definition of the comoving density contrast in (3.16).

Evolution of perturbations

As previously mentioned, the different sectors—scalar, vector, tensor— of the perturbations evolve independently in linear cosmological perturbation theory. Their equations of motion can be derived by solving the perturbed Einstein equations $\delta G_{\mu\nu} = 8\pi G \delta T_{\mu\nu}$, which can be opened to get a system of 10 equations. Yet the system contains redundant equations; however, we have an additional independent equation as Bianchi identities constraints $\delta G^{\mu}_{\nu;\mu} = 0$. Taking the tensorial part of the Einstein equation we can find the evolution equation for tensorial modes:

$$h''_{ij} + 2\mathcal{H}h'_{ij} + (2K - \nabla^2)h_{ij} = 8\pi G a^2 \sigma_{ij}, \tag{3.22}$$

describing the evolution of gravitational waves in the expanding perturbed spacetime.
For non-tensorial modes we will be working in conformal Newtonian gauge; taking vector modes into account, from the components G_{0i} and G_{ij} we can extract two evolution equations, and one constraint comes from the Bianchi identities:

$$\begin{aligned} (\nabla^2 + 2K)\Phi_i &= -16\pi G\bar{\rho}a^2(1+w)v_i^{\perp} \\ \Phi_i' + 2\mathcal{H}\Phi_i &= 8\pi G a^2 \sigma_i \\ v_i^{\perp\prime} + 3\mathcal{H}(1 - 3c_S^2)v_i^{\perp} &= -\frac{1}{2}\frac{w}{\bar{p}(1+w)}(\nabla^2 + 2K)\sigma_i. \end{aligned} \tag{3.23}$$

Nonetheless, vector modes do not play a major role in the evolution of structure because they have a decaying behaviour [27].
Turning to the scalar modes we can take into account the following combinations: $\delta G^0{}_0 + 3\mathcal{H}\,\nabla_i^{-1}\,\delta G^0{}_i$, $\delta G^i{}_j - \delta G^k{}_k \delta^i_j$, $\delta G^0{}_i$, $\delta G^i{}_i + 3c_s^2 \delta G^0{}_0$, $\delta G^{\mu}{}_{0;\mu}$ and $\delta G^{\mu}{}_{i;\mu}$ to obtain:

$$(\nabla^2 + 3K)\Psi = 4\pi G a^2 \bar{\rho}\Delta, \tag{3.24}$$

$$\Psi - \Phi = 8\pi G a^2 \sigma, \tag{3.25}$$

$$\Psi' + \mathcal{H}\Phi = -4\pi\bar{\rho}(1+w)V \tag{3.26}$$

$$\Psi'' + 2\,\mathcal{H}(1+c_S^2)\Psi' - K\Psi + \mathcal{H}\,\Phi' + (2\,\mathcal{H}' + \mathcal{H}^2)\Phi + \frac{1}{3}\,\nabla^2(\Phi - \Psi) = 4\pi G a^2 \delta S. \quad (3.27)$$

In this form, these equations relate the evolution of six parameter $\Psi, \Phi, \Delta, \sigma, V, \delta S$ between themselves are quite intricate, and one cannot expect to find a simple closed solution. To make things worse, we should also consider that until now we have only considered a single-component fluid, whereas we expect that different components comes into play, as e.g. the simplest case consider the universe as a two-components-fluid, namely matter and radiation; even though, more comprehensive models include more fluids. Within ΛCDM, the multi-component fluid comprises five constituents [52]: photons(γ), neutrinos(ν), baryonic matter(m)[5], dark matter(DM)[6] and dark energy(Λ). Needless to say, each component can be split into other subspecies; this is the case for PBHs: upon formation, they contribute as a part of the cold dark matter fluid.

The models of PBH formation usually take place in the universe, as such the evolution equations can be further adapted to suit our purposes. According to the scale of interest and the cosmic time it is reasonable to reduce the number of the components, because some of them were subdominant components or coupled to each other and in thermal equilibrium. To all intents and purposes, neglected components only affect the background and are said to be smoothed, thus $\delta\rho_a \approx 0$ and $\bar{\rho} = \sum_a \bar{\rho}_a$ where a spans the smoothed components [53].

Within the radiation epoch, evolution equations can be simplified by two assumptions. First, we can assume that the anisotropic stress vanishes; consequently, we can reduce to a single Bardeen potential $\Psi = \Phi$. This assumption is backed-up by the high degree of isotropy in CMB as opposed to the following matter epoch where the anisotropic stress grows with the scale factor [29]. The second assumption is to neglect the background intrinsic curvature, $K = 0$, which allows us to expand the perturbations in terms of their Fourier modes. In this way, the spatial gradient can be replaced with the comoving wavenumber of the specific mode, e.g $\nabla_i\,\Psi_{\mathbf{k}}(\eta, \mathbf{k}) = ik_i\Psi_{\mathbf{k}}(\eta, \mathbf{k})$ and $\nabla^2\,\Psi_{\mathbf{k}}(\eta, \mathbf{k}) = -\mathbf{k}^2\Psi_{\mathbf{k}}(\eta, \mathbf{k})$.

For $K \neq 0$ the Fourier modes are no longer eigenfunctions of the Laplacian operator and they cannot be used in the same way, in those cases one has to recur to spherical harmonics and Bessel functions [37]. The vanishing of K turns out to be a huge simplification that, in the case large scale density of the universe has stayed closed to the critical density, stands on a solid physical ground and it is not merely mathematical sleight of hand.

Hubble sphere and Jeans radius

One advantage of Fourier expansion is the introduction of a physical scale, given by $1/|\mathbf{k}|$ for each mode. It can be compared with the (comoving) Hubble radius

[5] In the cosmological context, the definition of baryon is relaxed to include also electrons and other heavy leptons conversely from a particle physics point of view.

[6] Dark matter can be parted in several classes, the hot/cold terminology refers to the typical kinetic energy of its components.

$1/\mathcal{H}$, which is the distance at which the speed of recession from the local reference frame is c [54]. Objects outside the Hubble sphere recede faster than the speed of light[7]. The comparison of these two scales gives us two regimes for studying the evolution equations: the super-Hubble regime for $|\mathbf{k}| \leq \mathcal{H}(\eta)$ and the sub-Hubble regime for $|\mathbf{k}| \geq \mathcal{H}(\eta)$. However, the comoving Hubble radius is not a quantity constant in time and depending on the cosmic epoch it can shrink or grow, thence modes are expected to exit or enter the sub-Hubble regime. This feature plays a paramount role in the formation of structures: modes enter the sub-Hubble regime either at radiation domination epoch or at matter domination—shorter wavelength modes enter first and modes with longer wavelength enter later.

The evolution equations for non-relativistic matter fluid reduce to the equations we would get from Newtonian mechanics: Poisson equation, Euler equation for fluids and continuity equation. Yet, we have to bear in mind that the expansion of the universe adds a feature that we could not deduce by Newtonian physics alone: it give rise to a damping behaviour, which can be easily understood in terms of the Hubble flow. Since cosmic fluids are moving in the expanding space, modes experience a form of dynamical friction even when there is no source. In this regime another important physical scale appears, the Jeans length or radius, which is the scale at which the pressure of the fluid has the same magnitude of its gravitational potential [55]: $R_J = c_s\sqrt{3\pi/8G\bar{\rho}}$. This length stands as the demarcation line between sound waves of baryons tight to radiation, known as Baryon Acoustic Oscillations(BAO), and the regime in which gravitational collapse takes over the thermal collisions.

Nonetheless, cold dark matter, being pressureless, has vanishing Jeans length, as opposed to other matter species which Jeans length vanishes only after entering the matter domination epoch, when the speed of sounds becomes negligible. The dark matter then tends to clump together at earlier times and after recombination the distribution of matter perturbations stops following the oscillatory behaviour of radiation to gather around the dark matter dwells, which are deemed to be the seeds of the first galaxies and stars.

The comoving Hubble radius in these two epochs—radiation and matter domination—is growing monotonically, so following it back in time we expect to see that wavelengths from higher to lower k re-entering the Hubble scale, and thus going back in time we can expect that almost all scales were lying outside the Hubble radius at some point in the past. The nicest feature of the super-Hubble regime is that the lack of causal contact makes the physics quite simple. In particular, if we contract the four-velocity with the conservation of the energy-momentum tensor $u^\nu T^\mu{}_{\nu;\mu} = 0$ [56] we obtain that:

$$0 = u^\mu \rho_{;\mu} + u^\mu{}_{;\mu}(\rho + p) \quad \Rightarrow \quad \zeta'_{\mathbf{k}} = \frac{\mathcal{H}}{\bar{\rho} + \bar{p}}\delta p_{\text{nad}} + \frac{1}{3}\mathbf{k}^2(E' + v). \tag{3.28}$$

On super-Hubble regime the second term is negligible and we obtain that primordial curvature evolution only depends on the non-adiabatic pressure, and it is constant if

[7] For this reason the Hubble radius is often referred as horizon in cosmology.

the latter is zero. This condition, as we will see soon, is satisfied in the inflationary epoch, and provides the means to establish the initial conditions for the perturbations re-entering the sub-Hubble regime. Moreover, by taking (3.21) together with (3.24), we attain:

$$\zeta_{\mathbf{k}} - \mathcal{R}_{\mathbf{k}} = \frac{2}{9(1+w)} \frac{\mathbf{k}^2 + 3K}{\mathcal{H}^2} \Phi_{\mathbf{k}}, \tag{3.29}$$

which tells us that in the linear regime, when the extrinsic curvature vanishes, the modes of comoving and primordial curvature perturbations coincide on super-Hubble scales ($k/\mathcal{H} \ll 1$).

The inflationary paradigm

To justify why the modes are located outside the Hubble sphere initially, it has been proposed that there was an earlier epoch in which the coming Hubble radius shrunk; to see how it happened we need to bring into play the paradigm of Inflation. The hot Big Bang model of cosmology alone has no causal explanation for the existence of perturbation on super-Hubble scales; for this reason, when the perturbation theory was first developed the initial conditions where just postulated, but through inflationary models these perturbations found a possible origin in the zero-point quantum fluctuations of a scalar field[8], the inflaton [57], which was once the dominant cosmic component.

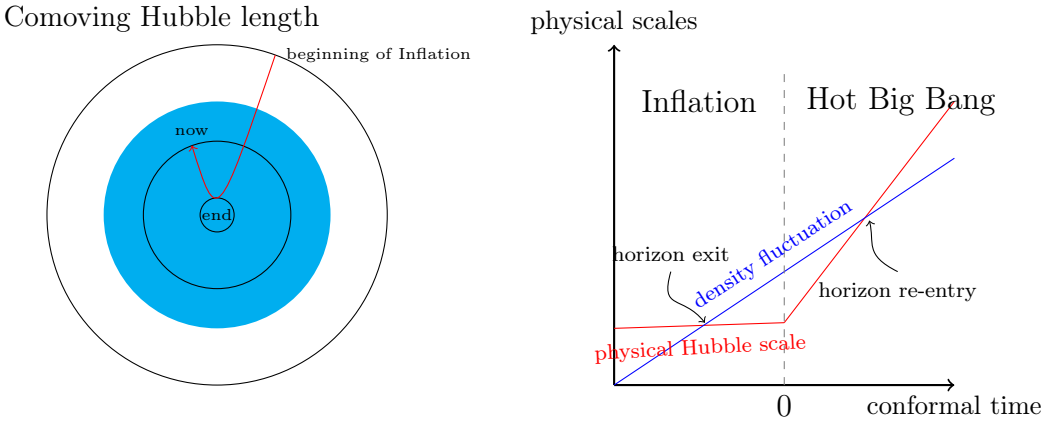

Figure 3.1. The picture shows the behaviour of the comoving Hubble sphere (left) and Hubble radius in comparison with a mode of comoving momentum k, which at some point exits the radius only to re-enter at later times, figure adapted from [51].

The inflationary epoch is a stage preceding the radiation domination epoch, in which the universe undergoes a phase of exponentially accelerated expansion, with scale factor $a(t) \sim \exp(Ht)$. This expansion has the virtue of smoothing out accidental inhomogeneities present in former stages of the universe and provides an explanations

[8] The inflationary paradigm might actually need more than one scalar field to work, the number of field required has not been establish yet, since the microscopic theory is still unknown.

for the similarity between causally-disconnected patches in the CMB [51]. Inflation can be specified by three equivalent conditions:

$$\frac{\mathrm{d}}{\mathrm{d}\,t}\frac{1}{\mathcal{H}} < 0 \quad \Leftrightarrow \quad \ddot{a} > 0 \quad \Leftrightarrow \quad \rho + 3p < 0, \tag{3.30}$$

where the first condition simply states that the comoving Hubble sphere is shrinking, the second asserts that the expansion is undergoing an acceleration phase and the latter formalizes the requirement for pressure to be negative in order to cause the expansion[9] [51]. A central assumption for inflation to work is that the observable universe, at the beginning of this phase, lies well within the Hubble radius—$\mathcal{H}(\eta_{\text{in}}) \ll \mathcal{H}_0$— and well outside it when this period stops—$\mathcal{H}_0 \ll \mathcal{H}(\eta_{\text{end}})$ [53].

Having specified the conditions, we now take into account a specific model of inflation, namely single-field, slow-roll inflation [50] . In this model, we consider a classical scalar field $\phi(t, \mathbf{x})$ living in the unperturbed spacetime in a non-equilibrium state, relaxing toward its true vacuum. The exact dynamics is still left unspecified and the field's action and equations of motion for the modes are given by:

$$S_\phi = \int d^4x\sqrt{-g}(g^{\mu\nu}\phi_{;\mu}\phi_{;\nu} - V(\phi)) \quad \Leftrightarrow \quad \ddot{\phi} + 3H\dot{\phi} - \frac{1}{a^2}\nabla^2\phi + V_{,\phi} = 0, \tag{3.31}$$

where in practice the inflaton field is considered to be homogeneous, so that the gradient term vanishes. The exact form of the potential is still unknown, and various potentials are actually explored in the literature [58], but they are generally required to slowly decrease toward a minimum in $\phi = 0$. The term $3\,\mathcal{H}\,\phi'_{\mathbf{k}}$ in (3.31) represents a friction term which, after an initial phase, allows the inflaton field to reach its terminal velocity and the Hubble parameter will remain almost constant, in a quasi-de Sitter phase, where the expansion of the scale parameter is approximately exponential [59].

One role of inflation is to drive the extrinsic curvature of spacetime toward flatness; this can be attained by considering the first Friedmann equation (2.11) rewritten in term of the curvature parameter $\Omega(a)$ for a non-flat universe:

$$|1 - \Omega(a)| = \frac{|K|}{(aH)^2}, \tag{3.32}$$

if H is kept constant, as the scale increase then the universe is driven toward the critical density, thus making $\Omega = 1$ an attractor solution for inflation [51][10].

By direct comparison of the energy-momentum tensor of the inflaton field with the source of an isotropic and homogeneous field in Einstein equations, we can infer the density and the pressure to rewrite the Friedmann equations in term of the inflaton:

$$\begin{aligned} \rho &= \frac{1}{2}\dot{\phi}^2 + V(\phi), & p &= \frac{1}{2}\dot{\phi}^2 - V(\phi) \Rightarrow \\ H^2 &= \frac{8\pi G}{3}\left(\frac{\dot{\phi}^2}{2} + V\right) - \frac{K}{a^2}, & H' &= \frac{8\pi G}{3}(V - \dot{\phi}^2). \end{aligned} \tag{3.33}$$

[9] In present time the negative pressure is ascribed to the dark energy, but in the early universe its contribution is negligible.

[10] This feature makes flatness a prediction of inflation, instead of being an ab-initio assumption.

From the second Friedmann equation, we recast one of the conditions of inflation as $V > \dot{\phi}$. The first slow-roll condition is given by the stronger assumption that the kinetic energy of the field is negligible with respect to the potential energy, $\phi'^2 \ll a^2 V(\phi)$. The second condition is given by the assumption that the former condition last long enough, so that that K goes to zero and we can have that $\mathcal{H}^2 \simeq \frac{8\pi G}{3} a^2 V(\phi)$; as a result, we can expect that the derivative with respect to the time of the first condition holds, or equivalently that $\ddot{\phi} \ll V_{,\phi}(\phi)$.
These approximations can be used in the equation of motion to obtain:

$$3H\dot{\phi} \simeq -V'(\phi) \quad \Rightarrow \quad \ddot{\phi} \simeq -\frac{\dot{H}}{H}\dot{\phi} - \frac{V_{,\phi\phi}\dot{\phi}}{3H}. \tag{3.34}$$

The two conditions can be reformulated in terms of the so-called slow-roll parameters ϵ and η[11] [50] defined by:

$$\epsilon = -\frac{\dot{H}}{H^2} = 4\pi G \frac{\dot{\phi}^2}{H^2} = \frac{1}{16\pi G}\frac{V_{,\phi}^2}{V^2}, \qquad \eta = \frac{1}{8\pi G}\frac{V_{,\phi\phi}}{V} = \frac{V_{,\phi\phi}}{3H^2}, \tag{3.35}$$

which must respect the conditions $\epsilon \ll 1$, $|\eta| \ll 1$. The parameters give the constraints the potential must respect for the inflation to occur in the slow-roll paradigm; conversely, when these inequalities do not hold anymore, as these parameters approach unity, it only means that inflation exits the slow-roll regime. After the slow-roll regime the universe must enter a reheating phase in which the energy is transferred from the inflaton to the other particle species. The ϵ parameter, which actually takes account of the variation of the Hubble parameter, is a good indicator of the end of inflation; indeed $\ddot{a} = a(\dot{H} + H^2) = a(1-\epsilon)H^2$ and when it passes unity, i.e. $\epsilon \geq 1$, inflation stops because the scale factor is no longer accelerating [50].
The duration of inflation is measured in terms of e-folds, the time interval in which the scale factor grows by a factor e:

$$N = \log\left(\frac{a_{\text{end}}}{a_{\text{in}}}\right) = \int_{t_{\text{in}}}^{t_{\text{end}}} H(t)\,\mathrm{d}\,t = \int_{\phi_{\text{in}}}^{\phi_{\text{end}}} \frac{V}{V_{,\phi}}\,\mathrm{d}\,\phi, \tag{3.36}$$

where the slow-roll approximations were used in the RHS. To solve the horizon and the flatness problems, the number of efolds is required to be $N \gtrsim 50 - 60$ [53].

The role of Inflation on perturbations

The reason we are interested in inflation is that it provides a mechanism to generate the primordial curvature perturbations. In a similar fashion with the perturbation theory for the metric, we now split the inflaton field into an homogeneous unperturbed part and a first-order perturbation: $\phi(x,t) = \bar{\phi}(t) + \delta\phi(x,t)$ in uniform density gauge. From the equation of motion for the perturbed inflaton field we can

[11] Not to be confused with the conformal time, which for inflation customarily varies from $-\infty < \eta \leq 0$.

derive the equation of motion of the perturbation, which can be written directly in terms of the modes:

$$\ddot{\delta\phi} + 3H\dot{\delta\phi} - \frac{\nabla^2}{a^2}\delta\phi + V_{,\bar{\phi}\bar{\phi}}\delta\phi = 0, \tag{3.37}$$

we can define an effective mass term $m^2(t) = \tilde{V}_{,\bar{\phi}\bar{\phi}}$. However, as we consider the Fourier expansion of this equation, modes behave as massless by virtue of the slow-roll condition on η, which allows us to neglect the last term until few Hubble times since exited the Hubble-sphere[12]. Thence, the equation of motion for the perturbations reduce to that of an harmonic oscillator for sub-Hubble modes, they acquire a damping term on near-Hubble scales and super-Hubble modes assume a constant dominant solution [45], in comoving coordinates, the particular solutions take the form:

$$w_{\mathbf{k}}(\eta) = \frac{e^{-ik\eta}}{\sqrt{2k}}\left(1 - \frac{i}{k\eta}\right). \tag{3.38}$$

On the other hand, taking the derivative with respect to time of equation (3.31), $\dddot{\bar{\phi}} + 3H\ddot{\bar{\phi}} + V_{,\bar{\phi}\bar{\phi}}\dot{\bar{\phi}} = 0$, we find that super-Hubble modes —for which the mass term is no longer negligible— share the same form for the evolution with $\dot{\bar{\phi}}$; thence, they are proportionally related by a constant which depend on time:

$$\delta\phi(t, \mathbf{x}) = -\dot{\bar{\phi}}(t)\delta t(\mathbf{x}) = -\bar{\phi}'(\eta)\delta\eta(\boldsymbol{\chi}), \tag{3.39}$$

therefore, $\phi(t, \mathbf{x}) = \bar{\phi}(t - \delta t(\mathbf{x}))$, the inflaton does not assume the same value in all space at the same time because the effect of perturbations is to delay its propagation [50].

We now assume that the perturbation field, can be promoted to quantum field on the small scale, which resides in its vacuum state. A de Sitter space contains an event horizon which coincide with the Hubble radius; as a result, the fluctuations of vacuum give rise to perturbations of the inflaton field, in a similar fashion of the Hawking radiation from a black hole [60]. The perturbations of the inflaton field are generated as quantum fluctuations of the vacuum which are stretched over the Hubble-radius; where they turn into a classical field and freeze to a constant value. Then, we can derive the expectation value for a single massless mode $\hat{\delta\phi}_{\mathbf{k}}(t) = a^{-1}(w_{\mathbf{k}}(t)\hat{a}_{\mathbf{k}} + w^*_{\mathbf{k}}(t)\hat{a}^\dagger_{\mathbf{k}})$[13] to arise from the vacuum [61] as:

$$\langle|\hat{\delta\phi}_{\mathbf{k}}|^2\rangle = \langle 0|\hat{\delta\phi}^\dagger_{\mathbf{k}}\hat{\delta\phi}_{\mathbf{k}}|0\rangle = \frac{|w_{\mathbf{k}}|^2}{a^2} = \frac{H^2}{2k^3}(1 + k^2\eta^2) \xrightarrow{k\ll\mathcal{H}} \frac{H^2}{2k^3}, \tag{3.40}$$

where the RHS express its value on super-horizon scales where the perturbations are constants. The result is independent on the direction of $\mathbf{k}$, so it is the same for their real and imaginary part. As a consequence of the fact that various modes are independent from each other, we expect the perturbations to arise as a Gaussian random

[12] This happens at time $t = t_*$, when $k = a(t_*)H(t_*)$. The equation of motion with the mass term neglected is known as Mukhanov-Sazaki equation.

[13] $\hat{a}_{\mathbf{k}}$ and $\hat{a}^\dagger_{\mathbf{k}}$ are creation and annihilation operators which satisfy the canonical commutation relations.

field [30], meaning that the probability of finding a perturbation of amplitude $|\delta\phi_{\mathbf{k}}|$ follows a gaussian statistics:

$$P(|\delta\phi_{\mathbf{k}}|^2) = \frac{1}{\sqrt{2\pi\sigma_{\delta\phi}}} \exp\left(-\frac{1}{2}\frac{|\delta\phi_{\mathbf{k}}|^2}{\sigma^2_{\delta\phi}} \right), \tag{3.41}$$

where $\sigma_{\delta\phi}$ is the variance of the distribution, given by the mean-square in (3.40). In position space, as this quantity depends on the superposition of all the Fourier modes, it is more useful to express it in terms of its logarithmic contribution in an infinitesimal interval of dk, also called spectrum $\mathcal{P}_{\delta\phi}(k)$ defined by relations:

$$\sigma^2_{\delta\phi}(\mathbf{x}) = \frac{1}{(2\pi)^3}\int_0^\infty \frac{\mathrm{d}\,k}{k}\mathcal{P}_{\delta\phi}(k) \quad \Leftrightarrow \quad \langle \hat{\delta\phi}_{\mathbf{k}} \hat{\delta\phi}_{\mathbf{k}'} \rangle = (2\pi)^3 \delta(\mathbf{k}+\mathbf{k}')\mathcal{P}_{\delta\phi}(k). \tag{3.42}$$

Since vacuum fluctuations continuously arise and get stretched by inflation we expect the final distributions of perturbations to be almost scale-invariant.

Quantum fluctuations act as a source in the energy-momentum tensor in Einstein equations, and thus induce metric perturbations, which in turn back-react to perturb the classical inflaton field. On flat-slices ($\psi = 0$), we can use (3.33) to relate the density perturbation to its inflationary counterpart [62]: $\delta\rho = \frac{\partial\rho}{\partial\phi}\delta\phi = V_{,\bar{\phi}}\delta\phi$. We can finally connect the primordial curvature perturbation with the inflationary perturbation:

$$\zeta = -\mathcal{H}\frac{\delta\rho}{\bar{\rho}'} = \frac{1}{3}\frac{\delta\rho}{\bar{\rho}+\bar{p}} = \frac{V_{,\bar{\phi}}}{3\dot{\bar{\phi}}^2}\delta\phi = 8\pi G\frac{V_{,\bar{\phi}}}{V}\delta\phi = 32(\pi G)^{3/2}\epsilon^{1/2}\delta\phi, \tag{3.43}$$

where, in the end, we used the slow-roll approximations for $\dot{\bar{\phi}}$ and H [63]. This allows us to derive the power spectrum for the Fourier modes of the curvature perturbation directly from the vacuum fluctuations of a single-field slow-roll inflaton [53]:

$$\mathcal{P}_\zeta(k) = \frac{\bar{H}^2}{4\pi^2}\left(\frac{\bar{H}}{\dot{\bar{\phi}}}\right)^2\Bigg|_{k_*}, \tag{3.44}$$

were the subscript k_* stands to remind that these quantities are evaluated at horizon exit, where their evolution enters the super-Hubble regime and stays frozen until they re-enter the horizon.

The scale dependence of the primordial curvature perturbations is one of the observables in the CMB fluctuations, and, to measure it, we introduce the tilt, $n(k) - 1$, and the spectral index $n(k)$ [53]:

$$n(k) \equiv \frac{\mathrm{d}\ln\mathcal{P}_\zeta(k)}{\mathrm{d}\ln k} + 1. \tag{3.45}$$

A perfectly scale-invariant spectrum has vanishing tilt[14], and so it is constant, $\mathcal{P}_\zeta(k) = A_\zeta$. Nonetheless, since inflation last for finite amount of time, or equivalently, because the Hubble parameter is not exactly constant, then the power

[14] This specific type of spectrum can be found in the literature as Harrison-Zel'dovich spectrum.

spectrum is only approximately scale-invariant; thence, it necessarily has a scale dependence [64]:

$$\mathcal{P}_\zeta(k) = \mathcal{P}_\zeta(k_p)\left(\frac{k}{k_p}\right)^{n-1} \equiv A_\zeta\left(\frac{k}{k_p}\right)^{n-1}, \tag{3.46}$$

where k_p is a pivot scale, serving the purpose of fixing the normalization A_ζ of the power law behaviour at $k_p \gg k$.
In addition, the spectral index could also be running [64]:

$$n(k) = n_s - \frac{1}{2!}\alpha_s \ln\left(\frac{k_p}{k}\right) + \frac{1}{3!}\beta_s \ln^2\left(\frac{k_p}{k}\right) + ..., \tag{3.47}$$

where we call $n_s(k)$ the slope, α_s the running of the spectral index, β_s the running of the running and so on, which are defined at the pivot scale:

$$n_s \equiv \left.\frac{\mathrm{d}\ln\mathcal{P}_\zeta}{\mathrm{d}\ln k}\right|_{k_p} + 1, \quad \alpha_s \equiv \left.\frac{\mathrm{d}\, n_s}{\mathrm{d}\ln k}\right|_{k_p}, \quad \alpha_s \equiv \left.\frac{\mathrm{d}^2\, n_s}{\mathrm{d}\ln^2 k}\right|_{k_p}. \tag{3.48}$$

Spectral parameters can be expressed in terms of slow-roll parameters [65]:

$$n_s - 1 = 2\eta - 6\epsilon, \qquad \alpha_S = 16\epsilon\eta - 24\epsilon^2 - 2\xi, \tag{3.49}$$

where $\xi = V_{,\phi}V_{,\phi\phi\phi}/(8\pi GV)^2$, is a parameter for the third derivative of the inflaton potential; thus, providing a link between the slow-roll parameters and observations. In conclusion, CMB data from Planck [23] measures $k_p = 0.05\mathrm{Mpc}^{-1}$, $A_\zeta = 2.101^{+0.031}_{-0.034}\times 10^{-9}$, $n_s = 0.9647 \pm 0.0043$, $\alpha_s = 0.0011 \pm 0.0099$ and $\beta_s = 0.009 \pm 0.012$, leaving open the possibility that there could be a weak dependence of the spectral index on the scale.

The Separate Universe Approach

The derivation of the spectrum for the primordial curvature perturbation of the last paragraph is based on the assumption of single-field slow-roll inflation. As a result of having only one field, the perturbations generated are granted to be gaussian and adiabatic [30], which in turn guarantees the constancy of the primordial curvature perturbations on scales beyond Hubble by virtue of equation (3.28). However, if more than one field takes part in the late stages of inflation, approximate scale-invariance gets necessarily broken at some scale; moreover, although observations still point toward a gaussian behaviour of the inflationary fluctuations, non-gaussianities are difficult to be ruled out [66]. In such cases, first-order cosmological perturbation theory might be insufficient because of non-linearities arising from spacetime with large-scale inhomogeneities; instead of recurring to higher-orders, Salopek and Bond [67] explored an alternative way of performing perturbation theory: where the long-wavelength perturbations are treated nonlinearly and the perturbative expansion is formulated in terms of their spatial gradients.

To consider a full non-linear characterization, perturbed spatial part of the metric can be written as [53]:

$$g_{ij} = a^2(\mathbf{x}, t)\tilde{\gamma}_{ij}(\mathbf{x}) \quad \text{with} \quad a(\mathbf{x}, t) \equiv a(t)e^{-\psi(\mathbf{x},t)}, \quad \tilde{\gamma}_{ij}(\mathbf{x}) \equiv \left(e^{\tilde{e}(\mathbf{x},t)}\right)_{ij}, \tag{3.50}$$

where $\tilde{e}$ is a traceless matrix of generators of the perturbations[15]. For the reason that the interesting scales are those lying beyond the Hubble scale, one can choose to expand in terms of the parameter $\varepsilon = k/aH$ which is small on these scales. The next step is, firstly, to assume that longer-than-Hubble wavelength modes have been smoothed by the inflation so that they will evolve as if they were homogeneous—making thus spatial gradients of order greater that ε negligible— and, secondly, that they look locally isotropic at each position. These two assumptions embody the so-called separate universe approach, which can be regarded as the first order approach of the gradient expansion [68]. In practice, smoothing over long-wavelength modes means to sum over the sub-ϵ scales, in a coarse-grained fashion:

$$\phi_{\mathbf{k},\text{smooth}}(t, \mathbf{x}) = \int d^3\mathbf{x}' W(t, \mathbf{x} - \mathbf{x}')\phi_{\mathbf{k}}(t, \mathbf{x}'), \tag{3.51}$$

by introducing a window function, $W(t, \mathbf{x} - \mathbf{x}')$, the Fourier transform of which has support only on scales $k < \mathcal{H}$. In this way, each region of size H^{-1} can be thought as a single point and its internal physics can be neglected.

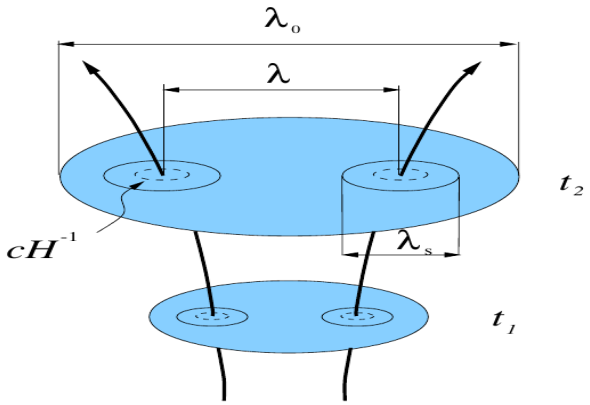

Figure 3.2. The picture illustrate the hierarchy of scales introduced by the separate universe assumption: $\lambda_0 \gg \lambda \gg \lambda_s \gtrsim H^{-1}$, taken from [69].

In practice, adopting this approach is tantamount to consider that regions smaller than the smoothing scale λ_s evolve as separate FLRW universes (with locally homogeneous perturbations), and large-scale perturbations of wavelength $\lambda = a/k$ can be formed by piecing these patches together. The FLRW background of cosmological perturbation theory must be valid for the present largest cosmological scale, $\lambda_0 = H_0^{-1}$, or larger scales if no additional structure exists beyond the large-scale

[15] $\tilde{e}$ is analogous to the quantity defined in (3.6) but subtracting the laplacian term of E which, instead, is included in ψ. All the generators no longer need to be considered infinitesimal; moreover, ψ can be taken to be $-\mathcal{R}$ comoving slices, and $-\zeta$ of slices of uniform density.

homogeneity and isotropy. Still, the role of the background can be now factored out when taking into account the curvature perturbation ψ, because it can be taken as the difference in the curvature perturbation of two points a and b at distance λ, $\psi = \psi_a - \psi_b$; hence, maintaining its non-linear role.

If we now consider a gauge transformation, $t \mapsto T = t + \xi^o$, the spatial metric in the context of the gradient at a given point transforms as: $\hat{g}_{ij}(T, \mathbf{x}) = g_{ij}(t, \mathbf{x}) + \mathcal{O}(\varepsilon^2)$. Therefore, using (3.50) and taking the determinant and the logarithm of both sides of the last relation: $\psi(T) + \ln a(T) = \psi(t) + \ln a(t)$, or equivalently, by the definition of e-fold (3.36):

$$\psi(T) = \psi(t) + \ln \frac{a(t)}{a(T)} \equiv \psi(t) + N, \tag{3.52}$$

the curvature perturbations on different gauges are related by the number of efolds occurring between the slices [70]. And so, the curvature perturbation at scale λ is given by the difference of the local number of efolds in the two separated patches, which in turn only depends on the perturbations of inflationary field. Still, this result could seem to be dependent on the gauge-choice in the initial an final slices. However, if we consider the initial slice to be a flat slice, and the final slice to be a constant-density slice, since these two gauges leave no residual degrees of freedom the problem do not arise [71]. For the reason that flat slicing requires the local curvature perturbation to vanish, whereas the curvature perturbation coincide with the primordial curvature perturbation on constant-density slices, we obtain the result known as δN formalism [53]:

$$\zeta = \delta N = N_{,a}\delta\phi_a + \frac{1}{2}N_{,ab}\delta\phi_a\delta\phi_b + \dots \tag{3.53}$$

where $\delta\phi_a$ are the scalar field components of the inflationary field[16] and $N_{,a} = \frac{\partial N}{\partial(\delta\phi_a)}$. For single-field inflation (3.53) shall reduce to the same result of the previous paragraph; otherwise, we can single out the inflaton, $\delta\phi$, contribution into the adiabatic part of ζ from the non-adiabatic, letting the summation run over the fields $\delta\sigma_a$ other than the inflaton, and the generalized power spectrum in the first order expansion in δN reads as [53]:

$$\mathcal{P}_\zeta(k) = \mathcal{P}_\zeta^{\text{ad}}(k) + \left(\frac{H}{2\pi}\right)^2 \sum_a N_{,a}^2 \Big|_k. \tag{3.54}$$

[16] Summation over the component indices is intended.

Chapter 4

Thresholds for Primordial Black Hole Formation

> Every physicists should know six or seven
> different representations of the same physics.
>
> Richard Feynman

In the previous chapter, we explored the origin of primordial perturbations; in this chapter, we describe how these perturbations can conglomerate to form PBHs. Several mechanisms have been proposed to account for the creation of PBHs in the literature, but the basic idea is the same: it all boils down to the local collapse of the distribution of matter-energy within the Schwarzschild radius.

What distinguish PBHs from stellar black holes, is that the first kind arise from primordial perturbations. For since universe was in the form of plasma of elementary particles, their formation can defy the Tolman-Oppenheimer-Volkoff limit [72], which sets a lower bound on the mass of black holes originating from stars. In addition, black holes arising from stars are modeled neglecting the expansion of the universe, collapsing in a asymptotically flat spacetime; for PBHs this assumption needs to be dropped because initially parallel geodesics diverge asymptotically in a FLRW spacetime [1].

After inflation, the comoving Hubble scale starts growing again, and the various modes of the primordial perturbations re-enter consecutively the physical Hubble scale. For all practical purposes, distances larger the Hubble scale recess faster than the speed of light, and so causal interaction is hindered; whence, once the causal contact is established again, perturbations might cumulate again. Moreover, by merit of inflation, we can assume that the background metric has been driven

[1] The main consequence is that stellar black holes, which keep their mass constant over the relevant time scales, have a well-defined event horizon, whereas in the dynamical context of an asymptotically curved spacetime such a surface might not exist. PBHs can be still characterized by the formation of an apparent horizon.

towards having the Friedman critical density $\rho_0(t) = 3H^2(t)/(8\pi G)$, so that the universe is flattened to $K = 0$.

We are going to review PBH formation under the following formalisms:

- simplistic two FLRW universes description;
- auto-solution method of two FLRW universes;
- critical collapse;
- quasi-homogeneous numerical methods;

In all cases, PBH formation is studied under the assumptions of fixed equation of state, and spherical symmetry. Later in the chapter, we relax these assumptions taking into account formation during a phase transition and ellipsoidal collapse.

Simplistic model of collapse

In the first paper [73] that attempted to study black holes in a cosmological background, Hawking and Carr took into account spherically symmetric, self-similar solutions of the Einstein equations in which the black hole radius expands at the same rate of the universe. They reached the conclusions that, in order to contain a black hole, a FLRW spacetime necessarily needs positive extrinsic curvature, and, in the radiation epoch, there is always a pressure gradient directed radially outward. The interest in this paper lies mainly in its pioneering character, and the $K > 0$ condition is a limitation towards viable applications to our universe.

Inspired by an earlier work of Harrison [74], Carr [75] studied again the formation by describing a spherical perturbation evolving as a closed, $K = 1$, FLRW universe embedded in an extrinsically flat unperturbed background. The overdense region evolves independently from the background, so it might grow for a while, but will eventually stop its expansion and start to collapse. Following the evolution of the density contrast, an upper- and lower-bound for the density contrast needed to obtain a PBH are established in the paper.

To put things into perspective, let us consider two coordinate charts: one describing the unperturbed extrinsically flat universe (t, r, θ, ϕ), and the other $(\tau, \xi, \theta, \phi)$ describing the perturbed universe of curvature K. At an initial time t_0, the perturbation of density contrast δ_0 is contained within a spherical region of physical radius R_0 in the flat chart; this radius corresponds to the areal radius of a sphere[2]. This means that we can take the metric for this setting to be [76]:

$$ds^2 = \begin{cases} -\,\mathrm{d}\,t^2 + \bar{a}^2(t)(\mathrm{d}\,r^2 + r^2\,\mathrm{d}\,{\Omega_2}^2) & \text{if } r \geq R_0/\bar{a}(t_0) \\ -\,\mathrm{d}\,\tau^2 + a^2(\tau)\left(\frac{1}{1-K\chi^2}\,\mathrm{d}\,\chi^2 + \sin^2\chi\,\mathrm{d}\,{\Omega_2}^2\right) & \text{if } \chi \leq \sin^{-1}(R_0/a(\tau_0)) \end{cases}, \quad (4.1)$$

[2]If A denotes the surface area of a sphere, the areal radius is defined as $\sqrt{A}/4\pi$. This definition is important because in the curved patch the proper distance from the origin is given by $a\chi$ in the curved chart, which does not match the areal radius.

where t and τ are the cosmic time for the flat and closed FLRW universes, r is the comoving radius defined in both charts, and χ the metric distance. By requiring the line elements inside and outside to match at time t_0, or $\bar{a}(t_0) = a(\tau_0)$ and $\left(\frac{\mathrm{d}\,\bar{a}}{\mathrm{d}\,t}\right)_0 = \left(\frac{\mathrm{d}\,a}{\mathrm{d}\,\tau}\right)_0$ equivalently; since $a^3(1+w)\rho$ and $\bar{a}^3(1+w)\bar{\rho}$ are constant in time, then the two time coordinates are related by [74]:

$$(1+\delta_0)^{w/(1+w)}\bar{a}^{3w}\,\mathrm{d}\,\tau = a^{3w}\,\mathrm{d}\,t, \tag{4.2}$$

when $w > -1$, being w the equation of state parameter(cf. 2.14). Synchronizing these time coordinates at the initial time, $t_0 = \tau_0$ and comparing the Friedmann equation (2.11) of the background and perturbed metrics, we obtain:

$$K = \frac{8\pi G}{3}\bar{a}_0^2\bar{\rho}_0\delta_0 = \frac{8\pi G}{3}a_0^2\rho_0\frac{\delta_0}{1+\delta_0} \quad \Leftrightarrow \quad \delta_0 = \frac{3K}{8\pi G\bar{a}_0^2\bar{\rho}_0} = \frac{3K}{8\pi G a_0^2\rho_0 - 3K}, \tag{4.3}$$

Plugging it back inside, it allows us to rewrite the first Friedmann equation for the perturbed patch as follows:

$$\left(\frac{\mathrm{d}\,a}{\mathrm{d}\,\tau}\right)^2 = \frac{8\pi G}{3}(\rho(\tau)a(\tau)^2 - \bar{\rho}_0\bar{a}_0^2\delta_0) = \frac{8\pi G}{3}\left(\rho(\tau)a(\tau)^2 - \rho_0 a_0^2\frac{\delta_0}{1+\delta_0}\right). \tag{4.4}$$

For the reason that background is extrinsically flat, the background density evolves as the critical density, so the evolution of the background quantities can be worked out to be:

$$\bar{a}(t) = \bar{a}_0\left(\frac{t}{t_0}\right)^{\frac{2}{3(1+w)}}, \quad \bar{H}(t) = \frac{2}{3(1+w)t}, \quad \bar{\rho}(t) = \frac{1}{6\pi(1+w)^2Gt^2}. \tag{4.5}$$

The specific evolution of the inner scale factor depends on the value of w, and finding an analytical solution is not straightforward. For the two cases of most interest—radiation and matter domination—it can be solved in terms of the conformal time in the inner patch $\mathrm{d}\,\tau = a(\eta)\,\mathrm{d}\,\eta$ [27]:

$$\begin{cases} a(\eta) = a_m(1-\cos\eta) & \text{for } w = 0 \quad \text{with } \tau = a_m(\eta+\sin\eta), \quad \eta \in [0, 2\pi] \\ a(\eta) = a_m\sin\eta & \text{for } w = 1/3 \quad \text{with } \tau = a_m(1-\cos\eta), \quad \eta \in [0, \pi] \end{cases}, \tag{4.6}$$

where a_m is the maximum value of the scale factor, at turnaround time when the scale factor stops expanding. Then, we can posit that every curved patch would start to collapse after some time t_m.

Instead of solving for the evolution of the density contrast in the inner patch, using cosmological perturbation theory, we consider it as a perturbation in background with the implicit assumption that its scale is much longer than the Jeans length, so that the contrasting pressure can be overcome. The Jeans radius is obtained at the crossover scale where the effects of gravity balance out the propagation of sound waves [55]: $\frac{32\pi G}{3}\bar{\rho}\delta = 2\frac{\dot{a}}{a}\dot{\delta} + c_s^2k^2\delta$. The Jeans length resulting is going to

be $\lambda_J = 2\pi/k$, and the Jeans radius is taken to be half of this value, which in our setting is more easily expressed as:

$$R_J = c_s\sqrt{\frac{3\pi}{8G\bar{\rho}}} = \frac{\sqrt{w}}{\bar{H}}. \tag{4.7}$$

Then, in the synchronous gauge δ the equations ((3.24)-(3.27) give:

$$\ddot{\delta} + \frac{4\dot{\delta}}{3(1+w)t} - \frac{2(1+3w)}{3(1+w)t^2}\delta = 0 \quad \Rightarrow \quad \delta(t) = At^{\frac{2(1+3w)}{3(1+w)}} + Bt^{-1}, \tag{4.8}$$

with A and B normalization constants. If we assume that the enough time has passed since the formation of the perturbation, so that the decaying part had time to become negligible by the time t_0, we get $\delta(t) = \delta_0(t/t_0)^{\frac{2(1+3w)}{3(1+w)}}$.The next assumption is that $\delta(t_m) \sim 1$ at turnaround time t_m, the moment in which the inner metric stops expanding and begin to collapse. This allows us to relate the turnaround time with t_0, and, as a result from the:

$$t_m \sim t_0\delta_0^{\frac{3(1+w)}{2(1+3w)}}, \quad R(t_m) \sim R_0\delta_0^{-\frac{1}{1+3w}}, \quad \bar{H}(t_m) \sim \bar{H}(t_0)\delta_0^{\frac{2(1+3w)}{2(1+3w)}}. \tag{4.9}$$

Finally, by imposing that the radius of the perturbation at turnaround time needs to be bigger that the Jeans length, $R(t_m) > R_J(t_m)$, to overcome the pressure, and smaller than the background Hubble scale, $R(t_m) < \bar{H}(t_m)^{-1}$, in order not to form a disconnected universe[3], we get [75]:

$$\frac{R_J^2}{R_0^2} < \delta_0 < \frac{R_{\bar{H}}^2}{R_0^2}. \tag{4.10}$$

As a final remark, in a radiation-dominated era($w = 1/3$), if the initial time is taken to be the time of re-entry from the super-Hubble regime($R_0 = \bar{H}_0^{-1}$), the initial density contrast is bound in the range $1/3 < \delta_0 < 1$, which we will refer to as Carr's bound.

Caveats of the simplistic model

The above limit, albeit very popular in the literature, presents a set of issues in its derivation, possibly due to its simplicity [76]. Due to the different evolution of the scale factors in the inner and outer patches, and the constancy of the extrinsic curvature K, the physical scale R_0 evolves faster in the flat universe patch than it does in the closed one, as shown in (4.1). This means that the evolution of the boundary radius should be followed in terms of the inner scale factor, a; however, this setting would still describe a top-hat distribution. Such a configuration, not only would be

[3]In its original derivation Carr denote this limit as the no-separate universe condition, which clashes with the nomenclature of the separate universe assumption described earlier in the text(3). In any case, the upper limit is better understood as the requirement that the collapse occurs inside the radius of causality, the Hubble scale.

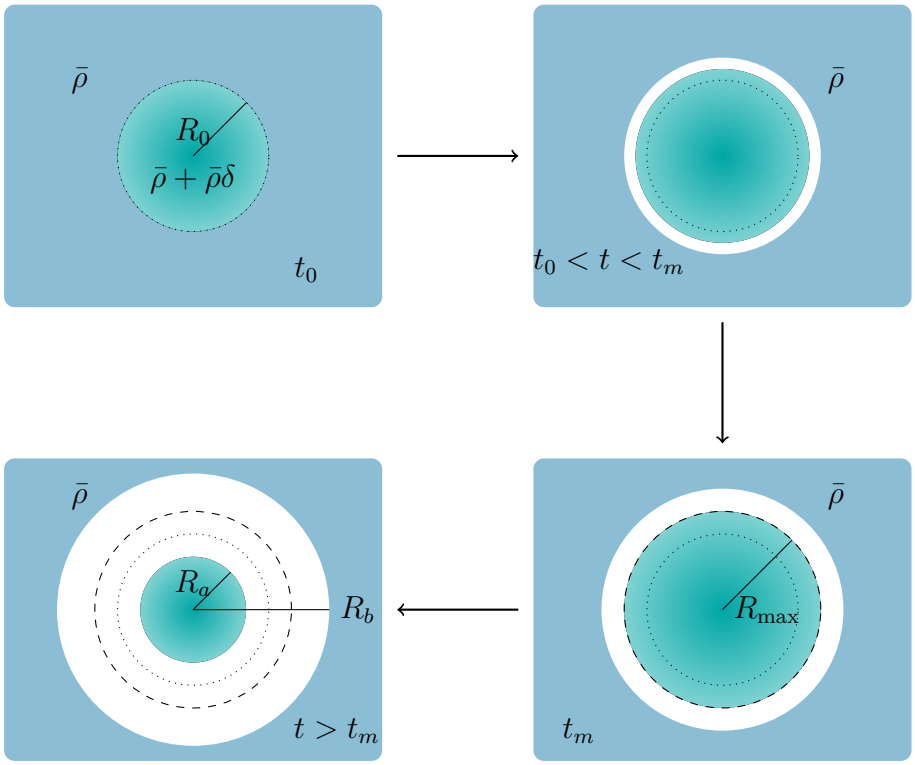

Figure 4.1. Following the evolution of the scale factors at later times, it appears like a region of vacuum surrounds the overdense core. This region is interpreted as an underdense region of width $W = R_b - R_a$ [77]. For small values of W strong pressure gradients will develop in this transition layer which can hinder the formation of the black hole.

quite artificial, but also it cannot account for the exact spatial flatness outside the perturbed region. In other words, there should be an underdense transition region that compensates the excess density in the core in order to reach asymptotically an exactly flat universe. Early numerical calculations [77] showed that the width of this region affects the formation of PBHs by creating pressure gradients inversely proportional to the core-boundary width.

Secondly, the cosmological perturbation theory breaks down well before the density contrast reaches the value of 1, so its evolution formula (4.8) is taken outside its range of validity. An alternative is represented by the application of gradient expansion to attack the non-linearities; indeed, recent numerical simulations prefer to resort to this method [78].

Another point deserving to be addressed more carefully is that the areal radius of the perturbed region, the line of demarcation between the extrinsically curved and flat patches, is obtained by cutting and gluing a closed universe model to the flat one at some comoving radius r_0. But since $r = \sin\chi$, for each value of r_0 there are two possible value of metric distance coordinate: χ_0 and $\pi - \chi_0$. Since, once a sphere is cut in two pieces, one can pick the lower- or the upper- dome; thence,

Kopp, Hofmann and Weller suggested there are two ways of choosing perturbations: those which $0 < \chi_0 < \pi/2$ (type I), and those for which $\pi/2 < \chi_0 < \pi$ (type II)[4] [79]. Using this argument, Kopp argued that the upper limit condition of Carr is too weak, and a stronger condition, geometric in nature, arises by asking that the $R_m < a_m$ and suggest a limit which is a factor π smaller than the condition that the universe stay connected. As a result, formation of PBHs in radiation-domination phase would be strongly suppressed if one insists in using δ as a determiner of the range[5]; instead, they advocate for the use of primordial curvature perturbation to characterize the PBHs formation range.

To address this issue, Carr and Harada repeated the calculation using a different formalism [76], where they used the method of auto-solutions. This consist in the observation that for any perfect fluid satisfying the continuity equation (2.13), then the quantity ρa^n is a constant in time when $n = 3(1+w)$. The Friedmann equation for the inner patch can be rearranged as follow:

$$\left(\frac{\dot{a}}{a}\right)^2 = \frac{8\pi G}{3}\rho - \frac{1}{a^2} \quad \Rightarrow \quad \dot{a}^2 = C_1 a^{-(1+3w)} - C_2, \tag{4.11}$$

with C_1 and C_2 are two constant quantities with respect to time:

$$C_1 = \frac{8\pi G}{3}\rho(t_0)a_0^{3(1+w)} = \dot{a}_0^2\Omega_0 a^{1+3w}, \quad C_2 = 1 = \dot{a}_0^2(\Omega_0 - 1). \tag{4.12}$$

Here $\Omega = 8\pi G\rho/3H^2 = (1+\delta)(\bar{H}/H)^2$ is the density parameter, that can be regarded as the specification of the initial amplitude of the perturbation[6].
At this point, one can define the proper radius $L = a\chi$ and follows its evolution up to turnaround time, where $a_m = (C_2/C_1)^{1/(1+3w)}$. Therefore, we have that:

$$L_m = a_m\chi_0 = a_0\chi_0\left(\frac{\Omega_0}{\Omega_0 - 1}\right)^{1/(1+3w)} = L_0(1+\delta_0)^{1/(1+3w)}. \tag{4.13}$$

Then, since the metric distance takes values between 0 and π, the PBHs can form if this distance is in the range $R_J < L_m < \pi a_m$; which can be reconverted to the original Carr's bound.

To conclude, I want to point out that if R_0 is chosen to be the Hubble scale of the background—meaning that we start to follow the perturbation at Hubble reentry—then the comoving radius r_0 is unambiguously fixed:

$$r_0 = \frac{R_0}{\bar{a}_0} = \dot{\bar{a}}_0 = \frac{3(1+w)}{2}t_0, \tag{4.14}$$

[4]The limiting cases $\chi_0 = 0$ and $\chi_0 = \pi$ correspond to the case of no perturbation, this can be understood as the closed universe is completely disconnected from the flat one up to a point.

[5]Nonetheless, they argue that this does not constraint the formation of PBHs, which for type II perturbations can happen even if part of the initial universe detach to form another closed universe, in their point of view.

[6]The subscript zero refers to the initial time t_0 and it is not related to the present time density parameter of ΛCDM.

depending only on the initial time t_0 and the equation of state variable. This tells us that PBHs cannot be described by this picture in a vacuum dominated epoch, $w = -1$, and (4.10) should not apply in such case.

The choice of Jeans radius and gauge

The previous analysis shows that there are still open issues with this specific way of modeling the perturbation, and further investigation are needed. The possibility that type II PBHs—producing a detached close universe []—may form leaded to the reinterpretation of the range for the density contrast as a range for its threshold value δ_c leaving opened the issue of this second, more exotic kind of black holes [76]. We will see in the next section how this threshold should be better understood. Before moving on to that topic, we think it is necessary discuss further the question of the threshold for type I PBHs; because, even if the problems raised earlier were fairly technical; another couple of points needs to be scrutinized and they bear a more physical character.

To begin with, the choice of the Jeans radius in equation (4.7) has been derived for the $K = 0$ metric; nevertheless, the perturbation is defined on the extrinsically curved metric. The gist of the problem is that several formulae has been presented in [80] and it is not clear what relation should be used for describing the competition between the contrasting effects of gravity against pressure. In line of principle, the Jeans length has been chosen to characterize the lower-bound without having to resort to the detailed description of the microscopic physics coming into play. Yet, the aforementioned formula was derived for the flat, radiation dominated, background spacetime, and later generalized to suit equations of state of the form $p/\rho \propto w$ [80]. For this reason, one could expect a different formulation for the interior of the perturbation, due to the fact that the formula (4.7) does not account for the extrinsic curvature.

Some alternative ways to calculate the Jeans radius have been proposed by Harada, Yoo and Kohri [81]; thus, altering the lower threshold of the allowed range for the formation of PBHs. Pressure gradients will force the overdensity away from the center; equivalently, the outgoing pressure can be characterized by the propagation of sound waves in the overdense medium. Therefore, if sound waves have time to propagate out of the overdense region before fluctuations collapse to a black hole, then the fluctuation distribution would be dispersed and the black hole would not form. Comparing th time a sound wave takes to reach the border of the overdense region with the time from turn-around to the total collapse into a point in a closed universe, the Jeans radius can be defined as:

$$R_J = a_{\max}\frac{1}{\sqrt{K}}\sin\frac{\pi\sqrt{Kw}}{1+3w} \quad \Rightarrow \quad \delta_c = \frac{R_J^2}{R_0^2} = \frac{1}{K}\sin^2\frac{\pi\sqrt{Kw}}{1+3w}, \tag{4.15}$$

which was originally provided in [81] for the case $K = 1$. In addition to this criterion, they also proposed a stronger and a weaker criteria. The first is obtained by asking

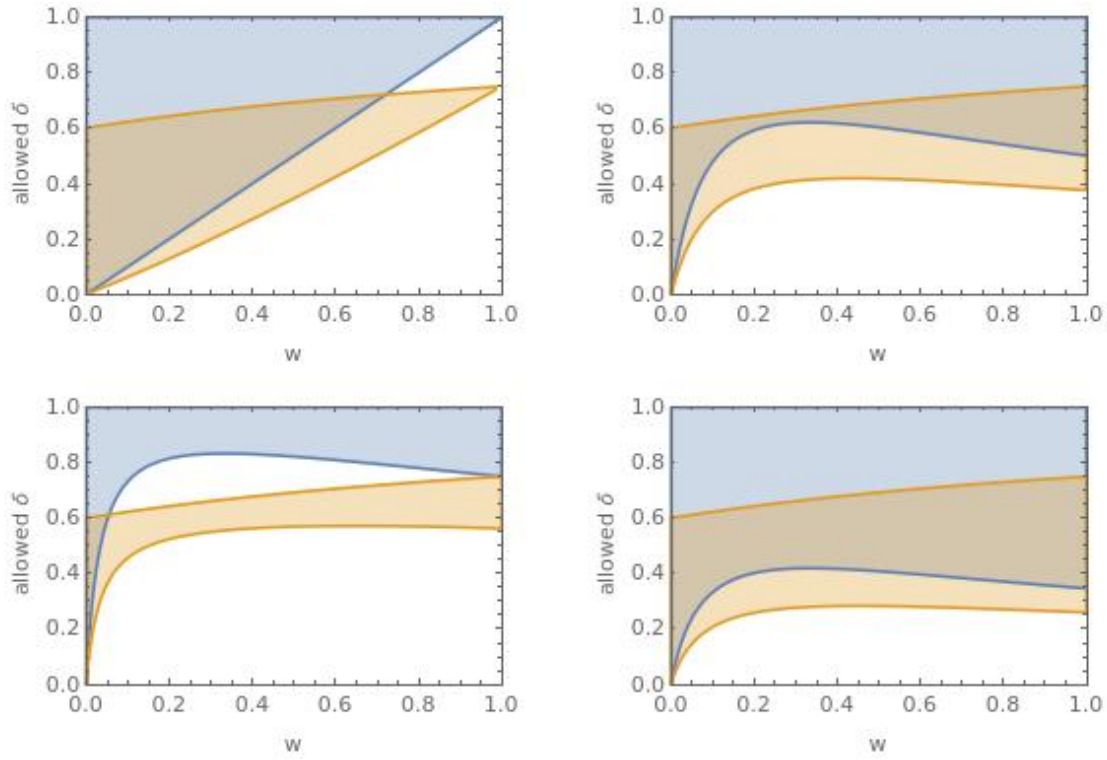

Figure 4.2. In the picture we can observe the allowed range for the critical density as a function of the equation of state, $\bar{p} = w\bar{\rho}$, in uniform Hubble gauge(blue) and in comoving gauge(orange). Different graphics refer to different definitions of the Jeans radius: the one used by Carr (4.7)—top left, the one obtained from the criterion imposing the sonic wave not to leave the perturbed region (4.15)—top right, and its stronger and weaker criteria (4.16)—bottom left and rigth.

that the distance along which the sound wave travels from the center should not exceed the radius of the future apparent horizon of the black hole. The weaker criterium is given upon the request that black hole horizon forms before a sound wave had time to travel from the edge the overdensity inward, and once it gets reflected by the center, out of the perturbation edge again [81]:

$$\delta_{c,\text{strong}} = \sin^2 \frac{2\pi\sqrt{w}}{1+2\sqrt{w}+3w}, \qquad \delta_{c,\text{weak}} = \sin^2 \frac{\pi\sqrt{w}}{1+\sqrt{w}+3w}. \tag{4.16}$$

Regardless of the way one choose to define the threshold, there is one last sensitive aspect that needs to be taken into account: the fact that neither the extrinsic curvature, nor the density contrast are gauge-invariant quantities; by the same token, the bounds of the allowed range are affected by the gauge choice. Earlier we assumed that the evolution of the density profile is attained in synchronous gauge [82]; the condition that Hubble parameter of the inner patch matches the Hubble parameter of the background at initial time is equivalent of choosing a gauge where the Hubble parameter is uniform(uniform Hubble gauge)[83], and the homogeneity of extrinsic

curvature is entailed in the Constant Mean Curvature(CMC) gauge [84]. Evolution of the density contrast is the same in these three gauges, but it differs in comoving gauge. The density contrast in comoving gauge, $\delta^{\rm COM}$ can be related to the density contrast in uniform Hubble gauge [81]:

$$\delta^{\rm COM} = \frac{3(1+w)}{5+3w}\delta(t_*)\left(\frac{R_{\bar{H}}}{R}\right)^2, \tag{4.17}$$

where t_* stands for the Hubble-crossing time, and $R_{\bar{H}}/R$ defines the relative size of the overdensity with respect to Hubble scale in the background. In comoving gauge, a time-independent density contrast can be defined in combination with the last quantity [81]:

$$\tilde{\delta} = \delta^{\rm COM}\left(\frac{R_0}{R_{\bar{H}}}\right)^2, \tag{4.18}$$

on which the bounds are conveniently derived in this gauge. This effectively implies that bounds one obtains in the comoving gauge are a factor $3(1+w)/(5+3w)$ smaller with respect to those in uniform Hubble gauge, as explicitly shown in figure (4.2). Note that if $R_0 = R_{\bar{H}}$ in this slicing, than $\tilde{\delta} \equiv \delta^{\rm COM}$; however, since the gauge changed this is no longer valid.

Numerical models: Critical Collapse

Albeit simplistic, one important conclusion can be drawn from Carr's model: since the allowed range for density contrast is of order of unity, we can expect that the mass of a PBH formed with this mechanism comes as a fraction of the Hubble mass $M_{\rm H} = \frac{4\pi}{3}\frac{\bar{\rho}}{\bar{H}^3}$—the mass contained inside the Hubble sphere assuming the density is the same of the flat spacetime. Indeed, it can be seen that:

$$M_{\rm PBH} = \frac{4\pi}{3}\bar{\rho}(t_c)\Big(1+\delta(t_c)\Big)R(t_c)^3 \propto \bar{\rho}_0 R_0^3 = M_{\rm H}, \tag{4.19}$$

under the assumption that the initial radius corresponds to the Hubble scale and that $t_c \approx t_m$ is the time at which the collapse happens.

To reinforce this conclusion, we now present the results of Choptuik [85]and Niemeyer & Jedamzik [86][87]. The first studied numerically the gravitational collapse of a massless scalar field ϕ immersed in a spherically symmetric time-dependent spacetime:

$$\mathrm{d}\,s^2 = -\alpha(r,t)^2\,\mathrm{d}\,t^2 + a(r,t)^2\,\mathrm{d}\,r^2 + r^2\,\mathrm{d}\,{\Omega_2}^2. \tag{4.20}$$

The Einstein equations, $G_{\mu\nu} = 8\pi(\phi_{;\mu}\phi_{;\nu} - 1/2 g_{\mu\nu}g^{\lambda\eta}\phi_{;\lambda}\phi_{;\eta})$, can be simplified upon the introduction of two generalized momenta: $\Phi(r,t) \equiv \phi_{,r}$ and $\Pi(x,t) \equiv a\phi_{,t}/\alpha$, so that the dynamics of the field can be described by the following set of equations:

$$\begin{aligned} &\Phi_{,t} = \left(\frac{\alpha}{a}\Pi\right)_{,r}, \qquad \Pi_{,t} = \frac{1}{r^2}\left(r^2\frac{\alpha}{a}\Phi\right)_{,r}, \qquad \frac{\alpha_{,r}}{\alpha} - \frac{a_{,r}}{a} + \frac{1-a^2}{r} = 0, \\ &\frac{a_{,r}}{a} + \frac{a^2-1}{2r} - 2\pi r(\Pi^2+\Phi^2) = 0, \qquad \frac{a_{,t}}{\alpha} - 4\pi r\Phi\Pi = 0. \end{aligned} \tag{4.21}$$

One can choose a numerical scheme in which the only quantity to evolve in time is the scalar field by using just the first four equations, so that a and α are numerically integrated form it at each step, and the fifth equation is a physical constraint that it is used to check the reliability of the computations.

In [85], it is also noted that these equations are invariant under arbitrary rescaling of time and radial coordinates by a positive constant k; hence, embodying a spacetime lacking a characteristic length scale. This was instrumental to understand that the formation of a black hole behaves as a critical phenomenon; id est following the evolution in phase space—the set of all possible initial data, in which every point is just a constant-time slice of the spacetime— trajectories evolve toward two fixed points: one representing a flat Minkowski spacetime, or the other representing a spacetime with a black hole. Because in the latter case, we have the emergence of a characteristic scale which is given by the black hole horizon; in turn, this implies the existence of a critical surface in phase space, characterized by a parameter p^*. Given $\mathcal{S}[p]$ a family of solutions depending continuously on the parameter p, then evolution will eventually converge toward the Minkowski critical point for $p < p^*$, or it will end up close to black hole spacetime for $p > p*$ [88]. The nature of this surface is universal, meaning that is independent of the specific form of ϕ's initial profile, and it presents a scaling behaviour, that becomes apparent in the form of a power-law for the mass of the resulting black hole:

$$M_{\rm BH} \simeq C(p - p^*)^{\gamma}, \tag{4.22}$$

where C and p^* depend on the particular choice of the initial family of profiles, meanwhile $\gamma \simeq 0.374$ is a universal exponent, profile-independent. The simplicity of this model makes it rather unsuitable for applications to stellar black holes, because the massless scalar field is not a good representation of the physics of virialization and quantum-mechanical interactions as they naturally introduce scales that invalidate the initial assumptions. However, it gave the idea that a critical surface might exist in the phase space and it motivated its search in numerical models.

Following this result, Niemeyer and Jedamzik went on to investigate the near-critical collapse of PBHs forming in a radiation dominated universe [86]. They argued that, for perturbations re-entering the Hubble sphere, the particular coincidence of scales provides the degree of fine-tuning required for the model to apply. They took into account three profiles for the perturbed energy density ρ:

$$\begin{aligned}
&\text{A)} && \rho(R) = \bar{\rho}\left[1 + A\exp\left(-\frac{R^2}{2(R_{\rm H}/2)^2}\right)\right], \\
&\text{B)} && \rho(R) = \bar{\rho}\left[1 + A\left(1 - \frac{R^2}{R_{\rm H}^2}\right)\exp\left(-\frac{3R^2}{2R_{\rm H}^2}\right)\right], \\
&\text{C)} && \rho(R) = \bar{\rho}\left[1 + \frac{A}{9}\left(1 - \frac{R^2}{R_{\rm H}^2}\right)\left(3 - \frac{R^2}{R_{\rm H}^2}\right)^2\theta\left(\sqrt{3}R_{\rm H} - R\right)\right],
\end{aligned} \tag{4.23}$$

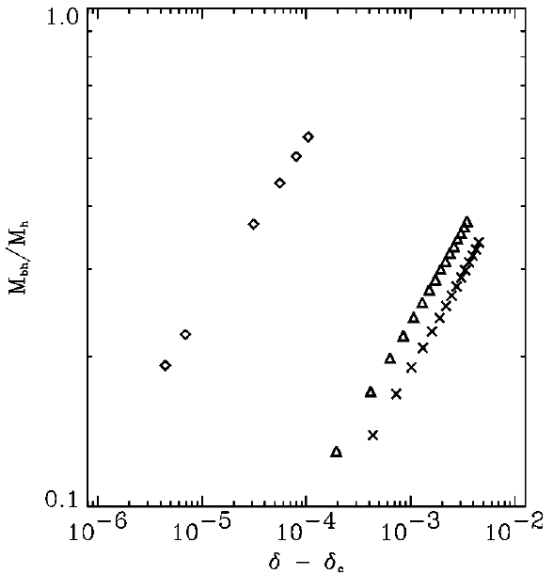

Figure 4.3. The results obtained in [86] for the different profiles: A) diamonds $\gamma_c = 0.34$, $K = 11.9$, $\delta_c = 0.7015$; B) triangles $\gamma_c = 0.36$, $K = 2.85$, $\delta_c = 0.6745$; C) crosses $\gamma_c = 0.37$, $K = 2.39$, $\delta_c = 0.7122$. The parameter δ was chosen to be the total mass excess for the Gaussian perturbation, the mass excess contained inside the Hubble sphere for the mexican-hat profile, and the perturbation amplitude for the polynomial case.

corresponding to A) a gaussian , B) a mexican-hat and C) a polynomial profiles for the perturbation. They numerically evolved the profiles varying the parameter A as to input different initial conditions, and so they managed to corroborate the PBHs mass follows a critical law:

$$M_{\mathrm{PBH}} = K(\delta - \delta_c)^{\gamma_c} M_{\mathrm{H}}, \tag{4.24}$$

at least for small values of the order parameter $\delta - \delta_c$. In order to fit the law so as to obtain approximately the same value of γ_c for different profiles, δ was chosen in different ways and datasets shown in Figure 4.3. The justification for why the power law is followed on a narrow range above the threshold δ_c is that PBHs forming closer to it develop a compression wave traveling outward and preventing further accretion. On the contrary, getting further from δ_c, the initial mass is high enough that surrounding material keeps falling into the horizon. All things considered, the choice of initial time when perturbations were well within the Hubble radius, was considered to be a weak point by following studies that, even if accepted the results, kept investigating the threshold. For instance, Musco, Miller and Rezzolla [89] reprised this work by including possible effects of the cosmological constant Λ. Eventually, they found that affects critical exponent and threshold as follow:

$$\begin{aligned} \gamma_c(\Lambda) &\simeq \gamma_c(0) - 8.3y \\ \delta_c(\Lambda) &\simeq \delta_c(0) + 0.98y, \end{aligned} \tag{4.25}$$

being $y = 4\Lambda M_{\rm H}^2/3$ the ratio between vacuum energy and the total energy inside the Hubble sphere. In other words, a positive cosmological constant would hinder the formation of PBHs. Yet, in a later paper [90] Musco and Miller commented that such modification of γ_c disappears around smaller values of $\delta - \delta_c \sim 10^{-3}$, and they justified it with the rationale that smaller mass implies higher compactness. So the effects of the cosmological constant again becomes negligible against the density of the collapsing fluctuation.

These results verified that the mass of a PBH should be indeed proportional to the mass contained in the Hubble sphere at the re-entry of the perturbation, but they also hint that the mass at which PBHs form could be very small, if the initial fluctuation is very close to the critical value.

Numerical models: Quasi-homogeneous formation

The studies we have presented this far evince that, for perturbations to clump into PBHs, the critical density must overcome a threshold value δ_c. Complications arising from different grounds hint that this parameter do not unambiguously provides a criterion for discriminating between density fluctuations that will eventually collapse and those which will not. As emphasized earlier, solutions of the Friedmann equations are difficult to find in a closed form, but for a limited number of models with specific parameters.One way to skirt the non-linearity of Einstein equations, is to recur to numerical simulations, to investigate how different initial conditions lead to the formation of a apparent horizon. Numerical models follow the evolution of a grid of characteristic lines; these are often chosen to be null geodesics, and follows their evolution.

Under the assumption of spherical symmetry, it is possible to set the problem in a way in which the Einstein's equations are expressed in a general relativistic hydrodynamics form, and describe the evolution of spacetime as a fluid. Fluid-dynamics can be formulated in two pictures: Lagrangian picture which refers to a frame in which coordinates follow the fluid, and Eulerian picture that fixes the coordinates with respect some arbitrarily chosen point—usually chosen to be the center of mass—and traces the evolution with respect to it[7].

Let us start by casting the metric in Lagrangian coordinates, corresponding to comoving coordinates in a cosmological context [91]:

$$\mathrm{d}\, s^2 = -A(r,t)^2\, \mathrm{d}\, t^2 + B(r,t)^2\, \mathrm{d}\, r^2 + R(r,t)^2\, \mathrm{d}\, {\Omega_2}^2, \tag{4.26}$$

where R plays the role of the Eulerian radius, which coincide with the areal radius introduced earlier. Next, we define U and Γ two quantities that express the comoving proper time- and radial-rate of change of the a spherical shell of Eulerian radius [92]:

$$U = A^{-1} R_{,t} \qquad \Gamma = B^{-1} R_{,r}, \tag{4.27}$$

[7] One mnemonic trick is: Lagrange likes to study the fluid while afloat; meanwhile, Euler watches him from the bridge.

The parameter U measures the radial speed of the fluid with respect to the center of coordinate, or equivalently how a point at fixed areal radius moves with respect to the center of mass. The other parameter can be considered as a generalization of the Lorentz factor of flat spacetime. Within this formalism, it is convenient to introduce a function of the comoving radius and time: the so-called Misner-Sharp-Hernandez (MSH)-mass[8]:

$$m(r,t) = 4\pi \int_0^r dr' \rho(r',t) R^2(r',t) R_{,r}(r',t), \tag{4.28}$$

which can be interpreted as a measure of mass inside a sphere of areal radius R at given time [94]; this quasi-local behaviour comes in handy to explore the formation of apparent horizons. These 3 quantities are related by the constraint equation [95]:

$$\Gamma^2 = 1 + U^2 - \frac{2Gm}{R^2}. \tag{4.29}$$

which is a first integral, and it might slightly deviate from the equality while running the numerical computation, but it serves the purpose of checking the accuracy of the simulation. At a given point of comoving radius r, the formation of the black hole can be checked by looking when $2m/R = 1$ and $U < 0$, or equivalently when $U + \Gamma = 0$. Similarly, if a spacetime point has $2m/R > 1$ and $U < 0$, then that point is situated inside the black hole horizon [96]. By the same token, one can locate the Hubble radius by looking when when $2m/R = 1$ and $U > 0$.

From Einstein's equations and the conservation of energy-momentum tensor, setting also $G = 1$, we obtain the hydro-dynamical equations of motion [95]:

$$\frac{\Gamma_{,t}}{A} = \frac{-U}{\rho + p} \frac{p_{,r}}{B}, \tag{4.30}$$

$$\frac{\Gamma_{,r}}{B} = \frac{-U}{\rho + p} \frac{\rho_{,r}}{A} + \frac{m}{R^2} - \frac{2U^2}{R} - 4\pi\rho, \tag{4.31}$$

$$\frac{U_{,t}}{A} = \frac{-\Gamma}{\rho + p} \frac{p_{,r}}{B} - \frac{m}{R^2} - 4\pi p R, \tag{4.32}$$

$$\frac{U_{,r}}{B} = \frac{-\Gamma}{\rho + p} \frac{\rho_{,t}}{A} - \frac{2u\Gamma}{R}, \tag{4.33}$$

$$m_{,t} = -4\pi p R^2 R_{,t}, \tag{4.34}$$

$$m_{,r} = -4\pi \rho R^2 R_{,r}, \tag{4.35}$$

$$A_{,r} = -\frac{p_{,r}}{\rho + p}, \tag{4.36}$$

$$B_{,t} = -\frac{\rho_{,t}}{\rho + p} - \frac{4R_{,t}}{R}. \tag{4.37}$$

The combination these equations with the equation of state allows to follow numerically the evolution of a grid of past- and future-directed null geodesics. In order

[8] This mass function can be presented in two distinct formulations: the Misner-Sharp formulation [92], or the Hernandez-Misner formulation when the time coordinate is replaced with the outgoing null coordinate [93]; equivalent to the null slicing of spacetime.

to perform such a computation, it is necessary to specify some initial conditions of the perturbation at some initial time; but particular attention should be put on how to impose these conditions: the perturbation size should be larger than the Hubble scale so to agree with the predictions from the inflationary arguments. This is especially important because, if the perturbation contains a decaying component, this might blow up close to initial time inducing spurious effects [97].

Numerical evolution will break down if either the characteristics cross the apparent horizon, in which case one chooses radial coordinates to define the mesh [95], or if parallel characteristics self-intersect, as though a shock forms. The latter problem had been addressed by the introduction of a viscosity parameter, that would impede the overlap; however, this scheme has been deplored because it introduces spurious quantities [98]. Both of these numerical difficulties can be alleviated by utilizing an Adaptive Mesh Refinement—which reduces the characteristics spacing close to regions where the spatial derivative become large—and by switching to null slicing, i.e. a foliation of spacetime along geodesics of outgoing null rays [99]:

$$F(u,r)\,\mathrm{d}\,u = A(r,t)\,\mathrm{d}\,t - B(r,t)\,\mathrm{d}\,r. \tag{4.38}$$

The quantity u is also referred as observer-time because it describe the time on the reference of a photon reaching an observer outside of the horizon. This requires to reformulate (4.30)-(4.37) in terms of the Hernandez-Misner formulation which, however, contains the same physics and shall be not be analyzed here.

The role of extrinsic curvature

Earlier we briefly commented on the fact that the extrinsic curvature is not gauge invariant, and since the numerical models are most conveniently set in the comoving gauge, we will now introduce a model in which it becomes a function of the comoving radius $K(r)$, and act directly as a source for the density fluctuations. This is the quasi-homogeneous model originally due to Polnarev and Musco [78]. Although it is not the first numerical models, it was the first to implement the gradient-expansion perturbation theory, and thus revived the research interests setting a new standard.

First of all, in this formalism, we set the description for the background by comparing the metric (4.26) with the flat Friedmann (2.6). Thence, we have:

$$\begin{aligned} \mathrm{d}^2\,s &= \begin{cases} -\bar{A}(r,t)^2\,\mathrm{d}\,t^2 + \bar{B}(r,t)^2\,\mathrm{d}\,r^2 + \bar{R}(r,t)^2\,\mathrm{d}\,\Omega^{\,2} \\ -\,\mathrm{d}\,t^2 + \bar{a}(t)^2(\mathrm{d}\,r^2 + r^2\,\mathrm{d}\,\Omega^{\,2}) \end{cases} \\ \Rightarrow \quad & \bar{A}(t,r) = 1, \qquad \bar{B}(t,r) = \bar{a}(t), \qquad \bar{R}(t,r) = r\bar{a}(t). \end{aligned} \tag{4.39}$$

As a result, we get $\bar{U} = \bar{H}\bar{R}$, which is equivalent to Hubble law, and $\bar{\Gamma} = 1$. For the reason that we are using comoving coordinates, the density contrast corresponds to the comoving density contrast Δ introduced in the setting of cosmological perturbation theory, but this does not prevent us to tackle the problem with the separate universe approach(cf. 3).

Now for the perturbed spacetime, we compare (4.26) with the Friedmann metric for positive value of extrinsic curvature:

$$\begin{aligned} \mathrm{d}^2 s &= \begin{cases} -A(r,t)^2\,\mathrm{d}\,t^2 + B(r,t)^2\,\mathrm{d}\,r^2 + R(r,t)^2\,\mathrm{d}\,\Omega^{\,2} \\ -\,\mathrm{d}\,t^2 + \bar{a}(t)^2\Big(\frac{1}{1-K(r)r^2}\,\mathrm{d}\,r^2 + r^2\,\mathrm{d}\,\Omega^{\,2}\Big) \end{cases} \\ \Rightarrow \quad & A(t,r) = 1, \qquad R(t,r) = \bar{a}(t)r \qquad B(t,r) = \frac{R_{,r}}{\sqrt{1-K(t,r)r^2}}. \end{aligned} \tag{4.40}$$

With an eye on the gradient-expansion, we also compare the perturbed metric to the one (3.50) of the separate universe approach. In doing so, we must be careful in not to mix the coordinates of the two slicings:

$$\begin{aligned} \mathrm{d}^2 s &= \begin{cases} -A(\hat{r},t)^2\,\mathrm{d}\,t^2 + B(\hat{r},t)^2\,\mathrm{d}\,r^2 + R(\hat{r},t)^2\,\mathrm{d}\,\Omega^{\,2} \\ -\,\mathrm{d}\,t^2 + \bar{a}(t)^2 e^{2\zeta(\hat{r})}(\mathrm{d}\,\hat{r}^2 + \hat{r}^2\,\mathrm{d}\,\Omega^{\,2}) \end{cases} \\ \Rightarrow \quad & A(t,\hat{r}) = 1, \qquad R(t,\hat{r}) = \bar{a}(t)e^{\zeta(\hat{r})}\hat{r} \qquad B(t,\hat{r}) = R/\hat{r}, \end{aligned} \tag{4.41}$$

where we denoted with $\hat{r}$ the radial coordinate for constant density slices. By comparison, we can derive the relation between the two radial coordinates: $r = \hat{r}e^{\zeta}$ and $(1-K(r)r^2)^{-1/2}\,\mathrm{d}\,r = e^{\zeta}(1+\hat{r}\zeta_{,\hat{r}})\,\mathrm{d}\,\hat{r}$, whence comes the relation between the extrinsic curvature to the primordial curvature perturbation:

$$K(r)r^2 = -\hat{r}\zeta_{,\hat{r}}(\hat{r})\Big[2 + \hat{r}\zeta_{,\hat{r}}(\hat{r})\Big]. \tag{4.42}$$

The no-disconnected universe condition of Carr's [75], which corresponds to the line of demarcation between type I and II types of density fluctuations for Kopp [79], can be reinterpreted in this formalism as the requirement that the $B(r,t)$ coefficient of the metric in (4.40) remains a real number, or again, that the metric remain positive definite. This translates into a bound for the extrinsic curvature or the primordial curvature perturbation profiles [100]:

$$K(r) < \frac{1}{r^2} \quad \text{or} \quad \zeta_{,\hat{r}}(\hat{r}) < -\frac{1}{\hat{r}}. \tag{4.43}$$

Furthermore, it is possible to distinguish between compensated— in which the overdensity(underdensity) is surrounded by underdensity(overdensity):

$$4\pi\int_0^\infty dr(\rho-\bar{\rho})r^2 = 0 \quad \Rightarrow \quad \lim_{r\to\infty} K(r)r^3 = 0 \quad \text{or} \quad \lim_{r\to\infty}\zeta(\hat{r})\hat{r} = 0, \tag{4.44}$$

or uncompensated profiles for which the two parameters asymptotically behave as $K(r)\sim r^{\alpha}$ and $\zeta(\hat{r})\sim\hat{r}^{\beta}$, with $-3\leq\alpha<2$ and $-1\leq\beta<0$; resulting in a non-flat universe on regions far from the perturbation.

Quasi-homogeneous solution in the gradient expansion

To discuss the solution of the MSH formalism together in the fashion of the gradient expansion, we introduce the time-dependent $\varepsilon(t) = 1/a(t)\bar{H}(t)r_k$, where r_k is the

comoving scale associated to the perturbation of wavelength k in momentum space []. In this way, the parameter fixes simultaneously the physical scale of and the time evolution of the system:

$$\frac{\dot{\varepsilon}}{\varepsilon} = \frac{1+3w}{2}\bar{H}(t). \tag{4.45}$$

Recalling that, within this approach, the metric evolves as the background solution up to second order; thus, we can perturb the parameters as follows [100]:

$$A = 1 + \varepsilon^2 \widetilde{A}, \tag{4.46}$$

$$B = \frac{\bar{a}(t)}{\sqrt{1 - K(r)r^2}}(1 + \varepsilon^2 \widetilde{B}) = a(t)e^{\zeta(\hat{r})}(1 + \varepsilon^2 \widetilde{B}), \tag{4.47}$$

$$R = \bar{a}(t)r(1 + \varepsilon^2 \widetilde{R}) = a(t)e^{\zeta(\hat{r})}\hat{r}(1 + \varepsilon^2 \widetilde{R}).\text{,} \tag{4.48}$$

$$\rho = \bar{\rho}(1 + \varepsilon^2 \widetilde{\rho}), \tag{4.49}$$

$$U = \bar{H}R(1 + \varepsilon^2 \widetilde{U}), \tag{4.50}$$

$$m = \frac{4\pi}{3}\bar{\rho}(t)R^3(1 + \varepsilon^2 \widetilde{m}). \tag{4.51}$$

The $\sim$ cap stands for the first-order quantities in the gradient expansion; virtually different from the first order perturbations of Cosmological Perturbation Theory. Since pressure is directly connected to density, pressure gradients are negligible ($\mathcal{O}(\varepsilon^4)$) in this approach when $\varepsilon \ll 1$. As a result, the equation of state maintains its form $p = w\rho$. The constraint equation (4.29) gives us the first link among the perturbations and the first connection among the curvature profile and the perturbations parameter:

$$K(r) = \bar{a}^2\bar{H}^2\varepsilon^2(\widetilde{m} + \widetilde{U}) \quad \Rightarrow \quad K(r)r_k^2 = \widetilde{m} + \widetilde{U}. \tag{4.52}$$

By the same token, perturbing Einstein equations, we attain how the growing modes of density and velocity perturbations depend on the curvature profile to the $\mathcal{O}(\varepsilon)$ order of the gradient expansion [100]:

$$\widetilde{\rho} = \frac{3(1+w)}{5+3w}\frac{(r^3K(r))_{,r}}{3r^2}r_k^2 = -\frac{2(1+w)}{5+3w}\frac{e^{2\zeta(\hat{r}_k)}}{e^{2\zeta(\hat{r})}}\left[\nabla^2\zeta(\hat{r}) + \frac{1}{2}\zeta_{,\hat{r}}(\hat{r})^2\right]\hat{r}_k^2, \tag{4.53}$$

$$\widetilde{U} = -\frac{1}{5+3w}K(r)r_k^2 = -\frac{1}{5+3w}\frac{e^{2\zeta(\hat{r}_k)}}{e^{2\zeta(\hat{r})}}\zeta_{,\hat{r}}(\hat{r})\left(\frac{2}{\hat{r}} + \frac{\zeta_{,\hat{r}}(\hat{r})}{2}\right)\hat{r}_k^2, \tag{4.54}$$

which are the two most important perturbations, and could be expressed in terms of each other:

$$\widetilde{\rho} = -\frac{1+w}{r^2}(r^3\widetilde{U})_{,r}, \qquad \widetilde{U} = -\frac{1}{(1+w)r^3}\int r^2 dr\widetilde{\rho}. \tag{4.55}$$

Similarly we can write the lowest order expressions for the other perturbations as [100]:

$$\widetilde{A} = -\frac{w}{1+w}\widetilde{\rho}, \tag{4.56}$$

$$\widetilde{B} = \frac{w}{(1+3w)(1+w)}r\widetilde{\rho}_{,r}, \tag{4.57}$$

$$\widetilde{R} = -\frac{w}{(1+3w)(1+w)}\widetilde{\rho} + \frac{1}{1+3w}\widetilde{U}, \tag{4.58}$$

$$\widetilde{m} = -3(1+w)\widetilde{U}. \tag{4.59}$$

Moreover, density contrast of cosmological perturbation theory can be related to the gradient expansion quantities through $\delta = \varepsilon^2\widetilde{\rho} + \mathcal{O}(\varepsilon^4)$and the lowest orders of the two approaches coincide when ε is set to 1, at Hubble crossing time, giving:

$$\delta = \frac{3(1+w)}{5+3w}\left(\frac{1}{\bar{a}\bar{H}}\right)^2\frac{(r^3K)_{,r}}{3r^2} = -\frac{2(1+w)}{5+3w}\left(\frac{1}{\bar{a}\bar{H}}\right)^2 e^{-2\zeta}\left[\nabla^2\zeta + \frac{1}{2}(\nabla\zeta)^2\right], \tag{4.60}$$

which has the advantage of connecting the density contrast with the primordial curvature perturbation.

The numerical evolution can then be launched: initial conditions are assigned on space-like slices at times larger than the Hubble crossing time, a typically when $\varepsilon \sim 10^{-2}$. The simulations generates a set of data according to the Misner-Sharp equations, which are used to initialize the Hernandez-Misner evolution for the null-slicing evolution. The perturbations grow initially, but slower than the Hubble horizon and start to compactify once they re-entered the horizon [90]. Depending on the steepness of their profiles, they might generate pressure gradients that, if large enough, generates voids or outward-propagating waves, thus hampering further collapse; this kind of behaviour is mostly followed by subcritical perturbations. Nonetheless, as the critical region is approached, perturbations generally shrink to a region of high compactness, and might settle to such a stage for long times without collapsing further and then disperse back into the background. Still, this interplay of growing and decaying modes, when perturbations are supercritical, eventually reach the point in which the black hole is formed [90]. This is similar to the observation discussed earlier from the work of Niemeyer and Jedamzik [87] that PBHs forming slightly above the critical threshold emit a shock wave screening them from subsequent accretion from the background.

The unequivocal footprint of formation of a PBH in the simulation is provided by a region in which the parameter $U(t,r)$ becomes negative together with the freezing of the lapse function $F(u,r) = 0$, meaning that a region of space has become unable to be probed by outgoing null rays [78]. Additionally, the function $2m(r,t)/R(r,t)$ tends to unity, signaling the formation of an apparent horizon that tends to the event horizon, as shown in Figure 4.4.

Critical Parameters

In the previous paragraph, the use of the separate universe approach provided a solid framework for discussing the evolution of prior to the re-entry and estimate it initial amplitude. Now, we want to discuss some quantities that could be used

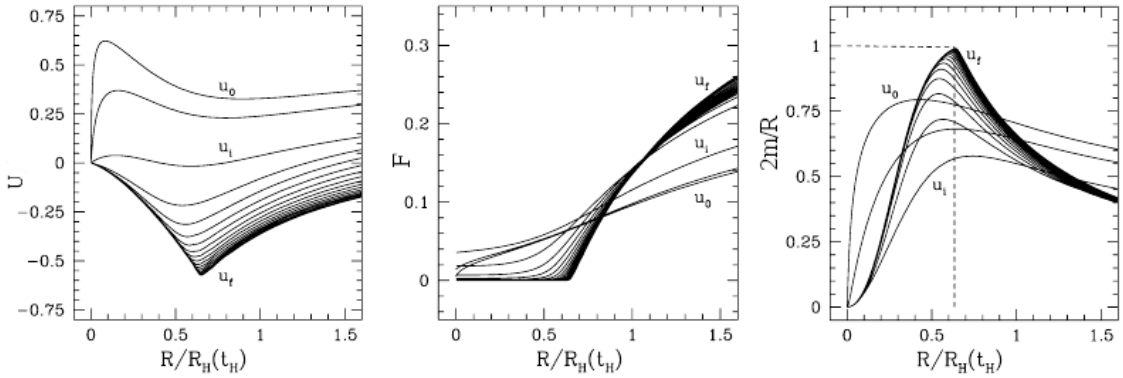

Figure 4.4. In the graphs, the evolutions of the Misner-Sharp-Hernandez functions U, F, $2m/R$ are shown from a initial configuration u_0, through an intermediate u_i and to the final formation of black hole u_f. The pictures are adapted form [78].

as critical parameters to assess whether initial conditions evolve into PBHs. Depending on the model, the extrinsic curvature profile can be parametrized by a several parameters and there is a considerable leeway for deciding which should be used to supply a criterion for the formation of PBHs. For instance, we shall use the compaction function $\mathcal{C}(r_m)$, the average density contrast $\tilde{\delta}(r_0)$ or the primordial curvature perturbation $\zeta(r_p)$ where r_p is the point where the scale at which the primordial curvature perturbation has a peak.

To quantify the amplitude of the whole perturbation one introduces the averaged mass excess inside a ball of radius R [90]:

$$\begin{aligned}\tilde{\delta}(r,t) &= \frac{1}{V}\int_0^R dR \int_0^{4\pi} d\Omega_2 \frac{\rho-\bar{\rho}}{\bar{\rho}} = \varepsilon^2(t)\frac{3(1+w)}{5+3w}K(r)r_k^2 + \mathcal{O}(\varepsilon^4) \\ &\simeq \left(\frac{1}{\bar{a}(t)\bar{H}(t)}\right)^2 \frac{3(1+w)}{5+3w}K(r),\end{aligned} \tag{4.61}$$

where $V = 4/3\pi R^3$ is the volume. We already came across this quantity in (4.18); in fact, this is its generalization for quasi-homogeneous models [100]. Yet, in order to gain full benefit out of this quantity, we also need to specify a scale for the perturbation size.

At this point, it comes in handy to define the compaction function $\mathcal{C}$, which firstly introduced in [97] as a supplementary parameter to constraint the PBH formation[9]:

$$\mathcal{C}(r,t) = \frac{2\delta m(r,t)}{R(r,t)}, \tag{4.62}$$

where $\delta m(r,t)$ is the mass excess enclosed within a spheres of areal radius $R(r,t)$. The compaction function turns out to be also very useful to characterize the extrinsic

[9]The original definition of this function was slightly different, being a factor 1/2 smaller, the provided definition follows from [100]

curvature. More explicitly, the mass excess is evaluated as the difference in MSH-mass between the perturbed universe and the background flat universe [101]; these two masses explicitly read as:

$$\begin{aligned} \bar{m}(r,t) &= \frac{1}{2}\bar{H}^2(t)\bar{a}^3(t)r^3, \\ m(r,t) &= \frac{3}{2}\bar{H}^2(t)\bar{a}^3(t)\int_0^r dr(1+\varepsilon^2(t)\widetilde{\rho}(r)) \\ &= \bar{m}(r,t) + \frac{3}{2}\bar{H}^2\bar{a}^3\varepsilon(t)^2\int_0^r drr^2\widetilde{\rho}(r). \end{aligned} \tag{4.63}$$

As a result, using (4.55) and (4.42) we can express the compaction function in terms of K and ζ:

$$\mathcal{C} = \frac{3(1+w)}{5+3w}K(r)r^2 = -\frac{3(1+w)}{5+3w}\hat{r}\zeta_{,\hat{r}}(\hat{r})\Big[2+\hat{r}\zeta_{,\hat{r}}(\hat{r})\Big]. \tag{4.64}$$

Owing to the choice made for the normalization of $\mathcal{C}$, the compaction function and the averaged mass excess agree at the comoving scale r_k, $\mathcal{C}(r_k) = \tilde{\delta}(r_k)$, at time for which the perturbation re-enters the Hubble scale when $\varepsilon = 1$; showing that these two parameters have equal footing on the description of the fluctuation.

In view of this last point, it would be nice to identify the scale r_k with the scale r_m in which the compaction function reaches its maximum [100]:

$$\mathcal{C}'(r_m) = 0 \quad \Leftrightarrow \quad K(r_m) + \frac{r_m}{2}K_{,r}(r_m) = 0 = \zeta_{,\hat{r}}(\hat{r}_m) + \hat{r}_m\zeta_{,\hat{r}\hat{r}}(\hat{r}_m), \tag{4.65}$$

which can be used to infer that $\tilde{\delta}(r_m,t) = 3\delta(r_m,t)$, independently from the curvature profile or the time; a point in favour of this scale.

It should be emphasized that the scale r_k, arising from the linear order of perturbation theory, is well suited to describe the idealized case of a single mode k evolving in Fourier space for which the Hubble crossing happens when $k/\bar{a}\bar{H} = 1$; nevertheless, the full non-linear process of collapse takes place in real space, where the perturbation is composed of several Fourier modes. So, in a general setting the comoving scale $r_0 = R_0/\bar{a}(t_0)$ at which the density contrast ultimately agrees with the background can be different from r_m and maintain dependence on the curvature profile [100]. In such cases, we will define the scale r_0 as the minimal value for which $\widetilde{\rho}(r_0,t_9) = 0$, or equivalently when $K(r_0) + r_0/3K_{,r}(r_0) = 0$.

Finally, there is another scale that can be used to quantify the strength of the perturbation, namely the scale r_p at which the density contrast assume a peak, $\delta_{,r} = 0$; this is particularly useful when used in conjunction with the primordial density perturbation [100].

Curvature profiles

Now we possess all the ingredients required to characterize the critical parameters and proceed to study how they emerge with specific profiles of the curvature. In

the following, we will describe the critical values for the parameters $\mathcal{C}_c \equiv \mathcal{C}(r_m)$, $\tilde{\delta}_c \equiv \tilde{\delta}(r_0)$ and $\zeta_c = \zeta(r_p)$. The black holes considered in these studies are assumed to form in radiation dominated era with $w = 1/3$.

To begin with, let us consider a simple gaussian distribution for the curvature profile and the density contrast that it yields [100]:

$$\begin{aligned} K(r) &= \mathcal{K} \exp\left[-\frac{r^2}{2\sigma^2} \right], \\ \delta(r,t) &= \frac{2}{3}\left(\frac{1}{\bar{a}\bar{H}}\right)^2 \left(1 - \frac{r^2}{3\sigma^2}\right) K(r). \end{aligned} \tag{4.66}$$

The parameters $\mathcal{K}$ and σ control the amplitude and the width of the perturbation, and the numerical factor in front of the density contrast is just the factor $3(1 + w)/(5 + 3w)$. The three scales of interest are given by:

$$r_m = \sqrt{2}\sigma, \qquad r_0 = \sqrt{3}\sigma, \qquad r_p = 0. \tag{4.67}$$

For a perturbation normalized to $\mathcal{K} = 1$ and $\sigma = 1$, the critical values for this profiles are $\tilde{\delta}_c \simeq 0.45$, $\mathcal{C}_c \simeq 0.5$ [100] and $\zeta_c \simeq 0.41$ [84]; so these value should be scaled with a factor K when this latter parameter moves away from unity. The strength of this model is that it gives rise to a mexican-hat profile for the density contrast, although it cannot model a compensated profile; in this sense the perturbation only asymptotically approaches a FLRW-flat spacetime.

The previous profile has been generalized [78][84] introducing an additional parameter α as follows:

$$\begin{aligned} K(r) &= \left(1 + \alpha\frac{r^2}{2\sigma^2}\right) \exp\left[-\frac{r^2}{2\sigma^2} \right], \\ \delta(r,t) &= \frac{2}{3}\left(\frac{1}{\bar{a}\bar{H}}\right)^2 \left[1 - \frac{5\alpha - 2}{3}\frac{r^2}{2\sigma^2} - \alpha\frac{r^4}{6\sigma^4}\right] \exp\left[-\frac{r^2}{2\sigma^2} \right]. \end{aligned} \tag{4.68}$$

The parameter gives the curvature a mexican-hat profile when negative, extend the half-width of the profile when $0 < \alpha \leq 1$, and add a off-centered peak when $\alpha > 1$. In the same way, $\alpha < 0$ makes deeper the underdensity trough and add an extra peak of overdensity after it, $0 < \alpha \leq 1$ widens the peak of the mexican-hat, and $\alpha > 1$ make an off-centered centered peak appear, turning the mexican-hat into a fedora. The overdensity regions are compensated by underdense one if $\alpha = -2$, but, for some reason, was only studied in ranges where α is positive by [84], and in the narrower range $0 < \alpha \leq 1$ by [78]. These studies shown that both α and σ affects the threshold values, still, whereas $\mathcal{C}_c$ and $\tilde{\delta}_c$ increase as α gets bigger, the ζ_c has an opposite trend and decreases.

In order to identify the most crucial parameters that effectively distinguish between which initial conditions lead to the formation of PBHs and which do not, a profile

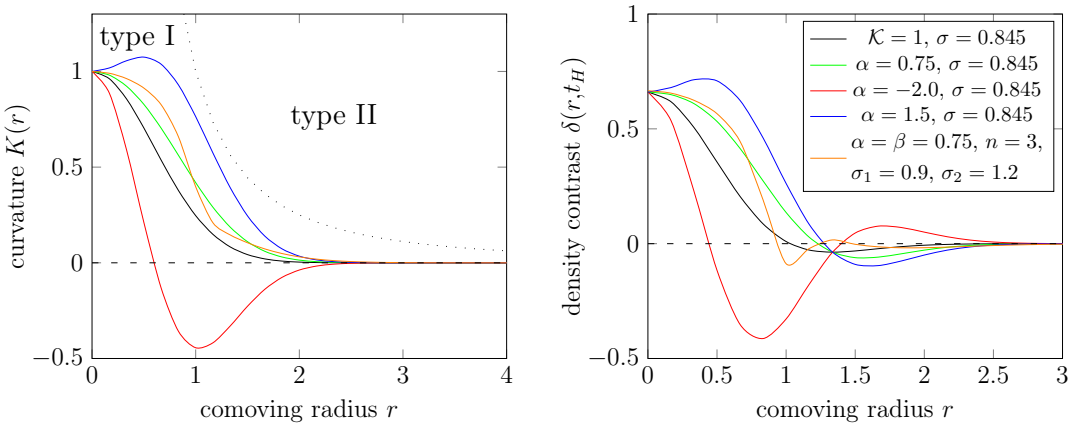

Figure 4.5. In the figures we can see different curvature profiles and the density contrast that they generate. The dotted line in the left plot stands for the boundary $K(r)r^2 = 1$ above which the perturbations give rise to type II black holes. Comoving radius is expressed in unit of Hubble scale.

with up to five parameters has been also studied [102]:

$$K(r) = \beta\left[1 + \alpha\left(\frac{r}{\sigma_1}\right)^{2n}\right]\exp\left[-\left(\frac{r}{\sigma_1}\right)^{2n}\right] + (1-\beta)\exp\left[-\left(\frac{r}{\sigma_2}\right)^{2}\right], \tag{4.69}$$

where $\sigma_1 \leq \sigma_2$. This profile reduces to the previous one if $\beta = 1 = n$, but the splitting in two gaussian profiles serves the purpose of adding a tail to the profile, while n regulate the steepness of the slope. The half-width of the profile is given by the scale σ attained at the point $\Omega \equiv \max_r |K_{,r}(r)|$, which can be taken as a measure of the density gradient. In [102] it was shown that, by plotting $\tilde{\delta}_c$ against Ω, the parameter $\tilde{\delta}_c$ fails to provide a clear-cut distinction between initial conditions that eventually collapse and the others when the profiles have different shapes in the center. Therefore, they went on to define empirically two parameters [102]:

$$\begin{aligned} \Delta_{p,q} &= r_p - r_q, \\ I_{s,j} &= \int_0^{r_s} r^j K(r) dr, \end{aligned} \tag{4.70}$$

where the scale of reference are set now defined by the relation $K(r_p) = p$. By random generating initial value for the profile's parameters, they managed to fit a demarcation line between the two kinds of critical behaviour. The best-fit functions obtained are $\Delta_{1/6,5/6}$ and $I_{3/5,2}$, which can be interpreted as the width of the underdense region and the integrated compaction function. In this sense the critical surface in the (Δ, I) space is given by the following broken line [102]:

$$[s_1(\Delta - \Delta_c) + I_c]\Theta(\Delta_c - \Delta) + [s_2(\Delta - \Delta_c) + I_c]\Theta(\Delta - \Delta_c), \tag{4.71}$$

with critical parameters $(s_1, s_2, I_c, \Delta_c) = (-0.021, 0.32, 0.79, 0.41)$ and Θ is the Heaviside function. A caveat is needed, though. The critical line just presented do not

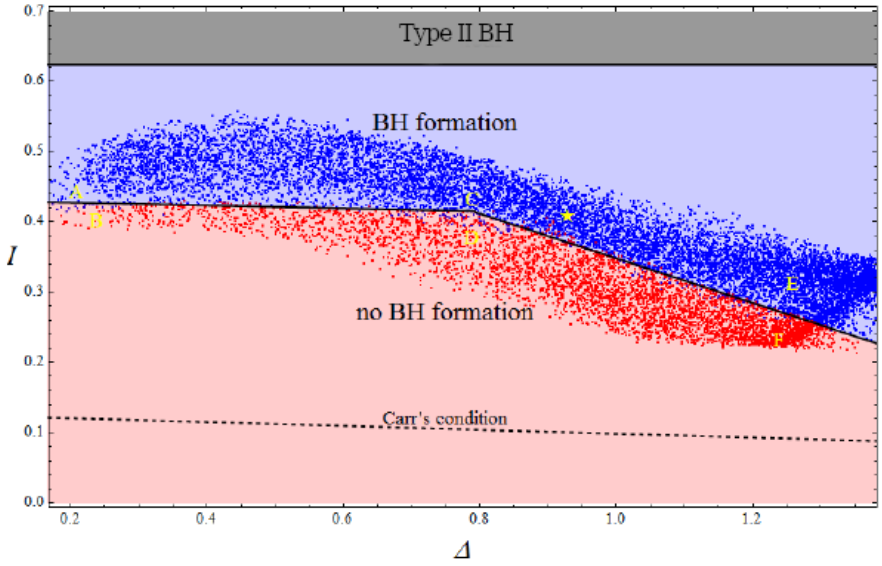

Figure 4.6. The space of parameters can be divided by a rather clear demarcation line between the two behaviours, up two an accuracy of 2.1%. The yellow stars represent the point which are inconsistent with the critical law. Picture is adapted from [102].

have a 100% accuracy, and there is a 2.1% of false positives—points that evolve into PBH in the sub-critical region or that do not collapse in the critical part. This could be taken as a point against the existence of a critical surface for more realistic scenarios of formation.

As a way around the usage of the extrinsic curvature as a source of the density contrast fluctuations, we could use a specificly gaussian profile for the primordial curvature perturbation [100]:

$$\begin{aligned} \zeta(\hat{r}) &= \mathcal{Z} \exp\left[-\frac{\hat{r}^2}{2\sigma^2} \right], \\ \delta &= \frac{2}{3}\left(\frac{1}{\bar{a}\bar{H}}\right)^2 \left[1 - \frac{\hat{r}^2}{3\sigma^2}\left(1 + \frac{\zeta(\hat{r})}{2}\right)\right] \frac{2\zeta(\hat{r})}{\sigma^2 e^{2\zeta(\hat{r})}}. \end{aligned} \tag{4.72}$$

Assessing the edge of the perturbation $\delta(r_0) = 0$ give us $\hat{r}_0^2 = 3\sigma^2(1 + \zeta(\hat{r}_0)/2)^{-1}$, which is only implicitly defined in terms of $\zeta(\hat{r}_0)$. When plugged inside $\tilde{\delta}$ it requires the non-analytical evaluation of the value $\mathcal{F}_0 \equiv -\hat{r}_0 \zeta_{,\hat{r}}(\hat{r}_0) = \hat{r}_0^2 \zeta(\hat{r}_0)/\sigma^2$ so that:

$$\hat{r}_0 = \sigma\sqrt{3 - \frac{\mathcal{F}_0}{2}}, \qquad \zeta(\hat{r}_0) = \frac{2\mathcal{F}_0}{6 - \mathcal{F}_0}, \tag{4.73}$$

which tell us that the value of $\tilde{\delta}(r_0)$ will depend both on $\mathcal{Z}$ and σ. Meanwhile, the scale $\hat{r}_m = \sqrt{2}\sigma$ which gives $\mathcal{C}(\hat{r}_m) = 8\mathcal{Z}(1 - \mathcal{Z}/e)/8e$, telling that this latter quantity depends only on $\mathcal{Z}$. The numerical simulations give the critical values of $\tilde{\delta}_c \simeq 0.55$, $\mathcal{Z} \simeq 0.8$ and $\mathcal{C} \simeq 0.55$. Altough technically more difficult, this way of

inputting the profile using ζ it is more convenient for relating the perturbation to the power spectrum $\mathcal{P}_\zeta$ from inflation; even though this possibility has been scarcely explored in the literature [100].

Threshold during Phase Transitions

Along the cosmic history, especially during the radiation-dominated epoch the universe could have gone along several phase transitions as it cooled down. Under the assumption that the universe is near thermal equilibrium, one can derive the energy density of the radiation fluid from the quantum distribution function of its relativistic particle [27]:

$$\rho(T) = g_*(T)\frac{\pi^2}{30}T^4, \tag{4.74}$$

where T is the temperature of the radiation fluid and g_* the effective number of degrees of freedom, which is the sum of the statistical weights of the fermionic and bosonic relativistic species composing the fluid.
When the temperature falls below the mass scale of a specific specie of particles, these decouple from the radiation fluid becoming non-relativistic and annihilating with their antiparticles, thus reducing $g_*(T)$. As the equation of state gets modified during the phase transition, the conditions for the formation of PBHs may differ from the purely radiation domination case. In light of this, it can be useful to understand how the critical parameters are affected around the turning points. In this analysis, we will consider PBH formation during two kind of phase transition: first order phase transitions—following the papers from Jedamzik [103], Cardall and Fuller [104] and Soubrinho [105]—and a crossover transition—following [106] and [107].

First-order Phase Transitions

First order phase transitions are characterized by the existence of a critical temperature $T_\star$, above and below which the system is in a high- and low-energy density state. When the critical temperature is reached, at some time t_-, the two phases will coexist in an intermediate phase. The pressure will vary continuously with a discontinuous slope, the two phases exchange latent heat at expenses of an entropy variation, while temperature is kept constant as parts of one phase turn into the other until the transition is completed, at some time t_+.

In the course of the transition, if the interaction rate of interested specie with the radiation fluid is larger than the Hubble expansion rate, $\Gamma/H \gg 1$ then the transition proceed with the formation of sub-Hubble bubbles and thermal and chemical equilibrium are approximately maintained [105]. In order for bubble to form the high-energy density phase must have some excess energy, as if it lays in a false

vacuum. Consequently, we can write [103]:

$$\begin{aligned} \rho_{\rm h}(T) &= g_{\rm h}\frac{\pi^2}{30}T^4 + B, \qquad & p_{\rm h}(T) &= g_{\rm h}\frac{\pi^2}{90}T^4 - B, \qquad & s_{\rm h}(T) &= \frac{4}{3}g_{\rm h}\frac{\pi^2}{30}T^3, \\ \rho_{\rm l}(T) &= g_{\rm l}\frac{\pi^2}{30}T^4, & p_{\rm l}(T) &= \frac{\rho_{\rm l}}{3}, & s_{\rm l}(T) &= \frac{4}{3}g_{\rm l}\frac{\pi^2}{30}T^3, \end{aligned} \tag{4.75}$$

where B is the energy of the vacuum in the high-energy density phase, and s the entropy density. At the transition temperature, we have $p_{\rm h}(T_\star) = p_{\rm l}(T_\star)$, which we can use to derive the energy of the vacuum:

$$B = \frac{1}{3}\frac{\pi^2}{30}(g_{\rm h} - g_{\rm l})T_\star^4. \tag{4.76}$$

The latent heat is given by $L = T_\star \frac{\partial}{\partial T}(p_{\rm h} - p_{\rm l})|_{T_\star} = T_\star(s_{\rm h} - s_{\rm l}) = \rho_{\rm h} - \rho_{\rm l} = 4B$. Conservation of entropy, $s_{\rm h} = s_{\rm l} + L/T_\star$, allows us to relate the scale factors at the beginning and the end of the transition to the effective degrees of freedom: $\bar{a}(t_+)/\bar{a}(t_-) = (g_{\rm h}/g_{\rm l})^{1/3}$. Energy density suffers a discontinuity from the interior to the exterior of a bubble, but we can assume that the average energy density changes continuously from $\bar{\rho}_-$ to $\bar{\rho}_+$ accordingly to the volume fraction of space in one phase, is given by [103]:

$$\langle\bar{\rho}\rangle(t) = \left(\frac{a(t_-)}{a(t)}\right)^3\left(\rho_{\rm h} + \frac{\rho_{\rm l}}{3}\right) - \frac{\rho_{\rm l}}{3} = \frac{\pi^2}{90}\left[4g_{\rm h}\left(\frac{a(t_i)}{a(t)}\right)^3 - g_l\right]T_\star^4, \tag{4.77}$$

and it term of it we can define the effective sound speed: $c_{s,\rm eff} = \sqrt{\partial p/\partial\langle\rho\rangle}$[10]. Bubble formation disrupts the propagation of acoustic waves; consequently, the effective sound speed drops to zero for wavelengths larger than the bubble typical size [109], and so sub-horizon overdense modes grow larger because the pressure gradients are largely suppressed.

The most direct consequence of the freezing of the speed of sound is a reduction of the Jeans Radius for overdensities re-entering the Hubble scale close to the phase transition. This means not that it drops to zero because the interior of the bubbles still behaves as a radiation fluid; but Cardall and Fuller [104] suggested it assumes an effective value, with repercussion on δ_c:

$$R_{J,\rm eff} = R_J\sqrt{1-f} \qquad \Rightarrow \qquad \delta_{c,\rm eff} = \delta_c(1-f), \tag{4.78}$$

where f is a qualitative parameter describing the fraction of overdense volume spent in the "dust-like" phase.
To evaluate this parameter, it is convenient to introduce $x = \langle\bar{\rho}\rangle_0/\bar{\rho}_-$ and $y = \bar{\rho}_-/\bar{\rho}_+$; where $\langle\bar{\rho}_0\rangle$ is the average energy density of the background at the time the overdensity re-enters the Hubble scale, $\bar{\rho}_{(i,f)}$ are the background energy densities

[10]The derivative is more easily evaluated as: $\frac{\partial\langle\rho\rangle}{\partial p} = f_{\rm h}\frac{\partial\rho_{\rm h}}{\partial p} + (1-f_{\rm h})\frac{\partial\rho_{\rm l}}{\partial p} + (\rho_{\rm h} - \rho_{\rm l})\frac{\partial f_{\rm h}}{\partial p}$, where $f_{\rm h}$ is the fraction of fluid in the high phase [108]

at the onset and offset of the phase transition [104]. The x parameter acts like a clock adjusted so that when it reaches unity the phase transition begins and stops when $x = y^{-1}$. The average density contrast is evaluated at time of reentry t_0 and at turnover time t_m. Based on the comparison of these two scales with the phase transition times, using (4.4) and (2.15), it is possible to relate the perturbed scale factor at turnaround time with the perturbed scale factor at Hubble re-entry:

$$a_m = a_0 \left(\frac{1+\delta_0}{\delta_0} \right)^{1/2}. \tag{4.79}$$

According to the phase in which the horizon-crossing time and the turn-around time fall, in [104], six classes of perturbations are distinguished:

A: both t_0 and t_m in the high-energy phase.
These are characterized by two conditions: $x\delta_0 > 1 - x$ for the constraint $t_0 < t_-$, and $x\delta_0^2 > (1+\delta_0)$ imposing $t_m < t_-$.

B: t_0 in the high-energy phase and t_m in the mixed phase.
These are characterized by three conditions: $x\delta_0 > 1 - x$, $x\delta_0^2 < (1+\delta_0)$ and $y\delta_0^3 > (1+\delta_0)^{3/2} x^{3/2}$ telling that $t_m < t_+$.

C: t_0 in the high- and t_m in the low-energy phase phase.
These are characterized the conditions: $x\delta_0 > 1 - x$ and $y\delta_0^3 < (1+\delta_0)^{3/2} x^{3/2}$.

D: both t_0 and t_m in the mixed phase.
These are characterized by three conditions: $x\delta_0 < 1 - x$, $y\delta_0^3 > (1+\delta_0)^{3/2} x^{3/2}$ and $xy\delta_0 > 1 - xy$ which states that $t_0 < t_+$.

E: t_0 in the mixed phase and t_m in the low-energy phase.
These are characterized by the conditions: $\delta_0 < x^{-1} - 1$, $y\delta_0^3 < (1+\delta_0)^{3/2} x^{3/2}$ and $xy\delta_0 > 1 - xy$.

F: both t_0 and t_m in the low-energy phase phase.
Simply characterized by $xy\delta_0 < 1 - xy$.

Let us denote a_i and a_f the perturbed scale factors of the overdensity when it first and last perceive the phase transition. Therefore, under the simplifying assumption that the collapse happens at turnaround, the fraction of volume spent during the softened epoch is given by [104]:

$$f = \frac{{a_f}^3 - {a_i}^3}{a_m^3}. \tag{4.80}$$

Now, for type A perturbation $f = 0$ because they are never affected by the phase transition. Type B have $a_0 < a_- = a_i$ and $a_f = a_m$. For type C, $a_0 < a_- = a_i$ and $a_f = a_+$. Type D have $a_0 > a_- = a_i$ and $a_f = a_m$, but since their region lays always on top of the regions for perturbation of type C and D, they are not constrained from below, but in principle they could be constrained from above against type II PBHs even if this has not been analyzed in the literature. Type E have $a_0 > a_- = a_i$

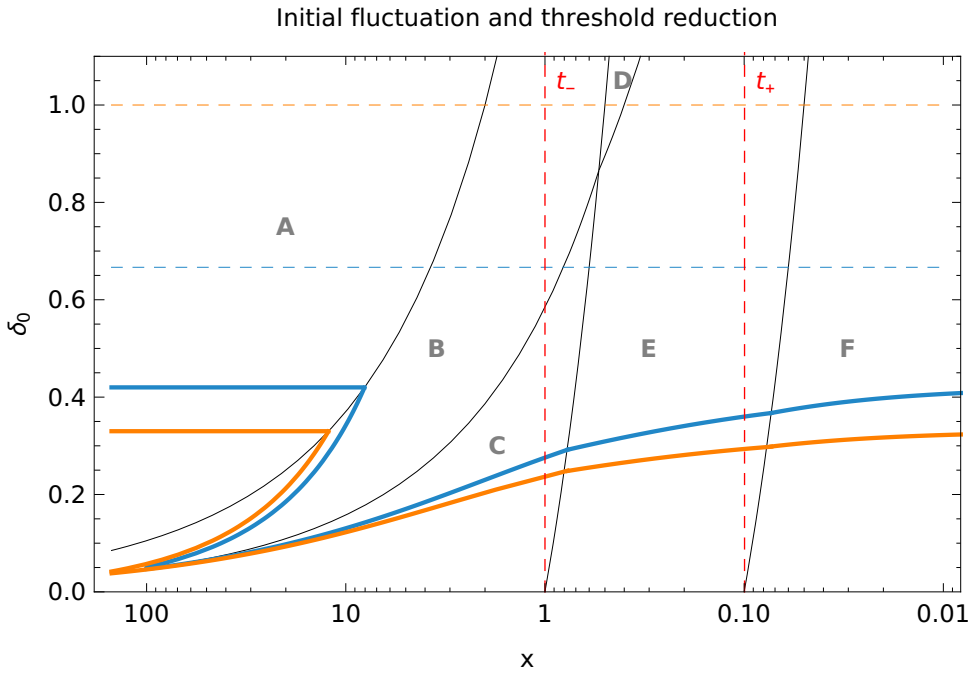

Figure 4.7. The gray lines show the boundaries between various perturbation types in proximity of the phase transition. The solid coloured lines give the effective threshold for the formation of type I PBH in the CMC(orange) and comoving(blue) gauses, while the dashed line give the threshold type II as unaffected by the transition; y is chosen to be 10, which corresponds to a duration of 2.3 e-folds.

and $a_f = a_+$, and, finally, type F have $a_- = a_i$ and $a_0 > a_f = a_+$. In the following table, we summarize the form of f with respect to the x, y, δ_0 parameters which can be obtained through Friedman equations for a two-FLRW universes model:

	A	B	C	E	F
f	0	$1 - \frac{x^{3/2}\delta_0^3}{(1+\delta_0)^{3/2}}$	$\frac{x^{3/4}\delta_0^{3/2}}{y^{1/2}(1+\delta_0)^{3/4}}(y-1)$	$\frac{(xy)^{1/2}\delta_0^{3/2}}{1+\delta_0}(1-y^{-1})$	$\frac{(xy)^{3/4}\delta_0^{3/2}}{(1+\delta_0)^{3/4}}(1-y^{-1})$

In this form, f is given in terms of the initial size of a perturbation and the x parameter, so it cannot be used directly the equation of the effective critical density contrast (4.78). To obtain the exact form one need to solve:

$$\begin{cases} \delta_{c,eff} = \delta_c(1 - f(\delta_0)) \\ \delta_{c,eff} = \delta_0 \end{cases}, \tag{4.81}$$

which give us a non-analytical bound for perturbation types C and F, as shown in Figure (4.7). One feature of the threshold near a first-order phase transition is the curve lose its monotonic behaviour and bends back. This can be understood as follows: fluctuations that re-enters the Hubble scale with a initial overdensity

between the crest and the critical threshold for radiation epoch are too heavy and reach turnaround before the onset of the phase transition and disperse back into background. The most significantly affected perturbation types that could then collapse into PBHs are of type B and C; type F are affected the slightest, and $\delta_{c,\text{eff}}$ rapidly tends to δ_c of a radiation dominated epoch again.

The speculation that the this kind of phase transition might have led to the generation of PBHs[11] in the QCD-phase transition was first proposed by Crawford and Schramm [110], but lattice QCD simulations later confirmed that QCD-transition happened as a crossover [107]. Nonetheless, the possibility that first order phase transitions might still have occurred at the end of EW-epoch has not been ruled out yet[105](for example in the scenario of an heavy Higgs) and it being first-order is paramount for having electroweak baryogenesis [111].

Crossover phase transitions

During a crossover phase transition the thermodynamics quantities varies without incurring any discontinuities. This seems to be the case for the QCD-phase transition in the early universe, which shall be the focal point of our discussion. Even though a smooth transition lack a net separation between two phases, it is still possible to introduce a critical temperature $T_\star \simeq 170\text{MeV}$ and a range ΔT in which the transition take place, which can be chosen to be $\Delta T = 0.1 T_\star$[12], so that now t_- and t_+ are now times associated with the epoch when the background had a temperature $T(t_-) = T + \Delta T$ and $T(t_+) = T - \Delta T$. In this light, the thermodynamic quantities (4.75) are still defined far from $T_\star$. The high phase will be the phase in which the universe was in a state of plasma of quarks and gluons, and in the low phase quark and gluons condensed in the form of an hadron-plasma.

To model a continuous variation in entropy, one can use a resolution of the step function [112] and write:

$$s(T) = \frac{2\pi^2}{45} g_{\text{l}} T^3 \left[1 + \frac{1}{2} \frac{g_{\text{h}} - g_{\text{l}}}{g_{\text{l}}} \left(1 + \tanh\left(\frac{T - T_\star}{\Delta T} \right) \right) \right]. \tag{4.82}$$

The speed of sound now will be a function of temperature, as such can be derived as follows:

$$c_s^2(T) = \frac{\partial p}{\partial \langle \rho \rangle} = \frac{\partial p}{\partial T} \frac{\partial T}{\partial \langle \rho \rangle} = s \left(T \frac{\partial s}{\partial T} \right)^{-1} = \left(\frac{\partial \ln S}{\partial \ln T} \right)^{-1}, \tag{4.83}$$

where we used the thermodynamics relations $s = \frac{\partial p}{\partial T}$ and $C_V = \frac{\partial \langle \rho \rangle}{\partial T} = T \frac{\partial s}{\partial T}$. During the transitions, the speed of sound reduces its value instead of dropping to zero. As a consequence, the equation of state gets softened in a similar fashion to first order

[11] Phase transitions do not generate the seeds for PBHs themselves; instead, an higher formation rate is obtained by reinforcing seeds that would have been too weak to collapse otherwise.

[12] First order phase transition result should be recovered in the limit $\Delta T \to 0$ [106].

phase transitions.
Following the treatment on first order phase transitions, we assume that PBHs form at turnaround and define an effective Jeans radius in the same way as equation (4.78) but we only need to generalize the definition of f, the volume fraction spent in the softened state. Sobrinho et al. [106] introduced the following expression:

$$f = \frac{1}{a_m^3} \int_{a_i}^{a_m} \frac{\tilde{c}_s - c_s(T)}{\tilde{c}_s} \, \mathrm{d}\, a^3, \tag{4.84}$$

where $\tilde{c}_s = 1/3$ is the speed of sound far from the transition. Then, using (4.79) in conjuction with the fact that during a radiation epoch $a \propto t^{1/2}$, allow them[13] to connect the cosmic time of re-entry and turnaround:

$$t_m = t_0 \frac{1+\delta_0}{\delta_0}. \tag{4.85}$$

Next, they express the temperature as a function of cosmic time by stacking backward the evolution of background scale factor:

$$T(t) = T_0 \left[\exp\left(\sqrt{\frac{\Lambda}{3}} (t_\Lambda - t_{\mathrm{now}}) \right) \left(\frac{t_{\mathrm{eq}}}{t_\Lambda} \right)^{2/3} \left(\frac{t}{t_{\mathrm{eq}}} \right)^{1/2} \right]^{-1}, \tag{4.86}$$

where T_0 is present time CMB temperature, t_{now} present time, t_Λ the time of matter-vacuum equality and t_{eq} the time of matter-radiation equality. Putting (4.79), (4.85) and (4.86) into (4.84), one can write:

$$f = \frac{3}{2} \left(t_0 \frac{1+\delta_0}{\delta_0} \right)^{-3/2} \int_{t_i}^{t_0 \frac{1+\delta_0}{\delta_0}} (1 - 3c_s(T(t))) \sqrt{t} dt. \tag{4.87}$$

From this formula, using (4.81) a non-analytical bound can be obtained as shown in figure (4.8).

The result, based on the use of formulas outside their regime and the stacking of scale factors, is numerically sensitive to six parameters from the cosmic epochs as such weak against their variation, still, it can be praised for its exploratory outlook into a plausible scenario of PBH formation
Another way to deal with these transitions has been implemented by Byrnes et al. [107]. As the thermodynamic quantities varies smoothly in a crossover, we can replace the discontinuous quantity g with two quantities $g_{\mathrm{eff}}(T)$ and $h_{\mathrm{eff}}(T)$. Then, starting from the form of quantities in (4.75), can be defined as:

$$g_{\mathrm{eff}}(T) = \frac{30\bar{\rho}(T)}{\pi^2 T^4}, \qquad h_{\mathrm{eff}}(T) = \frac{45\bar{\rho}(T)}{2\pi^2 T^3}. \tag{4.88}$$

Using the thermodynamic relation linking pressure, energy and entropy densities, $\bar{p} = \bar{s}T - \bar{\rho}$, the adiabatic index can be expressed as a function of the temperature:

$$w(T) = \frac{4h_{\mathrm{eff}}(T)}{3g_{\mathrm{eff}}(T)} - 1, \tag{4.89}$$

[13] This dependence actually applies only for the background scale factor as according to (4.6) the perturbed scale as a profile of the type $a(\tau) = a_m \sin(\arccos(1 - \tau/a_m))$.

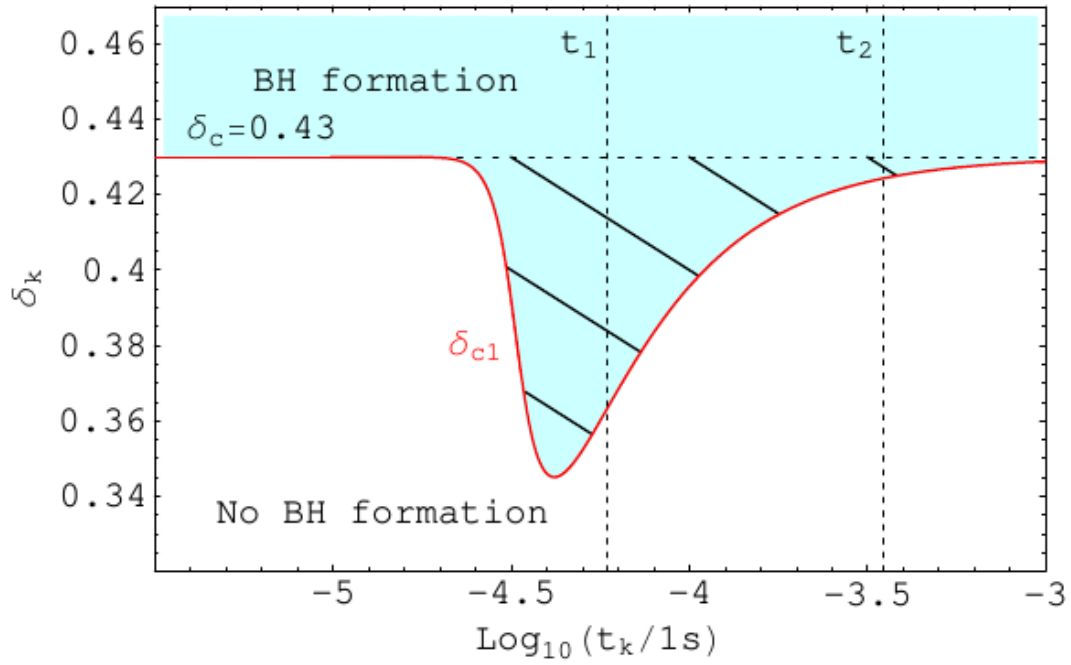

Figure 4.8. The softened critical density contrast found in [106]. Their notation differs from ours in $\delta_k \equiv \delta_0$, $t_k \equiv t_0$, $t_1 t_-$ and $t_2 \equiv t_+$.

from which one can obtain the effective speed of sound as a function of the temperature:

$$c^2_{s,\mathrm{eff}}(T) = \frac{4}{3}\frac{T h_{\mathrm{eff},T}(T) + 4h_{\mathrm{eff}}(T)}{T g_{\mathrm{eff},T}(T) + 4g_{\mathrm{eff}}(T)} - 1. \tag{4.90}$$

In [107], the numerical result of a lattice QCD study [113] is interpolate with a spline to calculate g_{eff} and h_{eff} and obtain the profiles of w and c_s^2, shown in figure (4.9) as a function of the time expressed in terms of the Hubble mass through the following relation:

$$M_H(T) \approx 1.5 \times 10^5 M_\odot \left(\frac{T}{1\mathrm{MeV}}\right)^{-2} \left(\frac{g_{\mathrm{eff}}}{10.75}\right)^{-1/2}. \tag{4.91}$$

Next, four possible thresholds for the density contrast are provided using the value of the adiabatic parameter at Hubble crossing time, at turnaround and two time averages [107]:

$$\begin{aligned} \delta_{c,\mathrm{eff}} &= \frac{1}{t_m - t_0}\int_{t_0}^{t_m} \delta_c(w(T))dt, \\ \delta_{c,\mathrm{eff}} &= \frac{1}{\ln(t_m/t_0)}\int_{t_0}^{t_m} \delta_c(w(T))\frac{dt}{t}, \end{aligned} \tag{4.92}$$

under the assumption that PBHs form once turnaround is reached. Nonetheless, they do not specify which relation they used for $\delta_c(w)$ but refer to the paper of Musco and Miller [90] which only provides some numerical result of the dependence of the threshold in terms of w.

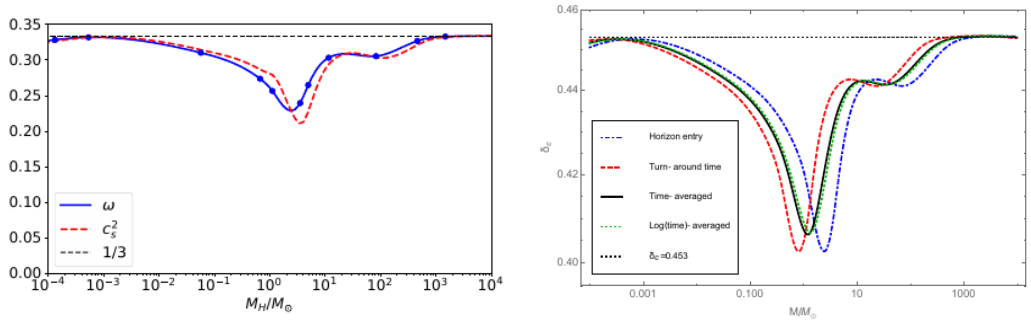

Figure 4.9. On top the adiabatic parameter w and the speed of sound c_s^2 as plotted by a spline interpolation in [107] of the data points(blue dots) generated by numerical lattice QCD simulations [113]. On the right the reduction of the threshold obtained with 4 different methods is compared to the numerical result of δ_c for a radiation dominated universe [90].

Ellipsoidal collapse

The critical thresholds we presented up to now were based on the assumption of spherical collapse. Spherical symmetry is a convenient assumption to simplify the calculation and to give a first-order approximation to investigate situations in which departures from sphericity are small or which recover it along the course of collapse. Nonetheless, since the universe is abundant with non-spherical configurations, to draw better conclusions on the formation of PBHs it might be useful to have a better understanding how the collapse is modified in configurations lacking this high degree of symmetry. The ellipsoidal configurations represent the simplest compromise between symmetry and more complexity. Inspired by a result conducted on the ellipsoidal gravitational collapse of galaxy haloes in an Einstein-de Sitter spacetime[14] [114], which relates the threshold of an ellipsoidal distribution to the threshold of a spherical one:

$$\frac{\delta_{ec}}{\delta_e} \simeq 1 + \kappa\left(\frac{\sigma^2}{\delta^2}\right)^{\gamma}, \tag{4.93}$$

Kühnel and Sandstad [115] advanced the argument that the same result holds for the case of PBHs in a arbitrary epoch.

To start with, we consider a ellipsoidal overdensity which is characterized by three axis parameters $a \leq b \leq c$, which can be thought as the eigenvalues of the deformation tensor. We use them to define the ellipticity e and the prolateness of the configuration as follows [115]:

$$e = \frac{b^2(c^2 - a^2)}{2(a^2b^2 + a^2c^2 + b^2c^2)}, \qquad P = \frac{a^2b^2 + c^2(b^2 - 2a^2)}{2(a^2b^2 + a^2c^2 + b^2c^2)}, \tag{4.94}$$

where $0 < e \leq 1$ and $|P| \leq e$. Maximal prolateness, $P = e$, is obtained with two equal small axes and a major one when $b = a$; maximal oblateness, $P = -e$,

[14] A matter-dominated universe with vanishing spatial curvature and cosmological constant.

is obtained for two equal large axes and one small axis when $b = c$. Finally, we can reduce back to a spherical scenario setting $c = a$, corresponding to $e = 0$. The smallest axis is the first that start the collapse, and longer axes will follow the collapse with a faster that linear dependence [116]. For this reason, ellipsoidal collapse can be compared with the collapse of the largest sphere embedded, with a radius equal to the smallest axis. The volume of the ellipsoid is related so to the sphere's volume by $V_e/V_s = (1+3e)/\sqrt{1-3e}$; thus, under the assumption of uniform energy density inside both objects, the masses scale as $M_e = M_s V_e/V_s$. As a result, the density contrast of the sphere $\delta(M_s)$ will be smaller by a factor $\delta(M_e - M_s)$. Referring Carr's paper, they used that density contrast scales a $\delta(M) \sim M^{2/3}$[15]. Therefore, comparing the critical density contrast of the sphere with the one of the ellipsoid, to the lowest order in ellipticity, one obtains:

$$\frac{\delta_{ec}}{\delta_c}\left(\frac{M_e}{M_s}\right)^{2/3} \simeq 1 + 3e. \tag{4.95}$$

Then considering a statistical Gaussian distribution of ellipsoidal overdensities of different shapes, from their power spectrum it can be calculated that the expectation values for ellipticity and prolateness read as [116]:

$$\langle e \rangle = \frac{3\sigma}{\sqrt{10\pi}\delta}, \qquad \langle p \rangle = 0. \tag{4.96}$$

Using these values in (4.95), a relation in the same form of (4.93) was obtained in [115]:

$$\frac{\delta_{ec}}{\delta_c} \simeq 1 + \frac{9}{\sqrt{10\pi}}\left(\frac{\sigma^2}{\delta_c^2}\right)^{1/2}. \tag{4.97}$$

The derivation is admittedly heuristic, but served their purpose to show that independently form the epoch of formation taking into account non-sphericity should hinder the formation of primordial black holes[16] and that this effect could be substantial. Interestingly, this can be used as argument for PBHs forming in a early matter era [117], where the Jeans criterion considerably lowers the spherical threshold, which to actually collapse need to have a shape very close the spherical; thus, lowering the probability of their formation based on the unlikeliness for such configurations to occur.

[15] However, in Carr's paper, the behaviour of the density contrast actually goes like $\delta(M)\ M^{2/3}$, and also later in their paper equation (6) as the same behaviour.

[16] Unfortunately, following the same line of reasoning with the actual dependence $M^{-2/3}$ leads to the opposite conclusion, that the ellipsoidal threshold is lowered. However, this result is counterintuitive and contrary to same behaviour in halos.

Chapter 5

Abundance of Primordial Black Holes and constraints

> Our hopes and expectations
> black holes and revelations.
>
> The Muse, "Starlight"

In the previous chapter, we inspected how various thresholds in the density contrast that lead to formation of PBHs when the density fluctuations re-enter the Hubble scale after inflation. The focus of this chapter is going to be on the relative abundance of a population of PBHs in the universe. This argument is strictly linked with the possibility that PBHs might constitute at least a fraction of the measured dark matter content of today universe, and can be used as a potential probe for constraining the Physics on small cosmological scales in the Early universe. In this sense, the most appealing feature of PBHs as a way to infer small scale characteristic of the universe is that it does not require their actual observation; indeed, the lack of PBH formation give us an upper bound on the spectrum of primordial density fluctuations and so it provides other cosmological models with guidelines that would help better constraints their form and feasibility.

The primordial black hole abundance function

In order to understand how to compute the abundance of primordial black holes and why it is useful, it might be convenient to summurized the picture and the assumptions attached to the emergence of seeds for PBHs. The genesis of the grains that are going to constitute the black holes stems from the generation of fluctuations in the vacuum of field—or fields—during the inflationary epoch. The assumption for these fluctuations is that they have a Gaussian statistics [118], and since spacetime is dilated by the quasi-exponential expansion, the fluctuations, through back-reaction, induce perturbations in the metric. The physical Hubble scale $\bar{H}^{-1}$ stays

approximately constant during this epoch, while the comoving Hubble scale $(\bar{a}\bar{H})^{-1}$ decreases so that perturbations grow and get stretched until they exit the Hubble scale. If the nature of these fluctuations is adiabatic, they eventually stop evolving far out of the Hubble scale, where their evolution gets frozen(cf. 3.28). Since the duration of inflation lasts for an high number of efolds($\sim 50 - 65$), the range of perturbations having exited the Hubble sphere spans several orders of magnitude. Once the inflationary epoch ends, it is followed by a reheating phase during which the energy of the inflaton field is transferred to the other fields—or directly into the radiation epoch. Irrespectively of which came first, the cosmic time is chosen in a way that at the onset of the radiation era it ticks $\eta = 0$. At this point, the physical Hubble scale grows quadratically in the scale factor and perturbations modes outside the Hubble scale progressively re-enters according to their physical wavenumber $k/\bar{a}$.

In order to describe the perturbations, we have two fields of choice: the primordial density perturbation ζ and the density contrast δ; briefly, we will see that this leads us to a two ways of calculating the abundance, which it has been only recently pointed out in the literature [119]. Nonetheless, within theseparate universe approximation in the gradient expansion framework, we derived a relation between the two quantities in equation (4.60), which can be linearized to relates their respective modes as follows:

$$\delta_{\mathbf{k}}(t) = \frac{2(1+w)}{5+3w}\left(\frac{k}{\bar{a}(t)\bar{H}(t)}\right)^2 \zeta_{\mathbf{k}}, \tag{5.1}$$

which becomes particularly simple at the time of horizon crossing of a specific mode, when $k/(\bar{a}\bar{H}) = 1$. Therefore, if the perturbation's amplitude exceeds a certain threshold value at the time of re-entry, a PBH will inevitably form with a fraction of the horizon mass $M_{\mathrm{PBH}} = \gamma M_H$, being γ the efficiency factor that depends on the details of the collapse.

After the formation, the mass of PBH contributes to increase the fraction of dark matter content of the universe. Naturally, the nature of dark matter is still undetermined at present day and so it is the speculative nature of primordial black holes, meaning that we still lack satisfactory evidence of their existence. Despite that, in order to seek for connections with potential observables, it is necessary to study their abundance and link it with available models.
To begin with, assuming that all the PBHs form in the radiation epoch—and that the mass spectrum is monocromatic—meaning that they all form with the same fraction γ—we can introduce the abundance function as follows [120]:

$$\beta(M_{\mathrm{PBH}}) = \frac{\rho_{\mathrm{PHB}}(t_*)}{\rho_{\mathrm{tot}}(t_*)} = \frac{M_{\mathrm{PBH}}\ n_{\mathrm{PBH}}(t_*)}{\rho_{\mathrm{tot}}(t_*)}, \tag{5.2}$$

where n_{PBH} is the number density of such black holes, and the whole expression is defined at the time of PBH formation t_*. This function has to be small at all the time during radiation domination, $\beta < 0.5$; otherwise, the fraction of PBHs would come to become the dominant component of the universe. This should be intended

as a conservative estimation of the abundance at a specific value of $M_{\rm PBH}$, and we will later discuss how it gets modified in the case of an extended mass spectrum.

The abundance function actually corresponds to the density parameter $\Omega_{\rm PBH}$, but it is convenient to maintain a distinction between the two functions. For instance,in the case of formation at radiation domination epoch, since the PBHs fluid can be assumed to behave as an ideal fluid of dust particles, the density parameter will grow with respect to the background density parameter until the time of matter-radiation equality. This is easily understood because the former goes down according to $\bar{a}^{-3}$ and the latter as $\bar{a}^{-4}$, then the expansion of the universe boost the density parameter during this era:

$$\Omega_{\rm PBH}(t_{\rm eq}) = \beta^{\rm eq}(M) \approx \frac{a_{\rm eq}}{a_*}\beta(M_{\rm PBH})\Omega_{\rm rad}(t_{\rm eq}), \tag{5.3}$$

which is derived under the assumption $\rho_{\rm tot} \approx \rho_{\rm rad}$ that becomes increasingly inexact as we approach $t_{\rm eq}$ because, at that time, one should have $\rho_{\rm tot} = \rho_{\rm rad} + \rho_{\rm mat}$ with $\rho_{\rm rad} = \rho_{\rm mat}$[1]; thus this should be considered a conservative approximation, as well.

If one drops the assumption of monocromaticity, then the mass fraction of the universe in the form of black holes should be given by the cumulative of the abundance [121]:

$$\Omega_{\rm PBH} = \int_{M(t_*)}^{M(t_{\rm eq})} \frac{{\rm d}\, M}{M}\beta^{\rm eq}(M). \tag{5.4}$$

This effect it will not be present in the following epoch, since the background goes as matter as well, so we can write $\Omega_{\rm PBH,0} = \Omega_{\rm PBH}(t_{\rm eq})/(1+z_{\rm eq})^3$ and introduce the current PBH to dark matter ratio as follows [120]:

$$f = \frac{\Omega_{\rm PBH,0}}{\Omega_{\rm CDM,0}}, \tag{5.5}$$

this quantity will come in handy in discussing the observational constraints.

Press-Schechter Formalism versus Peak Theory

The evaluation of the PBH abundance requires to evaluate the number density of the fraction of the universe in which either δ or ζ is above the critical value; to do so, one can resort to two different methods:

- Press-Schechter formalism [122] which derives the abundancy of PBHs by totting up their probability of formation,
- Peak theory [123] which derives the number of peaks of a gaussian random fields, based of their statistical properties.

[1]Moreover, we have to keep in mind that $\rho_{\rm mat} \approx \rho_{\rm barions} + \rho_{\rm CDM}$ and that $\Omega_{\rm PBH}$ is itself a fraction of Ω_{CDM}.

The Press-Schechter formalism was originally proposed to study the formation of large structures like galaxies and clusters, under the process of self-similar collapse. The self-similarity entails the phenomenon of a bottom up condensation of structures where the random aggregation of perturbations of smaller scales acts like point source for large scale ones. This is attained through coarse-graining, once a smoothing scale R is chosen, the density contrast is smoothed by convolution with a window function [124]:

$$\delta_R(r,t) = \int \mathrm{d}^3\,\mathbf{r}'\; W(R, r-r')\delta(r',t) = \frac{1}{(2\pi)^3}\sum_{\mathbf{k}}\int \mathrm{d}^3\,\mathbf{k}\tilde{W}(k,R)\delta_{\mathbf{k}}(t)e^{-i\mathbf{k}\cdot\mathbf{r}}, \quad (5.6)$$

where, for PBH settings, the scale is usually chosen to be the Hubble scale, $R = (\bar{a}\bar{H})^{-1}$, and the density contrast is taken to be in comoving gauge [124]. Two choices are often made for the window function, a top-hat or a gaussian profile; we are going to choose $\tilde{W}(k, 1/\bar{H}) = \exp(-k^2/2\bar{a}^2\bar{H}^2)$ following [119], [125]. Since at time of reentry, the relation (5.1) between $\delta_{\mathbf{k}}$ and $\zeta_{\mathbf{k}}$ is given by a simple numerical proportionality, the choice of the smoothing scale makes so that the gaussian statistics of the curvature perturbation modes is transferred transitively to the smoothed density contrast. As a result, assuming Gaussian statistics for δ, we can write the probability that a smoothed region has density contrast in an infinitesimal range $d\delta$ is given by [124]:

$$P(R,\delta)\,\mathrm{d}\,\delta = \frac{1}{\sqrt{2\pi}\sigma_\delta}\exp\left(-\frac{\delta_R^2}{2\sigma_\delta^2}\right)\mathrm{d}\,\delta, \quad (5.7)$$

where the variance of the cross-grained density contrast field reads as :

$$\sigma_\delta^2 = \int_0^\infty \frac{\mathrm{d}\,k}{k}\tilde{W}^2(k,R)\mathcal{P}_\delta(k). \quad (5.8)$$

Thence, integrating the probability over the allowed range for the formation of PBHs, give us directly the abundancy of PBHs [124]:

$$\beta = 2\int_{\delta_c}^{\delta_{\max}} P(R,\delta)\,\mathrm{d}\,\delta, \quad (5.9)$$

where the factor 2 is a correction taking into account wrong counting of embedded underdense in overdense regions[2]. If we assume that $\sigma_\delta \ll \delta_c$, motivated by the fact that the PBHs must be scarce, the abundance formula can be expressed as:

$$\beta \approx \frac{2}{\sqrt{2\pi}\sigma_\delta}\int_{\delta_c}^\infty \exp\left(-\frac{\delta_R^2}{2\sigma_\delta^2}\right)\mathrm{d}\,\delta = \mathrm{Erfc}\left(-\frac{\delta_c}{\sqrt{2}\sigma_\delta}\right) \approx \sqrt{\frac{2}{\pi}}\frac{\sigma_\delta}{\delta_c}\exp\left(-\frac{\delta_R^2}{2\sigma_\delta^2}\right), \quad (5.10)$$

where the last approximation derives from the asymptotic expansion of the complementary error function: $\mathrm{Erfc}(x) = 1 - \mathrm{Erf}(x)$.

As we saw, the use of the Press-Schechter formalism considers the average of the density contrast field, and sum its probability for values above the threshold for

[2]This problem is also known as cloud-in-cloud problem and it has been discussed in [126], [127].

the formation of the black hole, which is a quantity that was actually defined for the unsmoothed density contrast field. Motivated by the desire of improving this calculation and to link the abundance to the primordial curvature perturbation field, the Peak Theory was applied to the context of PBHs [119]. In addition, peaks in the density contrast field might not corresponds to peaks in the curvature perturbation field [101]. We begin by smoothing the curvature perturbation field within the Hubble scale, with the same window function used earlier:

$$\zeta(R = 1/\bar{H}, r) = \int \mathrm{d}^3\,\mathbf{r}'\; W(R, r - r')\zeta(r') \tag{5.11}$$

which can be expanded in Taylor-series around a point $\mathbf{r}_0$ as follows:

$$\zeta(R, r) \simeq \zeta_0(\mathbf{r}_0) + (\nabla_i\,\zeta_0)(\mathbf{r} - \mathbf{r}_0)^i + \frac{1}{2}(\nabla_i\,\nabla_j\,\zeta_0)(\mathbf{r} - \mathbf{r}_0)^i(\mathbf{r} - \mathbf{r}_0)^j, \tag{5.12}$$

where the short-hand $\zeta_0 = \zeta(R, r_0)$ has been adopted. The coarse-grained field can be considered gaussian [101] because the primordial curvature perturbations where generated by the inflationary bubbling of vacuum; thus, it makes sense to define its variance and higher-order statistical momenta:

$$\begin{aligned} \sigma_\zeta^2(R) &= \int \frac{\mathrm{d}\,k}{k}\tilde{W}^2(k, R)\mathcal{P}_\zeta(k), \\ \sigma_q^2(R) &= \frac{1}{\sigma_\zeta^2}\int \frac{\mathrm{d}\,k}{k}k^{2q}\tilde{W}^2(k, R)\mathcal{P}_\zeta(k), \end{aligned} \tag{5.13}$$

where the 0^{th} momentum is normalized to be just 1. In proximity of a peak of ζ, the first order derivatives in equation (5.12) vanish, and the hessian matrix $\boldsymbol{\zeta}_{ij} = \nabla_i\,\nabla_j\,\tilde{\zeta}_0$ is negative defined, so, in particular, it is invertible. We can use this to write the gradient of the field and define the position of the peaks [123]:

$$\boldsymbol{\eta}_i(r) \equiv \nabla_i\,\tilde{\zeta}(r) \simeq \sum_p \boldsymbol{\zeta}_{ij}(\mathbf{r} - \mathbf{r}_p)^j \quad \Rightarrow \quad \mathbf{r} - \mathbf{r}_p \simeq \boldsymbol{\zeta}^{-1}(\mathbf{r}_p)\cdot\boldsymbol{\eta}(\mathbf{r}). \tag{5.14}$$

In order to describe the peaks, the quantity $\nu = \tilde{\zeta}_0/\sigma_\zeta$ is introduced [101], which acquires a critical threshold ν_c directly from ζ_c; distinguishing regions that collapse into black hole from overdensities that disperse into the statistical background. Consequently, the number density of the peaks can be written as a Dirac's comb distribution, $n = \sum_p \delta^{(3)}(\mathbf{r} - \mathbf{r_p}) = \sum_p |\det(\boldsymbol{\zeta}(\mathbf{r}_p))|\delta^{(3)}(\boldsymbol{\eta})$ [123]. Finally, the number of peaks above the threshold value ν_c can be written as [125]:

$$n(\nu_c, R) = \frac{1}{(2\pi)^2}\left(\frac{\sigma_1^2(R)}{3}\right)^{3/2}(\nu_c^2 - 1)\exp\left(-\frac{\nu_c^2}{2}\right). \tag{5.15}$$

If we assume that the power spectrum is in the form $\mathcal{P}_\zeta(k) = A_\zeta(k/k_p)^{n_s-1}$; plugging it into (5.13), we get:

$$\sigma_\zeta = \frac{A_\zeta}{2(k_0 R)^{n_s-1}}\Gamma\left(\frac{n_s - 1}{2}\right), \qquad \sigma_1^2(R) = \frac{n_s - 1}{2R^2}. \tag{5.16}$$

It follows that the abundance of PBHs in peak theory reads as [125]:

$$\beta(\nu_c) = \frac{(n_s-1)^{3/2}}{4(3^3\pi)^{1/2}}\nu_c^2 \exp\left(-\frac{\nu_c^2}{2}\right) \approx \frac{(n_s-1)^{3/2}}{4(3^3\pi)^{1/2}}\frac{\zeta_c^2}{\sigma_\zeta^2}\exp\left(-\frac{\zeta_c^2}{2\sigma_\zeta^2}\right) = \beta(\zeta_c), \quad (5.17)$$

where the dependence on the smoothing disappears because we chose it to the same as the re-enter scale of the perturbation, and we approximated $\zeta_c(R) \approx \zeta_c$.

It should be emphasized that the two methods of Press-Schechter and Peak Theory do not agree. It has been advocated [119] that for abundances above $\Omega_{\rm PBH} \sim 10^{-20}$ the two are in good agreement. On the other hand, another study [125] have argued that such result included a mistake, and presented calculation should modified by taking into account the peaks in the density contrast. This would affect the calculation in the point of statistical momenta after having specified the power spectrum:

$$\sigma_\zeta = \frac{4(1+w)^2}{(5+3w)^2}\frac{A_\zeta}{2(k_0R)^{n_s-1}}\Gamma\left(\frac{n_s+3}{2}\right), \qquad \sigma_1^2(R) = \frac{n_s+3}{2R^2} \quad (5.18)$$

Therefore, the abundance of PBHs obtained from the peaks in the density contrast field:

$$\beta(\delta_c) = \frac{(n_s-1)^{3/2}}{4(3^3\pi)^{1/2}}\frac{\delta_c^2}{\sigma_\delta^2}\exp\left(-\frac{\delta_c^2}{2\sigma_\delta^2}\right). \quad (5.19)$$

Nonetheless, the assumption that the density contrast field acquires gaussianity from the linearized equation (5.1) has been challenged as being too simplistic, and if instead one consider the non-linear relation (4.60) then the density contrast will be inevitably non-gaussian and this kind of non-gaussianity reduces the abundance of PBHs [128].

As a final remark, we have worked under the assumption that primordial black holes form mostly in the radiation era; this assumption can be justified a posteriori by taking the result from the Pres-Schechter formalism. In line of principle, perturbations are going to re-enter the Hubble scales all the time, so in the matter dominated epoch that follows the radiation era, as well; however, a high-value of σ_δ is required for these to collapse into black holes [129]. After the time of recombination, baryonic matter will be in the form of atoms and black holes are likely to be of stellar origin and subdue the Chandrasekhar limit.

Time of formation, scale and e-folds

Earlier when discussing the collapse, we saw that the mass of PBHs comes as fraction of the Hubble mass. Under the assumption that this fraction is fixed we obtain an remarkable result that the black mass is proportional to the cosmic time. The mass of the black hole at formation time is proportional to ρR^3 at collapse time. Then, reprising equations (4.19) and assuming that formation happens in the radiation

epoch, $\bar{H} = 1/2t$ and $\bar{\rho} = 3/32\pi G t^2$, we can relate its mass to the time of re-entry of the perturbation:

$$M_{\rm PBH} = \frac{4\pi\rho R^3}{3} = \gamma \frac{4\pi c^3 \bar{\rho}(t_0)}{3\bar{H}^3(t_0)} = \gamma \frac{c^3 t_0}{G} \approx 7.76 \left(\frac{t_0}{1\rm s}\right) 10^{34} \rm g \approx 3.9 \left(\frac{t_0}{1\rm s}\right) 10^4 M_\odot \quad (5.20)$$

where the speed of light was temporarily restored for clarity. In the last formula, we used the used the value $\gamma = 3^{-3/2}$ for the efficiency factor, as it is frequently done in the literature [130]. This factor is estimated collecting the proportionality of the black hole mass to the Hubble mass. In the case of Carr's model then the proportionality is given by $(1 + \delta(t_*)\delta(t_0)^{-3/2})$, and δ_0 has a limited range for the formation to happen—cf. equation (4.10)—so we can use its lowest value w. Critical collapse hints that the efficiency factor could be as low as zero, still, because of the power law dependence $(\delta(t_*) - \delta_c)^{\gamma_c}$, low values of the mass require some fine tuning for $\delta(t_*)$, being at a fraction $\mathcal{O}(1)$ most of the time.

If we assume that the entropy of the universe is conserved between the time of formation and the matter-radiation equality, then the energy density evolves as $\bar{\rho} \propto g^{-1/3}\bar{a}^{-4}$ [131]—being g is the effective number of relativistic degrees of freedom of the radiation fluid. Following this proportionality, together with the fact that $\bar{a}\bar{H} \propto \bar{a}^{-1}$ in the radiation epoch, we can rewrite equation(5.20) as follows [132]:

$$M_{\rm PBH} = \gamma \left(\frac{k_{\rm eq}}{k_0}\right)^2 \left(\frac{g_{\rm eq}}{g_0}\right)^{1/3} M_{H,\rm eq}, \quad (5.21)$$

where $k_{\rm eq}$ is the comoving wavenumber at equality. In such a way, we have related the mass of the PBH to the Hubble mass at $t_{\rm eq}$, and transferred the dependence on time on the ratio between the re-entry scale and the matter-radiation equality scale. This is quite convenient as we can use the observed cosmological parameters [23] to get:

$$M_{\rm eq} = \frac{4\pi}{3} 2\bar{\rho}_{\rm rad,eq} \bar{H}_{\rm eq}^{-3} = \frac{8\pi}{3} \frac{\bar{\rho}_{\rm rad,0}}{k_{\rm eq}^3 \bar{a}_{\rm eq}}, \quad (5.22)$$

taking $k_{\rm eq} = 0.07\Omega_m h^2 \rm Mpc^-1$, $\Omega_m h^2 = 0.14314$, $\Omega_{\rm rad,0} h^2 = 4.17 \times 10^{-5}$ and $a_{\rm eq} \simeq 3441$, we obtain[3] $M_{\rm eq} \simeq 7 \times 10^{50}$g. Finally, we can use this to work out the scale of re-entry for the collapsing perturbations:

$$\frac{k_0}{\rm Mpc^{-1}} = 2.65 \times 10^{23} \left(\frac{g_0}{3.36}\right)^{1/6} \gamma^{-1/2} \left(\frac{1\rm g}{M_{\rm PBH}}\right)^{1/2}, \quad (5.23)$$

for reference $g_{\rm eq} = 3.36$, and its maximum according to SM particles is $g = 106.75$. Notably, the mass to scale proportionality is $M_{\rm pbh} \propto k^{-2}$ during radiation epoch. As candidates for dark matter, PBHs must have a mass larger than 10^{15}g at formation; this corresponds to scales smaller than $k \sim 10^{22}\rm Mpc^{-1}$.

Alternatively, we can use the time-dependence of the mass on the cosmic time to draw a link with the time the seeds where generated during the inflationary epoch.

[3] We worked under the assumption of 3 massless species of neutrinos.

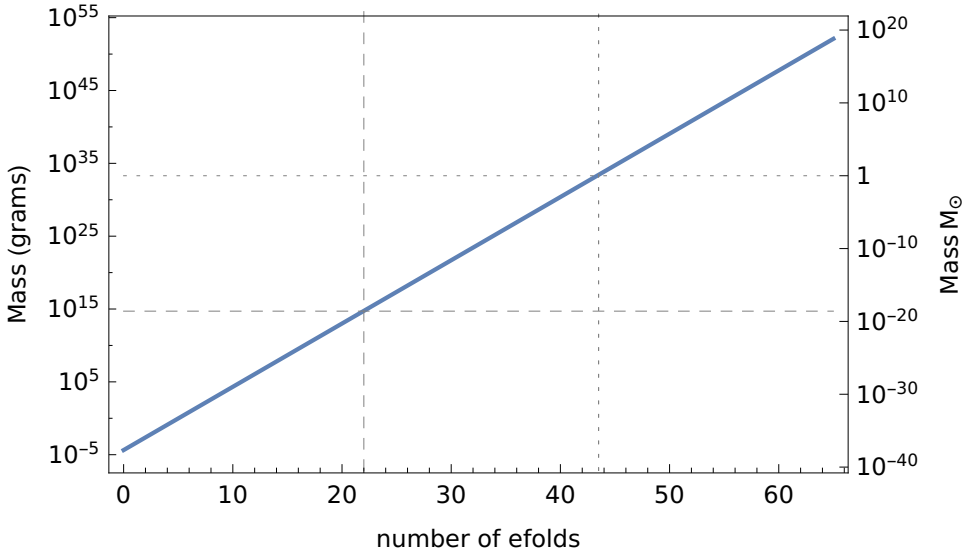

Figure 5.1. The mass of a PBH as a function of e-fold number neglecting reheating. For it we have approximated $H_N \approx H_{\rm end}$, as the Hubble parameter is approximately constant during inflation, and used the upper bound $H_{\rm end} < 2.7 \times 10^{-5} M_p$ set by the Planck collaboration [32]. The dotted and dashed lines serve as a reference for an easier reading of the e-folds corresponding to the solar mass and the critical mass distinguishing evaporated from non-evaporated PBHs respectively.

The point is that one the curvature perturbation where generated and stretched beyond the Hubble scale, they remain constant. Consequently, we can associate the physical radius of the curvature perturbation at time of re-entry with a comoving wavenumber $R_0 = \bar{a}(t_0) k_0^- 1$. This wavenumber exited the Hubble scale during inflation some N e-folds before the end of inflation, at which time $k_0 = \bar{a}_N \bar{H}_N = e^{-N} H_N$, being H_N the Hubble parameter at that time. If we follow [133] and take the radiation-dominated era to follow inflation, then using the evolution of the scale factor,one can write:

$$\bar{a}(t) = \left(\frac{t}{t_{\rm end}}\right)^{1/2} = \sqrt{2 H_{\rm end} t} \tag{5.24}$$

where the subscript *end* stands for the quantities being evaluated at the end of inflation. It follows that cosmic time of re-entry and black hole mass can be written as:

$$t_0 = \frac{\bar{H}_{\rm end} e^{2N}}{2\bar{H}_N^2} \approx \frac{e^{2N}}{2\bar{H}_{end}}, \quad \Rightarrow \quad M_{\rm PBH} = \gamma \frac{\bar{H}_{\rm end} e^{2N}}{2\bar{H}_N^2 G} \approx \gamma \frac{4\pi M_p^2}{H_{\rm end}} e^{2N}, \tag{5.25}$$

where the approximation used the fact that the Hubble parameter is approximately constant during inflation. If a period of reheating sits in between inflation and the radiation epoch, the evolution of the scale factor must be modified:

$$\bar{a}(t) = \left(\frac{t}{t_{\rm rh}}\right)^{\frac{1}{2}} \left(\frac{t_{\rm rh}}{t_{\rm end}}\right)^{\frac{2}{3(1+w)}} = \bar{H}_{\rm end}^{\frac{2}{3(1+w)}} \bar{H}_{\rm rh}^{-\frac{1-3w}{6(1+w)}} \sqrt{2t}, \tag{5.26}$$

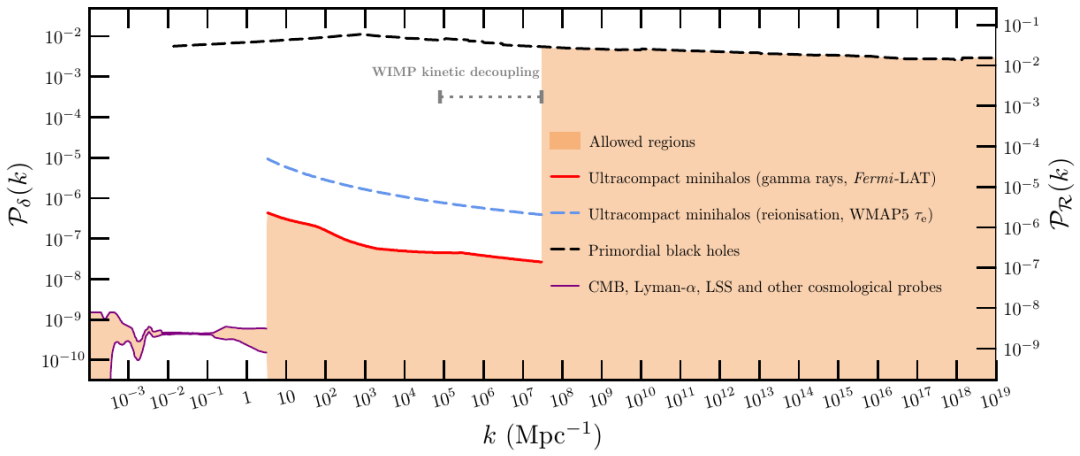

Figure 5.2. In the picture, taken from [134], constraints on the power spectrum are shown for different scales. The Strongest constraints are given by CMB and LSS on the left; whereas, the weakest constraints come from the lack of observations of PBHs on the right.

where now we introduced the time of the end of reheating and its associated Hubble parameter, and w is now the adiabatic parameter of the reheating epoch. The latter expression has the same form of (5.24), so we obtain the same result upon substitution of $\bar{H}_{\rm end} \to \bar{H}_{\rm end}^{4/3(1+w)}/\bar{H}_{\rm rh}^{(1-3w)/3(1+w)}$. The PBH mass is affected as follows:

$$M_{\rm PBH} = \gamma \frac{\bar{H}_{\rm end}^{4/3(1+w)} e^{2N}}{2G\bar{H}_N^2 \bar{H}_{rh}^{(1-3w)/3(1+w)}} \approx 4\pi\gamma M_p^2 \left(\frac{\bar{H}_{\rm end}^{-2-3w}}{\bar{H}_{\rm rh}^{1-3w}}\right)^{1/3(1+w)} e^{2N}. \tag{5.27}$$

hence evincing that the mass could be sensitive to the reheating phase.

As a result, the mass of primordial black holes could be related to cosmic time and the e-folds at which various modes of curvature perturbation exited the Hubble scale. For this reason, if ever observed, such black holes could allow to probe specific times of the inflationary period. The observations of Cosmic Microwave Background and Large Scale Structure also allow to probe these modes, even if the only probe a small window on the scales of its power spectrum. In fact, they span a range of wavenumber between $10^{-4}{\rm Mpc}^{-1} \lesssim k \lesssim 0.1{\rm Mpc}^{-1}$, a window of about 7 e-folds of perturbations that exited the inflation around $56-63$ e-folds [133]. They pose very stringent limits to the power spectrum, which seems to be in accordance with the adiabatic, single-field, inflationary picture presented in Chapter 3 and leading to the almost scale-invariant power spectrum of spectral index $n_s = 0.965 \pm 0.004$ and pivot scale $k_p = 0.005{\rm Mpc}^{-1}$.At smaller scales, observations from the y- and μ-distortions[4] of CMB and observation of Ultra-Compact Mini-Haloes(UCMH) pro-

[4]These stand for Compton scattering of photons off electrons, that creates a non-vanishing chemical potential(μ-) and blue-shifts the CMB's photons(y-type).

duce weaker constraints [134] on a window of $10^{-1}\text{Mpc}^{-1} \lesssim k \lesssim 10^{8} Mpc^{-1}$ corresponding to a range of 56 to 40 e-folds before the end of inflation [133]. The bound on the density contrast that can be derived ought to be respected by the primordial population of black holes, which in these two windows is strongly suppressed. Yet, as shown in picture 5.2 there is still a ~ 40 e-folds window leaving the density contrast fluctuations unconstrained.

Boosting the power spectrum

Although no exact mechanism prevent black holes to form during the inflationary epoch and some exact solutions exist for black holes in a cosmological background (e.g. Schwarzschild-de Sitter and McVittie solutions [135]), it is generally argued that the exponential expansion due to inflation dilutes black hole abundance to negligible values, and so eventual black holes formed during inflation would not be of particular interest and can be neglected in our discussion. Nonetheless, since the power spectrum of scalar perturbations is not exactly scale invariant, there are several mechanisms with which inflation generates the seeds for PBHs and, vice versa, primordial black holes can be used to constrain the inflaton potential. In order for PBHs to form the curvature perturbation's power spectrum needs to be enhanced from it value of 10^{-9} to its threshold value, this is excluded on scales between $10^{-4}\text{Mpc}^{-1} \lesssim k \lesssim 10^{8}\text{Mpc}^{-1}$. This could be attained by requiring special modifications to the inflationary picture, which we are going to discuss briefly.

Generating peaks with single field inflation

One way to boost the power spectrum was firstly proposed by Ivanov, Naselsky and Novikov [136] is by asking the slow-roll conditions to halt for some time at some scale that is unconstrained by the observations. They obtained this by exploiting that the proportionality of the curvature power spectrum(cf. 3.44) $\mathcal{P}_\zeta(k) \propto 1/V_{,\phi}^2$, so that, upon the requirement of presenting a plateau—i.e. $V_{,\phi} = 0$—the curvature power spectrum develops a spike at some small e-fold number. Following this line, other authors have proposed that the plateau could have been as well interchanged with the simpler requirement of local extrema [137], or an inflection point [138]. In all cases, the slow-roll conditions needs to be broken in a range somewhat larger than the region of interest in order to guarantee smoothness of the potential; yet, the duration of this break should not be to long, lest too many black holes are generated.

This lead to the realization [139] that this condition alone is not sufficient, as inflation might abruptly end too soon without reaching the needed number of e-folds; thence, an additional requirement is needed: the so-called ultra-slow-roll regime. This regime is characterized by a phase in which the slow roll ϵ stay small but the slow-roll η need not to be small, so that the inflaton field enters a phase of strong deceleration due to the almost vanishing of $V_{,\phi}$. In this way, it is possible to maintain the inflection point in the potential and have a successive long phase of ultra

slow-roll which does not kill inflation and boost the primordial curvature spectrum according to its duration, $\mathcal{P}_\zeta \propto e^{N_{\rm usr}}$. The increase in the power spectrum obtained it such way might still not be sufficient to guarantee the formation of PBHs in the radiation era, but it could be enough to generate seeds that would collapse during the QCD phase transition.

Two-field Inflation

An alternative mechanisms to boost the power spectrum at some smaller scale is to introduce a second scalar field in the inflationary picture, sometimes called spectator or waterfall in what is sometimes called hybrid inflation [132]. The inflationary potential $V(\phi, \psi)$ is given by the sum of two fields respective potentials, which as an example could read as:

$$\begin{aligned} V(\phi) &= V_0 + \frac{1}{2} m_\phi^2(\phi)\phi^2, \\ V(\psi) &= -\sqrt{\frac{V_0\kappa}{6}}\psi^2 + \frac{\kappa}{24}\psi^4, \\ V_{\rm int} = \frac{\lambda}{4}\phi^2\psi^2 \quad &\Rightarrow \quad V(\phi,\psi) = V_\phi + V_\psi + V_{\rm int}. \end{aligned} \tag{5.28}$$

In such scenario, the spectator field lives in a false vacuum for most of the inflationary epoch, without modifying the usual inflationary picture which is corroborated from observations at large scale. The inflaton dominated the as long as $\phi^2 > \sqrt{(8V_0\kappa/3\lambda^2)}$. At smaller scales(smaller e-folds from the end of inflation), once the inflaton drops below that critical value, the spectator acquire a non-zero expectation value and comes to dominate [132]. The alternating dominance of the two fields give rise to two period of inflation with a break in the middle, and it is during this latter period the slow-roll conditions are allowed to be violated and the primordial curvature perturbation are amplified [140]. One disadvantage of this kind of model is the generation of isocurvature perturbations due to the presence of two fields, which is disfavoured by observations at least on the CMB scale [32].

Parametric resonances

Another possibility is given by the case in which, toward the end of inflation, when $|V_{,\phi\phi}| \gg \bar{H}^2$, the long wavelength component of the dominant scalar field of inflation assumes an oscillatory behaviour. This might cause a resonance with either the inflaton, by self-interaction, or the spectator field in a case of hybrid inflation, which amplifies the small wavelength component [141]. This, in turn, results in a magnification of the curvature perturbation on sub-Hubble scales at late e-fold number, $N \sim 3$; thus making it easy for PBHs to form if inflation ends in a matter-like reheating phase [142], sometimes referred as early matter-domination epoch. These primordial black holes would be very light; hence, they would evaporate before Nucleosynthesis and have minor observational significance.

Nonetheless, a different kind of parametric resonance has been recently proposed [141], where the presence of a non-canonical kinetic term of the inflaton results in

an oscillating sound speed for the curvature perturbation inside the Hubble sphere. If we denote by k_* the oscillation frequency, then the curvature perturbation power spectrum would present peak at harmonic frequencies, $k = 2k_*, 3k_*, ...$, in addition of its usual form. Albeit a bit contrived, such a scenario has the advantage of producing several windows at different scales for eventual seeds of primordial black holes without affecting particularly the scale-invariant spectrum.

Observational Constraints

We now turn to discuss the present observational constraints of PBHs. As emphasized earlier, PBHs are still speculative, an unobserved prediction of cosmology. Upon formation, their mass abundance contributes to increment the total of dark matter content of the universe. This can be understood under the assumption that the effects due to eventual charges are negligible. Again, assuming the formation happens in the radiation era, the largest window for the mass of black holes is given by:

$$\gamma\left(\frac{k_{\rm eq}}{k_{\rm rh}}\right)^2\left(\frac{g_{\rm eq}}{g_{\rm rh}}\right)^{1/3} M_{H,\rm eq} \lesssim M_{\rm PBH} \lesssim \gamma M_{H,\rm eq} \sim 10^{50}\text{g} \equiv 10^{16} M_\odot, \tag{5.29}$$

where we used (5.21) to determinate the extrema. The lower bound depends on the specifics of reheating, which are still unclear and unconstrained by observations as it involves very small scales.If one ignores the details of reheating and naively assumes that radiation epochs follows directly after inflation, then it could conclude that the minimal mass of black holes could be as low at zero; this prediction can be expected to fail sooner than the Planck's scale it is reached.

In addition, another effect should be taken into account when considering black holes of low mass, notably their evaporation, a process discovered in 1975 by Hawking [4]. In its original derivation, he considered the quantization of a massless scalar field in the background of a Schwarzschild spacetime and found out that black holes emit quanta of this field with a blackbody spectrum[5] with a temperature: $T \propto 1/M$. The same process was derived again with various formalisms and for massive field of various spin [143][144][145] and it is considered a solid theoretical prediction. In this way, black holes lose eventual charges and angular momentum by emission of lighter quanta on a time scale smaller than they lose their mass [146].

In each case, the evaporation happens when the temperature of the black hole is higher than that of the surrounding universe. This allows us to determine a critical mass $M_{\rm cr} = 5.1 \times 10^{14}\text{g} = 2.5 * 10^{-19} M_\odot$, which can be obtained by comparing the black hole lifetime (.22) with the age of the universe, $t_{\rm now} = 13.8\text{Gyr}$. Black holes lighter than $\sim 10^{15}\text{g}$ will have been evaporated by present time, and constraint can be placed on their mass spectrum by following the requirement of not having altered the understood processes in the early universe. Heavier black holes are either undergoing evaporation now or are so massive that this process is negligible; thus,

[5]Details on the derivation of the Hawking radiation can be found in the appendix.

they are still gravitationally relevant today. In the following we are going to focus on these two classes separately.

Constraints on evaporated Black Holes

We will now discuss the origin of some of the constraints on the mass function of small PBHs which have evaporated in the early universe. Once again, we are going to assume a monocromatic mass spectrum to get conservative bounds. For this purpose, once we write the mass of the PBHs in terms of the Hubble mass, $\beta(M)$ becomes dependent on the γ and γ, which are rather uncertain, so it is convenient to define $\beta'(M) = \gamma^{1/2}(g/106.75)^{=1/4}\beta(M)$ in order to factor out the dependence.

The critical mass $M_{\rm cr}$ corresponds to a black hole temperature of 21MeV; consequently, all particles with mass lower than this value will be produced by the evaporation. The spectrum of injected particles will have to components: a primary component which create the particle directly, and a secondary component made by the decay and hadronization of primary component. The spectrum of secondary photons emitted is peaked at $m_{\pi^0}/2 \approx 68$MeV independently of the mass of a black hole due to the decay of soft pions [144], black holes less massive than this temperature will have the photon emission dominated by secondary component. These can be used for the constraints coming from the observation of x- and $\gamma-$ray background. The total spectrum of photons emitted from primordial is peaked at M_{cr} because photons from black holes with $M > M_{\rm cr}$ are at lower temperatures because the secondary emission is hindered; whereas photons from $M < M_{\rm cr}$ have lower energy because they get redshifted. This correspond to a sharp discontinuity at $M_{\rm cr}$ that it is transferred to a discontinuity in the upper bound of β' [120]:

$$\beta'(M) < \begin{cases} 3\times 10^{-27}(M/M_{\rm cr})^{-5/2-2\epsilon} & M < M_{\rm cr}, \\ 4\times 10^{-26}(M/M_{\rm cr})^{7/2+\epsilon} & M > M_{\rm cr}, \end{cases} \tag{5.30}$$

where ϵ is a parameter that depends on the observations and fluctuate between 0.1 and 0.4. The discontinuity is a consequence of the requirement of monocromatic mass spectrum for the primordial black holes and it is expected to be smoothed in a more realistic scenario in which mass are spread [120]. Moreover, if PBHs are clustered into the galactic bulge, instead of being uniformly distributed in the universe, we can also use the galactic gamma ray background to constrain their abundance[120]. The bound from energetic photons lose validity for $M < 3\times 10^{13}$g as below this limit the interaction with matter activate processes of pair-production off of hydrogen and helium nuclei.

This gives us a way to compare the effects against the characteristic of Big Bang Nucleosynthesis(BBN), which would have been affected if a too numerous population of primordial black holes had occurred. For instance, the production of high-energy pair of neutrinos-antineutrinos would change the neutron-proton ratio at electroweak scale resulting in an increased ^4He production in the range 10^9-10^{11}g [120]. Another effect of evaporation during BBN epoch is the increase in entropy: if too abundant,

the radiation from black holes would modify baryon-to-entropy with consequences on the ratio of ^4He to deuterium D; in a similar manner, emission of either neutron-antineutron or nucleon-antinucleon pairs would as well increase the abundance of D by spallation processes of ^4He, affecting black holes of mass $10^9 - 10^{13}$g. Then, for black holes of mass $> 10^{10}$g too copious photon emission could dissociate D, ^6Li, ^7Li and ^3He [120].

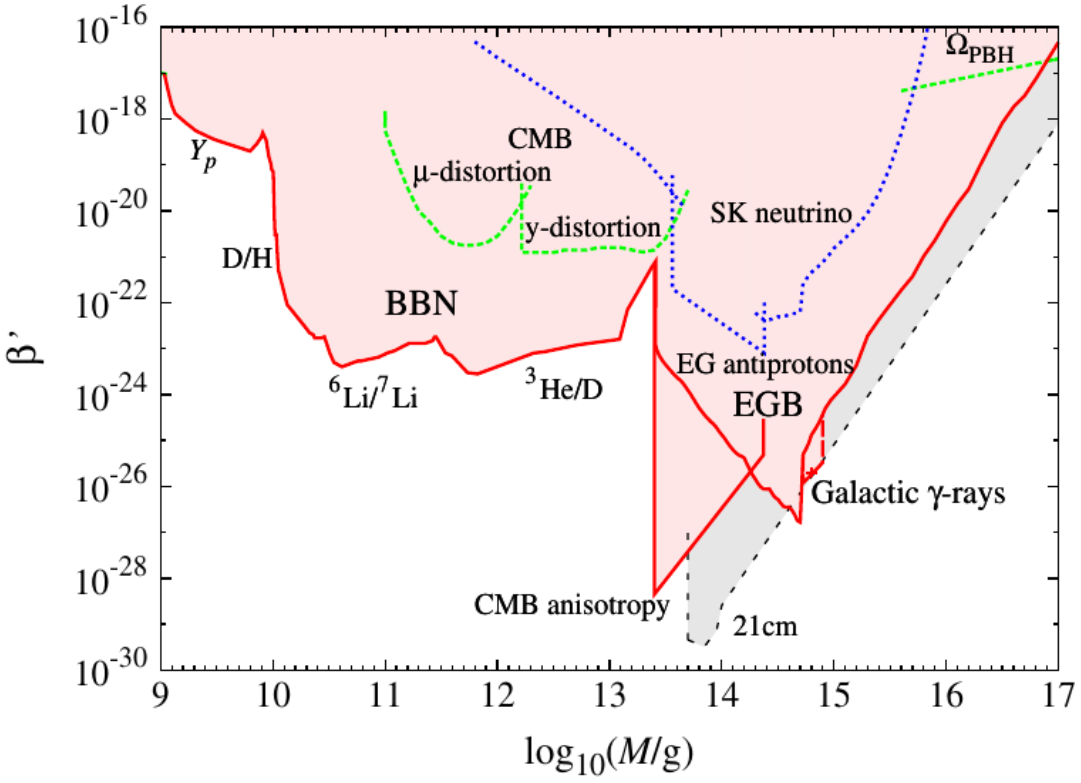

Figure 5.3. The constraints on evaporated PBH mass abundance for a monocromatic mass spectrum. The red line gives the strongest bounds due to Big Bang Nucleosynthesis and gamma ray background. The picture is taken from [120].

Bounds obtained from the Big Bang Nucleosynthesis [147] are shown on the left part of figure 5.3. The right part is dominated by the already discussed gamma ray background constraints. In between these two, the CMB anisotropies limit the initial mass abundance; this is because black hole evaporation would make more uniform small scale anisotropies after recombination. The emission of e^{-e^+} pairs from black holes would scatter off CMB photons in an energy region above the reionisation threshold; this means that before the recombination the same process had happen by the mean of thermal collisions which kept the hydrogen nuclei ionized. The lowest mass at which these observations serve as a useful constraint for PBH is $M = 2.5 \times 10^{13}$g, which is the mass above which evaporation continues after recombination; on the other hand, the heating of CMB by electron-positron pair is no longer effective once opacity falls too low, which takes place at redshift $z = 6$ or

equivalently $M = 2.4 \times 10^{14}$g. The related bound on the initial mass abundance is [120][6]:

$$\beta'(M) < 3 \times 10^{-30} \left(\frac{M}{10^{13}\text{g}} \right)^{3.1}. \tag{5.31}$$

Weaker constraints can be obtained by taking into consideration the photon-to-baryon ratio, observed at $\sim 10^9$, it can be used to constraints $\beta'(M) < 10^9 (M_{\text{Pl}}/M) \approx 10^4\text{g}/M$ [148]; telling that only black holes smaller than 10^4g could generate all of the CMB. Otherwise, photon emission from $10^{11}\text{g} < M < 10^{13}\text{g}$ black holes would produce CMB distorsions by emission of photon after freeze-out of the double Compton channel, leading to the development of a chemical potential for photons. The flux of cosmic rays reaching Earth contains an antiproton-to-proton ratio lower that 10^{-4}; PBHs, which produce them in equal amount, should be responsible to the antiprotons flux because the production by evaporation has a cut-off below $0.2GeV$, whereas cosmic rays production of antiproton by spallation off interstellar medium has a cut-off below $2GeV$. Another minor constraint comes from the emission of neutrinos from PBHs, the spectrum of which is similar to that of photons up to a normalization factor [120]. The observation of the neutrino background could in principle help to constraint very precisely the black holes with a longer lifetime than the time of neutrino decoupling. In any case, observation of electronic antineutrinos in the Super Kamiokande(SK) experiment gave us a way of constraining the initial abundance of primordial black holes, which is weaker than the gamma ray background [120].

At last, one last prospective constraint on evaporated black holes could come from absorption band of hydrogen, the 21-cm line [149]. In fact, evaporation of PBHs would heat up the intergalactic medium in region of the universe at red-shift $z \gtrsim 6$ and consequently would cause emission rather than absorption of hydrogen clouds not yet bounded into stars. This bound is shown in the Figure 5.3 by the dashed line on the left. This is of particular interest because the results of EDGES [150] experiment shown an existing discrepancy between the ΛCDM model and observations, hinting that either the intergalactic medium was colder or the CMB hotter than expected.

Constraints on non-evaporated Black Holes

Now we turn our attention to the constraints to primordial black holes with a lifetime longer than the age of the universe, thus that did not have time to evaporate completely. This class of primordial black hole are suitable candidates for constitute part of the Dark Matter present in the universe. As such, we can immediately pose

[6]The actual paper includes a factor $(0.1/f_H)$, with f_H is the fraction of emission coming out in electrons and positron. However, we did not included this factor in the formula because the numerical value used in the same paper is $f_H = 0.1$ which cancels out in the end.

a constraint by requiring $\Omega_{\rm PBH} < \Omega_{\rm CDM} \approx 0.12/h^2 = 0.27$, it can be written [120]:

$$\beta'(M) < 2.04^{-18}\left(\frac{\Omega_{\rm CDM}}{0.25}\right)\left(\frac{h}{0.72}\right)^2\left(\frac{M}{10^{15}{\rm g}}\right)^{1/2}, \tag{5.32}$$

additional constraint will be lower than this value and are usually expressed in terms of the fraction to dark matter $f = \Omega_{\rm PBH}/\Omega_{\rm CDM} = 4.1 \times 10^8 \beta'(M)(M/M_\odot)^{-1/2}$. The constraints we are going to comment are summarized in Figure 5.4.

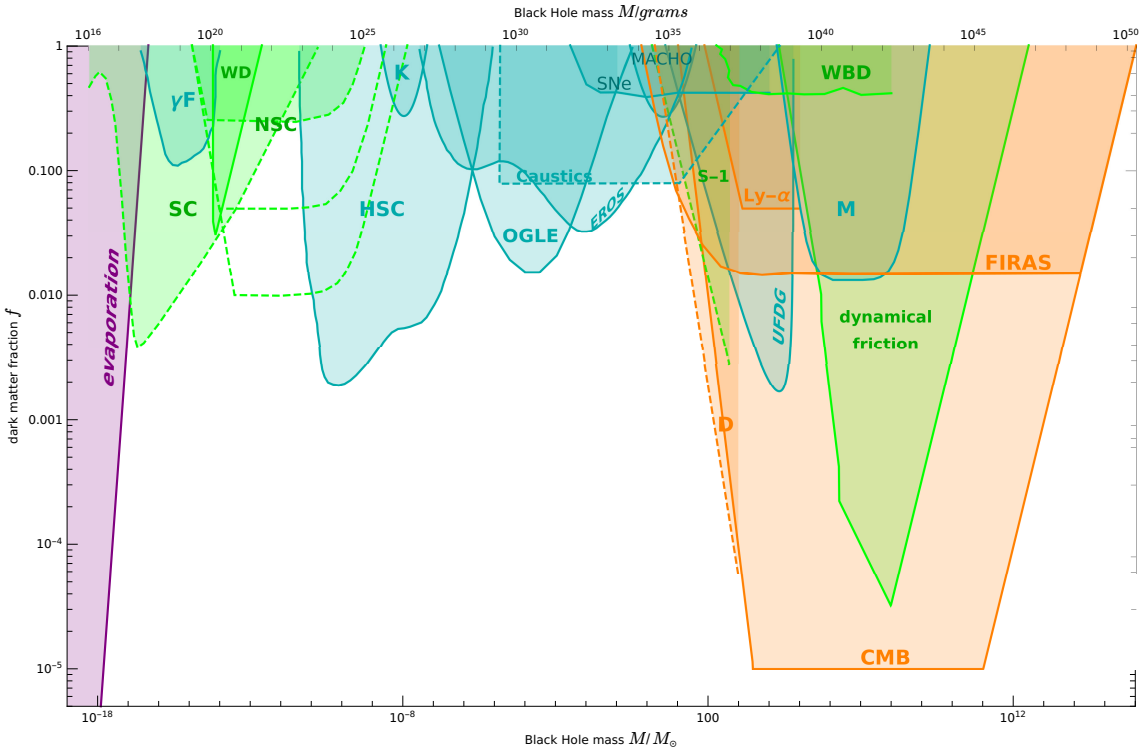

Figure 5.4. The constrained region is shown by the shade areas in the figure color-coded according to their character: purple is the constraint of evaporation, green stand for dynamical constraints, blue are constraints due to gravitational lensing and orange constraints coming from accretion of black holes by absorption of radiation. Dashed lines stand for possible constraints whose robustness needs to better assessed or criticized. In this figure we updated a similar exclusion plot firstly produced in [130] with the studies cited in this section.

Starting from lower masses, the first constraint comes from gamma ray emission from black holes that have not completed their evaporation yet; gamma ray observations pose the severest constraint on the possibility that PBHs could be part of dark matter.

Even if PBHs might not to be responsible for the gamma ray bursts we observe, PBHs in the mass range $10^{17} - 10^{20}$g possess a Schwarzschild radius comparable to wavelength of gamma ray photons, and so they can cause interference patterns known as femtolensing(γF); observations [151] constraint the fraction of dark matter in the form of black hole to be less that $10 - 20$

Small black holes in the range $10^{20} - 10^{22}$g if too abundant could disrupt the stability of white dwarfs(WD), small stars whose nuclear reaction are in balance with the gravitational effects thanks to the electron degeneracy pressure. If small black holes were to pass through white dwarf, they would have negligible gravitational effects, but could instead heat up the region surrounding their trajectory and thus cause runaway processes that triggers the explosion of the star [152].

In a similar fashion, constraints can be obtained by asking that the gravitational interaction between stars and black holes is such that when the latter passing through them lose enough kinetic energy to get captured in their core; nonetheless disturbing their stability. These constraints have been analyzed in the case of stars in the process of formation(SC) [153] or for neutron stars(NSC)[7] [154] in the region of $10^{17} - 10^{25}$g, black holes in the sublunar-mass range $10^{-17} - 10^{-9} M_{\odot}$.

Going higher, from lunar- to solar-masses, the fraction to dark-matter is heavily constrained above $\sim 1\%$ by numerous gravitational microlensing experiments:

- the Kepler telescope(K) having an main goal the observation of planets transiting in front of their stars [155];
- the Subaru Hyper Suprime-Cam(HSC) experiment which performed a millilensing survey in the halos of Milky Way and Andromeda galaxies, which up-to-date constitute the strongest and more robust constraint [156];
- the EROS [157] and MACHO [158] experiments which looked for microlensing events in the Magellanic Cloud, constrained to less than $\sim 10\%$ the possibility of dark matter being composed of compact objects in the $10^{-7} - 1 M_{\odot}$ range;
- the OGLE [159] experiment, observing stars in the Galactic Bulge, surveyed microlensing events and pushed to $\sim 1\%$ the constraints in the region $10^{-6} - 10^{-2} M_{\odot}$. Nonetheless, they claimed to have observed 6 events which could be compatible with the possibility of PBHs of earth-mass, due to the low probability of observing free-floating planetary objects in such a region. However, independent confirmation is needed to confirm this claim;
- microlensing of light coming from explosions of Super-Novae(SNe) [160] reduced to less than $\tilde{3}0\%$ fraction of PBH of stellar mass as component of Dark Matter. This region in of particular interest for the gravitational interferometry experiments on Earth;
- another possible constraint, in this the Earth-to-solar mass range, could come from the observation of caustic crossing[8] events, in which case the caustic

[7] In the Figure 5.4 this constraint is presented for 3 different dark matter density profiles: $\rho_{\rm DM} = (4 \times 10^2, 2 * 10^3, 10^4) {\rm GeVcm}^{-3}$. Only the most conservative bound is shaded.

[8] The caustic of an extended gravitational lens is a region around the magnifying source in which the magnification becomes infinity. In practice, magnification does not diverge because of finite size of the objects.

would be broken or its magnification reduced due the strong field of the compact object transiting through it [161].

These constraints leave an open window for the possibility of PBHs forming more than $\sim 10\%$ at solar mass ranges $\sim 1 - 100 M_\odot$.

Above this mass window, tighter constraints come from the accretion of PBHs at the expense of the surrounding gas. In the radiation era, PBHs are not expected to accrete appreciably, massive ones could do so in between the matter-radiation equality and recombination and therefore could leave footprints in the cosmic microwave background. This has been analyzed for spherical accretion a in [162] using the data from the FIRAS(Far Infrared Absolute Spectrometer) and WMAP3 observations and in [163] using Planck15 data together with a model of accretion into a disk; thus, limiting to less than 10^{-5} the possibility of PBH to form dark matter in the range $10^3 - 10^{11}_\odot$.

Within these bounds, other constraints reinforce this conclusion. Most notably, the effect of dynamical friction [164] which consists in the transfer of kinetic energy from PBHs to nearby passing objects inside galaxies by sling-shot mechanism. As a result, the more massive PBHs spiral down toward the center of the galaxies and their abundance can be constrained by requiring that the mass concentration of the center of galaxies do not exceed the observed limits.

In a similar fashion, if massive PBHs dwelt inside Ultra Faint Dwarf Galaxies—satellite galaxies to the Milky Way and Andromeda which possess lower luminosity and higher mass within their half radius, thence being ideal places for a concentration of dark matter—then stars and black holes would frequently interact gravitationally. So while massive black holes experience dynamical friction, stars are subject do dynamical heating which, in average, would spread the star distribution wider. On the contrary, if dark matter is composed of objects lighter than the stars, the roles are swapped and stars cool down. Following this line of though, an upper bound for f in ranges $> 10 M_\odot$ was obtained in [165](UFDG) for ultra-faint dwarf galaxies together with the cluster in Eridanus, and in [166] for the specific case of Segue 1(S-1), a Milky Way's satellite.

If PBHs were present during the dark ages, they could have contributed to early formation of structures; in such case, hydrogen clouds would have been illuminated by the light emitted from the accretion around black holes. This has been used in conjunction with the observation of Lyman-α forest[9], originally by [167], to argue that if primordial black holes with mass $\gtrsim 10^4 M_\odot$ formed all dark matter that the flux would have been incompatible with observations. This analytical result overestimated some parameter, but it has been worked out again by comparing numerical simulations to observations in [168] and with updated observations in [169] which is the curve($\mathsf{Ly} - \alpha$).

[9]Lyman-α are the transitions lines between the ground and the excited states of hydrogen's electron orbitals.

Another bound was obtained by requiring PBHs not to disrupt wide star binaries, which being loosely bound would be easily separated if experienced dynamical heating by a massive black hole passing by. The disruption could be catastrophic, if the disruption happens as a consequence of a single encounter, or diffusive for multiple events. Comparing time scales of the disruption to the age of the binaries, a bound(WBD) is obtained in [170] out of 4 possible wide binary systems.

We conclude with a constraint coming from millilensing(M), which takes its name from the fact that supermassive compact objects are expected to produce a two-fold image of the same object with a separation of milliarcseconds. The result [171] of Very-Long Baseline Interferometry(VLBI) observation of 300 radio sources was inconclusive, thus limiting the possibility of uniformly distributed supermassive($\sim 10^6 - 10^8 M_\odot$) PBHs to less that $\sim 1\%$ of Dark Matter.

Consequences and generalizations of constraints

The constraints that have been considered this far allow to exclude the possibility that PBHs form the totality of dark matter at any mass range. It is possible to identify at least three possible windows for the possibility that they form a significant fraction of total dark matter:

- sublunar-mass black holes: this window lies between the constraints for neutron stars capture and the microlensing experiments. The first study depends on the assumption that dark matter is present in globular cluster which is often criticized; if neglected then f can be extended up to unity in the region between brown dwarf disruption and the HSC experiment.

- earth-mass black holes: between the HSC and OGLE microlensing surveys, the fraction could attain values of $\mathcal{O}(1) - \mathcal{O}(10)\%$, and as already mentioned some observational anomalies might have been spotted around this window.

- intermediate-mass black holes: this window stretches between the microlensing and accretion bounds. It is of particular interest because the LIGO-VIRGO black-hole mergers event observed with the first detection of gravitational waves are in this window, and it is still debated if these events have primordial—formed during the QCD phase transition—or astrophysical origin—forming from the collapse of binary of population III stars [172]. If primordial, these black holes would have already cast doubt on some of the bound obtained by accretion argument.

For completeness, the bound on capture by stars is often neglected by many papers, for the same reason of the doubtful assumption on the dark matter density, but this has the consequence of opening another window for subatomic-sized black holes, and depending on the ϵ parameter of the gamma-ray bound f could vary between $0.55 - 0.8$ in this window [130]. Of minor relevance, especially because of their theoretical uncertainty, there are two other possible windows that lie below the Big

Bang Nucleosynthesis constraints—if evaporation of black holes could leave stable relics [173]—and above the CMB bounds for super-massive black holes.

All things considered, it must be stressed that the constraints are obtained under the assumptions of 1) a monocromatic mass function, 2) the mass of PBHs is fixed-fraction of Hubble mass, 3) PBHs are uniformly distributed in the universe after formation.

The assumption 1), as stated previously, is admittedly over-simplifying and it is used to derive conservative bounds. However, one simple extension one could make is to considered a more realistic case of an extended mass-function; corresponding to a scenario that different black holes form with different masses and at different times. To account for the spread in mass, instead of using $\beta = M_{\rm PBH} n/\bar{\rho}_{\rm tot}$, it is more convenient to introduce [121] the following abundance function:

$$\psi(M) \propto M \frac{\mathrm{d}\, n(M)}{\mathrm{d}\, M}, \tag{5.33}$$

where M is intended as the mass of PBHs, i.e. we dropped the subscript. As our purpose is to work with the fraction to dark matter, we pick the normalization of the previous function to be:

$$f = \int \mathrm{d}\, M \psi(M). \tag{5.34}$$

The monocromatic bounds on f can be generalizes to this case by reparametrizing a given astrophysical observable that depends on the abundance, i.e. $O[\psi(M)]$, in such a way to functionally expanded:

$$O[\psi(M)] = O_0 + \int \mathrm{d}\, M \psi(M) K_1(M) + \int \mathrm{d}\, M_1\, \mathrm{d}\, M_2 \psi(M_1)\psi(M_2) K_2(M_1, M_2) + \dots \tag{5.35}$$

where O_0 is the contribution of the background and K_j depend on the physical details of the observable which can be obtained as follows. If a given measurement yields $O[\psi] \leq O_{\rm exp}$ for the monocromatic case, equation (5.35) implies[10]:

$$f \leq \frac{O_{\rm exp} - O_0}{K_1(M_0)}, \quad \Rightarrow \quad K_1(M) = \frac{f_{\rm max,mono}(M)}{O_{\rm exp} - O_0}, \tag{5.36}$$

where $f_{\rm max,mono}$ is the monocromatic bound at the scale M.
For the non-monocromatic case, we replace the latter value of $K_1(M)$ in (5.35) so as to get:

$$\int \mathrm{d}\, M \frac{\psi(M)}{f_{\rm max}(M)} \leq 1, \tag{5.37}$$

which can be integrated over a mass range (M_1, M_2) to obtain $f_{\rm max}(M)$ in the non-monocromatic case, once $\psi(M)$ is specified. The exact form of $\psi(M)$ is actually

[10] Using $\psi_{\rm mono}(M) = M_0 \delta(M - M_0)$.

dependent on the specific model of PBH formation; however, a common choice is a quasi-lognormal form:

$$\psi(M) \propto \frac{1}{\sqrt{2\pi}\sigma M} \exp\left(- \frac{\log^2(M/M_c)}{2\sigma^2} \right), \tag{5.38}$$

where M_c is defined by the peak of the function $M\psi(M)$ [121]. The reason it represents a good choice is that it has been shown to approximate a large class of models as long as they a produce smooth symmetric peak in the power spectrum. For this specific case, the lognormal bounds found[11] in [121] are tighter than the monocromatic case, but might allow for the totality of dark matter to be in the form of PBHs if some dynamical constraints are relaxed. Independently from the specific form of $\psi(M)$, using this conscription to generalize the bounds can only result in stricter bounds than the monocromatic case, tough.

It is important to notice that if, instead of the assumption 2), critical collapse is taken into account, then the mass function necessarily spreads and the abundance function get broader than the monocromatic case, as studied in [107]. It has also been argued that critical collapse or inclusion of non-sphericity could make unreliable some of the constraints by modifying the underlying principles within which they were obtained [174]. Yet, quantitative studies on how these could affect the bounds have not been performed.

On the other hand, the assumption 3) seems to be the weakest. In fact, if PBH distribution were not to be uniform, and instead their formation were likely to happen in clusters as a result of successive generations [175] or by the introduction of a scale-dependent bias[12] [176], then they would be able to merger with a certain frequency at later times; thence, clustering could substantially help to evade the microlensing and CMB accretion constraints. This argument has been challenged in [177] by the reason that mergers would so contribute to the Stochastic Gravitational Wave Background which has not been observed to date. To present, no consensus has been reached on the possibility of clustering; in [178] a neutral stance was taken and some arguments on both sides were re-assessed with the final conclusion that clustering should not be relevant for the intermediate-mass window.

[11] The paper considers only the constraints coming from evaporation, femtolensing, microlensing and CMB.

[12] E.G. If perturbations are sitting on the crest of a long-wavelength mode the threshold of formation could be lowered with respect to those lying in the trough.

Chapter 6

Conclusion

In this thesis, we have explored the concept of PBHs, from the origin of the cosmological perturbations that might lead to their formation, to their formation mechanisms and, finally, the actual observational status of this prediction of Cosmology. Motivated by the assumption that the Universe must have undergone through a phase in which matter and radiation where coupled in a state of hot dense plasma, regions too dense might have encountered favourable conditions for the collapse in the form of black holes of different sizes, some of which could have survived until present time and, as such, constitute a possible component for at least part of the Dark Matter content of the Universe.

We considered how these kind of black holes are characterized by a scalar perturbation in the metric, or equivalently the energy density, of the a background, homogeneous and isotropic, expanding spacetime. These perturbations can be described by the use of two formulations of perturbation theory, namely the Cosmological Perturbation Theory and the Gradient Expansion, which differ in the definitions of what can be considered a small quantity in a cosmological context. In addition, we justified how this scalar field perturbations emerge as a result of the inflationary paradigm.

A significant part of this thesis was devoted to examine some models of PBHs formation and the thresholds above which the perturbations would inevitably collapse into PBHs. A basic way to estimate this is by asking the characteristic length of the perturbation to be larger than the Jeans radius, the length above which the pull induced by gravitational effects prevails over the pressure of the particles, which a reductionist approach to quantify our poor understanding of the interacting physics in a era where exotic processes are expected. This is expected to be a over-simplifying assumption, which indeed lead to some ambiguity on how to properly defying the Jeans radius. We reviewed that the concept of critical collapse, and some of the numerical studies that have been conducted in this regard. Additionally, we discussed how can the threshold might be lowered by a phase transition or increased by inclusion of non-sphericity, which is expected in a more realistic situations.

Later, we inspected the actual possibility that PBHs exist in the Universe, by presenting two theoretical ways to account for their abundance, the Press-Schechter formalism and the theory of peaks. We draw a connection between the mass of PBHs to the cosmic time, the scale of perturbations and the number of e-fold at which the curvature perturbation left the sphere of causality during inflation. Since the observations on the Cosmic Microwave Background and Large Scale Structure contraindicate the presence of dense fluctuations on large scales, we presented three scenarios which in which the curvature perturbations could be amplified on smaller scales. In relation to this particular point, a line had to be drawn in taking into account what could be useful for our purposes, and so other theoretical scenarios were left out by the reason that they deserved a more detailed discussion, and that they involved a picture somewhat detached from the inflationary picture. Some instances of these other scenarios involve the possibility of creation of curvature perturbations from axion-curvaton interaction, bubble wall collisions or collisions of cosmic strings.

We concluded the thesis by discussing observational constraints of PBHs of small mass, which would have already evaporated by present date, and higher mass primordial black holes. The latter have stirred particular interest in the scientific community, in the wake of the observation of gravitational waves by the mergers of binary systems of black holes of high mass and low angular momentum, which had been taken as an hint of the possible primordial origin, reviving the possibility that at least part of dark matter is in the form of black holes. With this in mind, we briefly discussed the robustness of the presented constraints.

Appendix

Geodesics in General Relativity

A geodesic is a curve $\gamma(\lambda)$ which extremizes the interval between two points [179]; it can specified by some parameter λ, which does not necessarily need to be the time. The curve can be explicitly found by solving the geodesics equation:

$$\frac{\mathrm{d}^2 x^\mu}{\mathrm{d}\lambda^2} + \Gamma^\mu{}_{\alpha\beta}\frac{\mathrm{d}x^\alpha}{\mathrm{d}\lambda}\frac{\mathrm{d}x^\beta}{\mathrm{d}\lambda} = 0, \tag{.1}$$

where $\mathrm{d}x^\mu/\mathrm{d}\lambda = u^\mu$ is the 4-velocity of the curve. The parameter used to describe the geodesics is completely arbitrary; as a matter of fact, we can define an other parameter σ through the relation $\mathrm{d}\sigma = f(\sigma)\,\mathrm{d}\lambda$ [40], to obtain:

$$\frac{\mathrm{d}^2 x^\mu}{\mathrm{d}\sigma^2} + \Gamma^\mu{}_{\alpha\beta}\frac{\mathrm{d}x^\alpha}{\mathrm{d}\sigma}\frac{\mathrm{d}x^\beta}{\mathrm{d}\sigma} = -\frac{f'(\sigma)}{f(\sigma)}\frac{\mathrm{d}x^\mu}{\mathrm{d}\sigma}, \tag{.2}$$

this equation is sometimes referred as autoparallel equation. When the two parameters are related by a linear relation, i.e. $\lambda = a\sigma + b$ with a and b arbitrary constants, then $f'(\sigma) = 0$ and the equation is in the same form of (.1), in which case the parameters are said to be affine parameters. The inhomogeneuous term in (.2) can be interpreted as a forcing term acting tangentially to the geodesic at every point.

Schwarzschild solution and its extensions

Using spherical coordinates $\{t, r, \theta, \phi\}$, we can write line element of the Schwarzschild metric as:

$$\mathrm{d}s^2 = -\left(1 - \frac{r_s}{r}\right)\mathrm{d}t^2 + \left(1 - \frac{r_s}{r}\right)^{-1}\mathrm{d}r^2 + r^2\,\mathrm{d}\Omega_2{}^2, \tag{.3}$$

where $r_s = 2GM$ is the Schwarzschild radius, and M is the mass of a point-like distribution. This metric describes the spacetime around a static, spherically symmetric distribution of mass.
Studying the behaviour of light-like geodesics, the spherical surface at this radius is called event horizon, as following any future-directed, null geodesics crossing this surface are either incoming or tangent to the spherical surface, but cannot be outgoing. Strictly speaking, the metric is valid only outside the event horizon where no

matter is present. As a result, it is not suitable to describe the interior of a massive objects; nonetheless, Birkhoff's theorem assures that as long as any spherical object has a radius larger than the Schwarzschild radius, we can use it to describe exactly the spacetime outside a spherical body [18]. When the density of such an object is higher that $\rho_S = 3/32\pi G^3 M^2$, then the mass distribution is completely enveloped inside the event horizon and we call it a Black Hole.

In Schwarzschild coordinates the lightcones around the black hole tend to get narrower the closer they get to the event horizon, and close completely on it, but this is an effect arising from the choice of coordinates [17]. To better understand the behaviour of lightlike geodesics around a black hole, we introduce the tortoise coordinate $r^* = r + 2GM \log\left|\frac{r}{2GM} - 1\right|$, which stretches the radial coordinate of the right amount needed to maintain the ordinary causal structure of lightcone, and then define the outgoing and incoming null coordinates, $u = t - r^*$ and $v = t + r^*$, a couple of coordinates naturally apdapted[1] to outgoing and incoming null geodesics. Swapping one of these two coordinates to the Schwarzschild time coordinate we get the incoming and outgoing Eddington-Finkelstein metrics, the line element of which are given by:

$$\begin{aligned} \mathrm{d}\, s^2 &= -\left(1 - \frac{r_s}{r}\right) \mathrm{d}\, v^2 + \mathrm{d}\, v\, \mathrm{d}\, r + r^2\, \mathrm{d}\, \Omega_2{}^2 \qquad \text{Incoming,} \\ \mathrm{d}\, s^2 &= \left(1 - \frac{r_s}{r}\right) \mathrm{d}\, u^2 - \mathrm{d}\, u\, \mathrm{d}\, r + r^2\, \mathrm{d}\, \Omega_2{}^2 \qquad \text{Outgoing.} \end{aligned} \tag{.4}$$

Despite these coordinates are useful to parametrize geodesics around a black hole, the parametrization fails to be affine at the event horizon [179]. To see it we need to consider a generator vector of time translationkilling[0] $\xi^\mu = \delta^\mu_v$ [181], outside of the horizon it behaves as timelike vector, but on the horizon $\xi_\mu \xi^\mu = 0$, so there it appears as a null vector[2]. It is on the event horizon where the geodesics equation acquire a non-homogeneous term proportional to the surface gravity $\kappa = 1/4GM$:

$$\frac{\mathrm{d}^2 x^\mu}{\mathrm{d}\lambda^2} + \Gamma^\mu{}_{\alpha\beta} \frac{\mathrm{d}x^\alpha}{\mathrm{d}\lambda} \frac{\mathrm{d}x^\beta}{\mathrm{d}\lambda} = \kappa \frac{\mathrm{d}x^\mu}{\mathrm{d}\lambda}, \qquad \lambda = u, v. \tag{.5}$$

In order to obtain an affine parametrization and maximally extend the geodesics of Schwarzschild metric, we establish a further set of coordinates: the Kruskal null coordinates $U = -e^{-\kappa u}$ and $V = e^{\kappa v}$, which can be turned back into the Kruskal-Szekeres coordinates $T = 1/2(V + U)$ and $R = 1/2(V - U)$ to write the interval as:

$$\mathrm{d}\, s^2 = \frac{32(GM)^3}{r} e^{-2\kappa r}(-\mathrm{d}\, T^2 + \mathrm{d}\, R^2) + r^2\, \mathrm{d}\, \Omega_2{}^2 \tag{.6}$$

[1] A coordinate is said to be naturally adapted to a geodesic curve when it can be used as a time parameter for describing the motion along the geodesic.

[2] Since Schwarzschild spacetime is static, then time translation is a symmetry of the metric. Generators of the isometries are also called Killing Vectors. In particular, hypersurfaces where Killing vectors vanish are called Killing horizons, and those surfaces are characterized by a constant surface gravity [135].

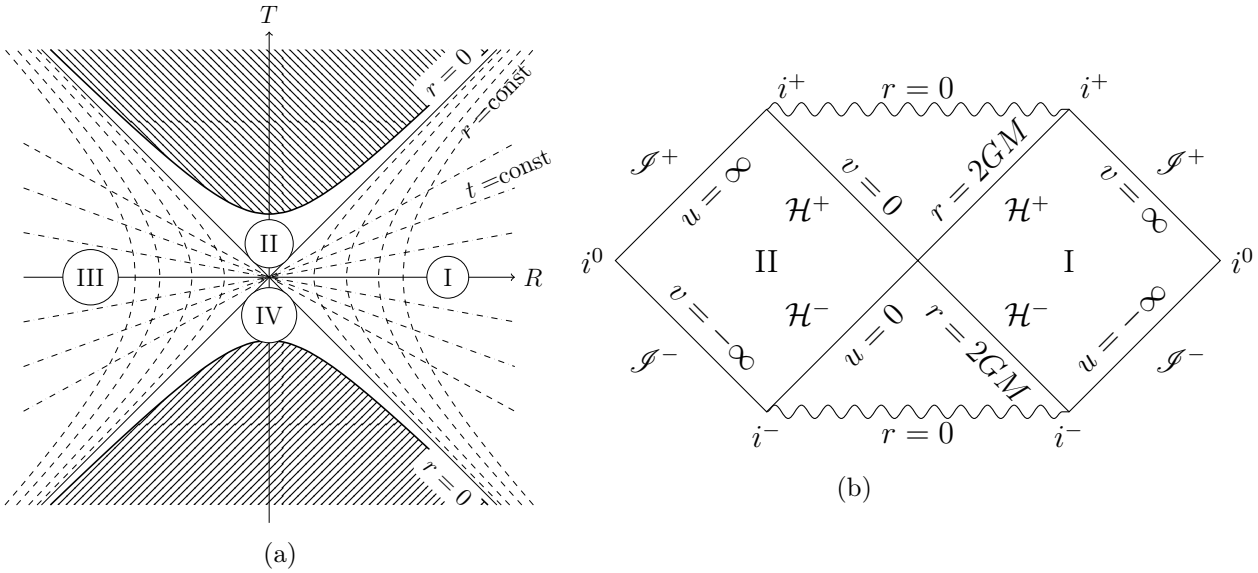

Figure 1. (1a) The Kruskal-Szekeres coordinates; the 45° lines correspond to the event horizons of the Black Hole (II) and White Hole (IV) wedges, regions (I) and (III) describe two separated exterior regions. (1b) $\mathcal{H}^{+/-}$ describe the Black/White Hole's horizon. $i^{-/+}$ past/future temporal infinity and i^0 present spatial infinity indicates regions asymptotically far from the origin at different times. $\mathscr{I}^{-/+}$ are the past/future null infinity are the limit of convergence of the light cones [180].

This set of coordinates evince that the Schwarzschild solution is describes one of four disjointed patches of a broader manifold, as shown in Figure 1a.

It can be useful, when dealing with null geodesics, to represent all the manifold in a compact way, this is attained by the use of Penrose diagrams, which are obtained by a compactification of null coordinates $\tilde{u} = 2\tan^{-1} u$, $\tilde{v} = 2\tan^{-1} v$. The nicest feature of such kind of diagrams, is that null geodesics are represented as 45° degrees lines, and hence the causal structure is made explicit. Furthermore, along these lines u and v assume always a constant value. In Figure 1b the conformal diagram of Kruskal-Szekeres manifolds is unraveled [182].

Field theories in curved background

Taking into account quantum fields reveals us that Black Holes, are indeed not Black, by this we mean they evaporate by emission of quantum excitations.To understand how this process occurs let us first analize how to treat a scalar field Φ of mass m in a curved spacetime. The field must satisfy the Klein-Gordon equation of motion:

$$g^{\mu\nu}\Phi_{;\mu\nu} - m^2\Phi = \frac{1}{\sqrt{|g|}}(\sqrt{|g|}g^{\mu\nu}\Phi_{,\nu})_{,\mu} - m^2\Phi = 0, \tag{.7}$$

the effects due to curved background are enforced by substitution of the ordinary flat Minkowski metric $\eta_{\mu\nu}$ with the curved one and the promotion of ordinary partial

derivatives to their covantiant form [183]. This can be solved in terms of its Fourieur modes, where ϕ is expanded in terms of its modes $\{f_{\mathbf{k}}, f^*_{\mathbf{k}}\}$, with $\omega^2 = \mathbf{k}^2$. The next step is to upgrade the classical field to a quantum field, by introducing the canonical creation and annihilation operators $\hat{a}^\dagger_{\mathbf{k}}$,$\hat{a}_{\mathbf{k}}$, so:

$$\hat{\Phi} = \int d\mathbf{k}(\hat{a}^\dagger_{\mathbf{k}} f_{\mathbf{k}} + \hat{a}_{\mathbf{k}} f^*_{\mathbf{k}}). \tag{.8}$$

An observer, with proper time τ, will discriminate between particles and antiparticle by the sign of their frequency dependence: $\frac{D}{\mathrm{d}\tau} f_{\mathbf{k}} = -i\omega f_{\mathbf{k}}$ and $\frac{D}{\mathrm{d}\tau} f^*_{\mathbf{k}} = +i\omega f^*_{\mathbf{k}}$ being $\omega > 0$. This is analogous to how the discrimination it is done in ordinary Quantum Field Theory, the only difference being $\frac{D}{\mathrm{d}\tau}$, which indicates the directional derivative along the direction of its timelike Killing vector [18]. For this same reason, in curved spacetimes the concept of particle is related to the observer; being more specific, two observers with a relative acceleration will disagree on the number of field modes because their respective timelike Killing vectors are not related by a Lorentz transformation. Nevertheless, the requirement that their respective creation and annihilation operators must be canonical ensures that modes observed in the two frames, say $\{f_{\mathbf{k}}, f^*_{\mathbf{k}}\}$ and $\{g_{\mathbf{k}'}, g^*_{\mathbf{k}'}\}$, must be connected by a Bogoliubov transformation:

$$\begin{aligned} g_{\mathbf{k}} &= \int d\mathbf{k}'(\alpha_{\mathbf{k}\mathbf{k}'} f_{\mathbf{k}'} + \beta_{\mathbf{k}\mathbf{k}'} f^*_{\mathbf{k}'}), \\ f_{\mathbf{k}} &= \int d\mathbf{k}'(\alpha^*_{\mathbf{k}\mathbf{k}'} g_{\mathbf{k}'} - \beta_{\mathbf{k}\mathbf{k}'} g^*_{\mathbf{k}'}), \end{aligned} \tag{.9}$$

here $\alpha_{\omega\omega'}$ and $\beta_{\omega\omega'}$ are the Bogoliubov coefficients and can be determined by expanding the modes of one observer, in term of the modes or anti-modes of the other, through the following inner product:

$$(f, g) = -i \int_\Sigma \sqrt{|\gamma|} d^{n-1}x (f \nabla_\mu g^* - g^* \nabla_\mu f) n^\mu \tag{.10}$$

where Σ is an Cauchy hypersurface[3], $\gamma_{\mu\nu} = g_{\mu\nu}|_\Sigma$ the induced metric on the surface and n^μ a vector normal to the surface. To be specific, this allows the expectation value of number operator $\hat{n}$ to be non-zero in one of the two frames, even if the other observer perceive only vacuum:

$$\langle 0_f | \hat{n}_{g_{\mathbf{k}}} | 0_f \rangle = \int d\mathbf{k}' |\beta_{\mathbf{k}\mathbf{k}'}|^2 \quad \text{whereas} \quad \langle 0_f | \hat{n}_{g_{\mathbf{k}}} | 0_f \rangle = 0. \tag{.11}$$

Hawking Radiation

Here, we will review 'en passant' some of the basic concepts of black holes and some consequence of including quantum theory in curved spacetimes.

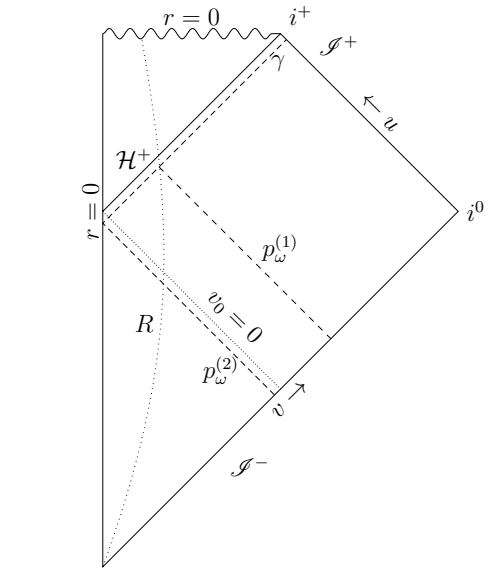

][!h]

Figure 2. The conformal diagram of a Black Hole obtained by spherical collapse.

Temperature of a black hole

The formation of a Black hole by spherical collapse has the main effect of creating two causally disjoint regions of spacetime, but this—contrary to the eternal Kruskal-Szekeres geometry— does not happens at all the time: the event horizon arise only when matter gets sufficiently compressed. As a result, the Penrose diagram for a collapsing body (Figure 2) can be formed by tracing the trajectory of the radius of the spherical body on the Penrose diagram, using the fact that the Schwarzschild solution describe a vacuum spacetime, the interior of the object would not be described by the Kruskal-Szekeres metric [4].

The main consequence is that prior to its formation, to describe a field Φ we only need a complete set of modes on a Cauchy surface which can be conveniently choose to be the past null infinity $\mathscr{I}^-$; there we choose a complete set $\{f_{\mathbf{k}}, f^*_{\mathbf{k}}\}$. On the other hand, after its formation, a Cauchy surface must include both the interior and the exterior of the black hole, we can choose it as the event horizon and the future null infinity $\mathcal{H}^+ \cup \mathscr{I}^+$, and take two separate sets, $\{g_{\mathbf{k}}, g^*_{\mathbf{k}}\}$ on $\mathcal{H}^+$ and $\{p_{\mathbf{k}}, p^*_{\mathbf{k}}\}$ on $\mathscr{I}^+$:

$$\hat{\Phi} = \int d\mathbf{k}\hat{(}a_{\mathbf{k}} f_{\mathbf{k}} + h.c.) = \int d\mathbf{k}(\hat{b}_{\mathbf{k}} g_{\mathbf{k}} + \hat{c}_{\mathbf{k}} p_{\mathbf{k}} + h.c.) \tag{.12}$$

This will lead us to a Bogoliubov transformation between modes on $\mathscr{I}^-$ and $\mathscr{I}^+$ [18]. For simplicity, we will consider a massless scalar field and solve (.7) on $\mathcal{I}^{+/-}$

[3] A Cauchy hypersurface is a spacelike hypersurface that intersects each geodesics exactly once [180].

using infalling/outgoing Eddington-Finkelstein coordinates (.4):

$$\begin{aligned} f_{\omega lm} &= \frac{1}{\sqrt{2\pi\omega}} \frac{e^{-i\omega v}}{r} Y_l^m(\theta,\varphi), \\ p_{\omega lm} &= \frac{1}{\sqrt{2\pi\omega}} \frac{e^{-i\omega u}}{r} Y_l^m(\theta,\varphi). \end{aligned} \tag{.13}$$

where $\omega^2 = \mathbf{k}^2$ is the angular frequency, and $Y_l^m(\theta,\varphi)$ the spherical harmonics[4].

The event horizon, being a null-surface, can be characterized by considering the last outgoing null ray reaching the asymptotic null infinity, this rays is associated with one incoming null ray, identified as v_0; earlier rays—with $v < v_0$— are reflected by the the origin and propagate as outgoing null rays to $\mathscr{I}^+$. Conversely, later incoming rays having $v > v_0$ cross the event horizon and fall inevitably toward the singularity at $r = 0$. In general, rays approaching the spherical distribution will feel the effect of an effective potential which should be taken into account as a scattering source, which could be rather cumbersome. To overcome this complication the modes p_ω are traced backwards through the geodesic γ, and will be split into two parts: a $p_\omega^{(1)}$ summing up the reflected part of the modes, and $p_\omega^{(2)}$ for the part emerging from the collapsing body which is given by a $\Gamma(\omega)$ fraction of the package p_ω, this quantity is called greybody factor. The Bogoliubov coefficients between the modes $\{f_\omega, f_\omega^*\}$ and $\{p_{\omega'}^{(1)}, p_{\omega'}^{(1)*}\}$ will be proportional to a $\delta(\omega - \omega')$ because this are reflected modes.

The radiation arises from Bogoliubov coefficients between f-modes and $p^{(2)}$-modes, but to calculate the Bogoliubov coefficients we need to find a way to relate the u and v coordinates. This can be attained by solving the geodesic equation (.1) for infalling and outgoing geodesics (.4) in terms of an arbitrary parameter λ. This will give us that near the horizon $u(\lambda) \approx -1/\kappa \ln(\lambda)$ for incoming geodesics, and $v(\lambda) = v_0 - \lambda$ for outgoing geodesics.
If unite them, we get: $u(v) \approx -\kappa^{-1} \ln(v_0 - v)$ [184]. Once we substitute this inside the Bogoliubov's $\alpha^{(2)}_{\omega\omega'} = (f_\omega, p^{(2)}_\omega)$ and $\beta^{(2)}_{\omega\omega'} = (f^*_\omega, p^{(2)}_\omega)$, together an argument about the analyticity of the integrals [185], it turns out that $|\alpha^{(2)}_{\omega\omega'}| = e^{\pi\omega/\kappa}|\beta^{(2)}_{\omega\omega'}|$, and we can expand:

$$p^{(2)}_\omega = \int d\omega' \beta^{(2)}_{\omega\omega'} \Big(e^{\pi\omega/\kappa} f_{\omega'} + f^*_{\omega'} \Big), \tag{.14}$$

and from the fact that $(p^{(2)}_\omega, p_{\omega'}) = \Gamma(\omega)$ we reach the conclusion that:

$$\langle 0_f | \hat{n}_{p_\omega} | 0_f \rangle = \int d\omega' |\beta^{(2)}_{\omega\omega'}|^2 = \frac{\Gamma(\omega)}{e^{2\pi\omega/\kappa} - 1}. \tag{.15}$$

For $\Gamma(\omega) = 1$, the expectation number is in the form of the blackbody distribution, which can be interpreted as the the black hole is emitting termal radiation like a

[4] A mode can be uniquely specified by either $\mathbf{k}$ or equivalently the triplet ω, l, m. However, as the physics is not affected by l, m, we will drop them and identify modes only by ω from now on.

greybody of absorbivity $\Gamma(\omega)$. Adopting this analogy we can extract the Hawking temperature of a black hole which reads as:

$$T = \frac{\kappa}{2\pi} = \frac{\hbar c^3}{8\pi k_B G M} \approx 1.06 \left(\frac{10^{10}\text{g}}{M}\right) \text{TeV}, \tag{.16}$$

we restored the fundamental constants for completeness and provided an useful formula for mass-temperature confrontations.

One interesting corollary of Hawking radiation is that, in order for Black Holes to emit thermal radiation, mass of BHs should decrease,so as to maintain energy conservation. The temperature is inversely proportional to the mass, this implies that BH have negative specific heat, meaning that it heats up as it lose energy. From this insight we can extrapolate an estimate of their lifetime. To do so we neglect the back-reaction of the radiation on spacetime, and we assume that the total power radiated is following the Stefan-Boltzmann law for a blackbody:

$$P = A\sigma T^4, \tag{.17}$$

being $A = 4\pi r_S^2 = 16\pi G^2 M^2$ the surface area, and σ the Stefan-Boltzmann constant[5]. Then, if we collect in α all the constant terms:

$$\frac{\mathrm{d}M}{\mathrm{d}t} = -P = -\frac{\alpha}{M^2} \quad \Rightarrow \quad M(t) = (M_0^3 - 3\alpha t)^{1/3}. \tag{.18}$$

According to their temperature they could emit different particle species from the Standard Model: $M \gg 10^{17}$g emit particle which are effectively massless, $10^{15}\text{g} < M < 10^{17}$g can emit electrons, $10^{14}\text{g} < M < 10^{15}$g muons and for smaller mass ranges QCD species production could be allowed, as well [145].

An electrically charged, rotating black hole can characterized by 3 parameters: mass M, electric charge Q and angular momentum J. These quantities are related to one another by the first law of black-hole thermodynamics:

$$\mathrm{d}\,M = \frac{\kappa}{8\pi}\,\mathrm{d}\,A + \Omega\,\mathrm{d}\,J + \Phi\,\mathrm{d}\,Q, \tag{.19}$$

being A the area, Ω surface angular velocity and Φ surface electric potential of a black hole. It must be specified that the surface gravity in this case is different from the Schwarzschild black hole:

$$\kappa = \frac{4\pi\sqrt{M^2 - Q^2 - (J/M^2)^2}}{A}. \tag{.20}$$

Such black hole will emit a mode $|\omega lm\rangle$ with energy in a range $(\omega, \omega + \mathrm{d}\,\omega)$ at a rate described by [144]:

$$\mathrm{d}\,\dot{N} = \frac{\Gamma_s\,\mathrm{d}\,\omega}{2\pi}\left(\exp\left[2\pi\frac{\omega - m\Omega - q\Phi}{\kappa}\right] - (-1)^{2s}\right)^{-1}, \tag{.21}$$

[5] A more detailed study should also include the particle species cross-sections, a study for massless particles emission was performed by [143], but included only two species of massless neutrinos.

where s is the particle spin and q its charge. In the above formula Γ_s is the absorption probability for a mode of spin s of a given particle specie, which the exact form depends on the cross-section and needs to be calculated numerically [143]; however, at high energies, since the cross-section of each species approaches the geometric optics limit, and so $\Gamma_s \sim 27G^2M^2Q^2$. To simplify things, we can introduce a factor $f(M)$ to account for the number of emitted particle species, normalized to unity when the emission involves only massless particles are emitted($M \gg 10^{17}$g), but otherwise its value it is a non-trivial function of the black hole's mass and the specific masses of the emitted species [145]. Finally, we can write an estimated lifetime for the black hole as:

$$\tau \approx 407\left(\frac{f(M)}{15.35}\right)\left(\frac{M}{10^{10}\text{g}}\right)^3 \text{s}. \tag{.22}$$

When we substitute for the age of the Universe($t_{\text{now}} \approx 13.7$Gyr) and use $f(M_{\text{cr}}) = 1.9$, we get a critical mass $M_{\text{cr}} \approx 5.1 \times 10^{14}$g [13]. Thence, we expect primordial BHs with a mass lower than $\sim 10^{15}$g to be evaporated by present age.

Horizons and Misner-Sharp-Hernandez mass

Up to this point, in this appendix, we have considered Black Holes in a spacetime which is asymptotically flat[6]. Unfortunately, the notion of event horizon is ill-defined if one considers spacetimes which do not have the property of asymptotic flatness; the FLRW metric describes constitutes such an example.

In fact, for this spacetime the Riemann tensor is nowhere vanishing and the Ricci tensor, or in other words the curvature of spacetime, is given by:

$$R = \frac{6}{a^2}(\mathcal{H}^2 + \mathcal{H}' + K), \tag{.23}$$

where $\mathcal{H}$ is the comoving Hubble parameter, and K the extrinsic curvature; hence, globally curve since the scale factor is a parameter that depends only on time. To understand why in this spacetime the notion of event horizon is ill-defined, let us consider it at a fixed time t in matter domination phase; we see that the Hubble scale $1/H$ acts in a similar fashion to the event horizon of a black hole: future-directed, null geodesics are either incoming or tangent to the Hubble sphere, because incoming geodesics at a distance further than the Hubble radius recess faster then the speed of light—this is also why the Hubble radius is often called horizon in a cosmological context. The problem lies in the fact that the Hubble scale is evolving and at earlier(later) times it would have smaller(larger) values. In this sense, the lack of an event horizon is due to a lack of static nature of this horizon, as events which are out of the horizon at some point might not be at a later point. Finding the

[6]We do not provide the proper definition of asymptotic flatness, but it coincides with the intuitive idea that the metric in spherical coordinates reduces to the Minkowski metric for $r \to \infty$.

event horizon of a spacetime, is therefore a teleological problem—one that requires the knowledge of the entire evolution of spacetime [17].

With the insight that, horizons are defined by the behaviour of geodesics at a spacetime point, we denote by the expansion parameters:

$$\theta_+ = k^\mu_{+,\mu}, \qquad \theta_- = k^\mu_{-,\mu}, \tag{.24}$$

where $k^\mu_+(k^\mu_-)$ is the tangent vector to a radial, outgoing(incoming), future-directed, null geodesic at a point [186]. It is easy to see that if any of the two parameters assume a positive value than at a congruence of geodesics will be diverging, and, conversely, $\theta_\pm < 0$ yields a converging congruence at later times. Now, taking into account a spherical surface of radius r, the metric sphere is said to be [187]:

- trapped: if $\theta_+\theta_- > 0$. In addition, the sphere is also called future trapped if both positive, $\theta_\pm > 0$, and past trapped if both negative, $\theta_\pm < 0$. An example of future trapped surface is any sphere having a radius larger than the Hubble scale in a FLRW spacetime, whereas a past trapped instance is a sphere of radius smaller than the Schwarzschild radius in a Schwarzschild spacetime.

- untrapped: if $\theta_+\theta_- < 0$. A typical case of untrapped surface is that of positive θ_+ and negative θ_- indicating that a congruence of outgoing, null geodesics diverge, and the incoming converge.

- marginal: if $\theta_+\theta_- = 0$. A sphere having null θ_+(outgoing geodesics cannot expand outside the region) is said to be future(past) marginal if $\theta_- < 0(\theta_- > 0)$ or bifurcating if also θ_- is null. Furthermore, we can make an additional distinction: a marginal surface is said to be outer(inner) if $\mathcal{L}_{k_-}\,\theta_+ < 0(\mathcal{L}_{k_-}\theta_+ > 0)$ or degenerate if $\mathcal{L}_{k_-}\theta_+ = 0$.

Nomenclature aside, these definitions help us to better explore the various kinds of horizons, with all of its nuances; and despite their abstract appearance, they extricate our understanding from the messy jungle of causality in a curved space. According to our definition these surfaces are always two dimensional spheres, but, in line of principle, any closed two-dimensional surface shall suffice as long as we consider incoming and outgoing, normal, null geodesics to its surface. Nonetheless, we proceed to define several kind of horizons using these spherical surfaces as building blocks, under the assumption that the spacetimes we are going to consider are spherically symmetric.

- Event horizon. An Event horizon is the causal boundary between two region of spaces one untrapped, and the other trapped. This is taken to be as the past boundary of the region from which all null geodesics reach the asymptotic null infinity, and as such is a null surface.

- Apparent Horizon. We define it as the closure of a (2+1)-surface foliated by future(past),marginal surfaces, which constitute its time slicings.

- Trapping Horizon. A trapping horizon is a particular case of apparent horizons, in which we also require the 3-surface to be foliated by past(future), inner(outer) marginal time slicings.

It is important to remark that,thanks to their quasi-local definition, both Apparent and Trapping Horizons are different from Event Horizons, which is defined as a global characteristics of spacetime instead. In other words, Event Horizons are static regions while Apparent Horizons can evolve with time(and so do Trapping Horizons) [135]. In any case, Apparent Horizons lie inside or share their boundary with the Event Horizon.

It can be shown [187] that the Misner-Sharp-Hernandez mass, in spherically symmetric spacetime, takes the same form of the Hawking-Israel mass function:

$$M(t,R) = \frac{1}{2G} R(1 - g^{\mu\nu} R_{;\mu} R_{;\nu}), \tag{.25}$$

where R is the areal radius. It follows, that in a region where $2GM/(R) < 1$, one has $\theta_+\theta_- < 0$, meaning that this region is untrapped; still, regions where $2GM/R > 1$ correspond to trapped regions ($\theta_+\theta_- > 0$) and that along marginal surfaces, where the product of the expansion parameters is null, we recover $2GM/R = 1$, which in a Schwarzschild spacetime corresponds to the Event Horizon. To conclude, we want to stress that this result is more general, because the Misner-Sharp-Hernandez mass $M(t,R)$,which it is a quasi-local function that accounts for the total gravitational energy contained inside a region of areal radius R at time t, give us an important tool to search and identify when and where an Apparent Horizon arises in a spherical spacetime; as a result, it allows to define Black Holes in spacetimes which are not asymptotically flat.

Acknowledgements

I want to express my gratitude to my supervisor Professor Sami Nurmi for the patience and the independence that he gave me during the writing of this thesis, for its comments, and for always giving me possibility to participate to the events in Cosmology that he organized. These changed my understanding of the Universe, literally. Many thanks are directed to all the participants of Kosmokahvi.
A special thanks goes to my dear friend Mathieu Renzo, PhD student at Anton Pannekoek Institute, Amsterdam University; he has always been there for me with advices and rebukes, he acted as a second supervisor.

A word of love goes to my parents and sibilings which helped me in their own way. I give my appreciations to all my friends that has always believed in me, even more than I did, with special mentions of Earric and Ana for their pressing me to be a better person every day, Niyati for running the journal club, Luca for being my man regardless of the distance, Wivi for the encouragements, all the Lorentz Group for the japing, Hussam(i), Ayan, my Sami, Erkka, Terhi, Mikko, Juls, Rai, Sile, Afrina and all the others that I am forgetting at the moment(sorry). I believe that a scientist is a quasi-particle dressed of the people who surround her/him.

I want to thank the Department of Physics and the Faculty of Science for the scholarships that have made possible my desire of living and studying abroad.

And, last but not least: спасибо Вика, моя муза, за хорощее и плохое.

Bibliography

[1] A. Einstein, "Die Feldgleichungen der Gravitation," Sitzungsberichte der Königlich Preußischen Akademie der Wissenschaften (Berlin), Seite 844-847., 1915. [Online]. Available: http://adsabs.harvard.edu/abs/1915SPAW.....844E

[2] K. Schwarzschild, "Über das Gravitationsfeld eines Massenpunktes nach der Einsteinschen Theorie," Sitzungsberichte der Königlich Preußischen Akademie der Wissenschaften (Berlin), 1916, Seite 189-196, 1916. [Online]. Available: http://adsabs.harvard.edu/abs/1916SPAW.....189S

[3] A. S. Eddington, "A Comparison of Whitehead's and Einstein's Formulæ," , vol. 113, p. 192, Feb. 1924. [Online]. Available: http://adsabs.harvard.edu/abs/1924Natur.113..192E

[4] S. W. Hawking, "Particle creation by black holes," Communications in Mathematical Physics, vol. 43, pp. 199–220, Aug. 1975. [Online]. Available: http://adsabs.harvard.edu/abs/1975CMaPh..43..199H

[5] I. Bombaci, "The maximum mass of a neutron star." , vol. 305, p. 871, Jan. 1996. [Online]. Available: http://adsabs.harvard.edu/abs/1996A%26A...305..871B

[6] S. E. Woosley, A. Heger, and T. A. Weaver, "The evolution and explosion of massive stars," Reviews of Modern Physics, vol. 74, pp. 1015–1071, Nov. 2002. [Online]. Available: http://adsabs.harvard.edu/abs/2002RvMP...74.1015W

[7] S. Hawking, "Gravitationally collapsed objects of very low mass," Monthly Notices of the Royal Astronomical Society, vol. 152, no. 1, pp. 75–78, 1971. [Online]. Available: http://dx.doi.org/10.1093/mnras/152.1.75

[8] Y. B. Zel'dovich and I. D. Novikov, "The Hypothesis of Cores Retarded during Expansion and the Hot Cosmological Model," , vol. 10, p. 602, Feb. 1967. [Online]. Available: http://adsabs.harvard.edu/abs/1967SvA....10..602Z

[9] B. P. Abbott and L. et al., "Observation of Gravitational Waves from a Binary Black Hole Merger," Physical Review Letters, vol. 116, no. 6, p. 061102, Feb. 2016. [Online]. Available: https://ui.adsabs.harvard.edu/abs/2016PhRvL.116f1102A

[10] S. Bird, I. Cholis, J. B. Muñoz, Y. Ali-Haïmoud, M. Kamionkowski, E. D. Kovetz, A. Raccanelli, and A. G. Riess, "Did LIGO Detect Dark Matter?" Physical Review Letters, vol. 116, no. 20, p. 201301, May 2016. [Online]. Available: https://ui.adsabs.harvard.edu/abs/2016PhRvL.116t1301B

[11] S. Clesse and J. García-Bellido, "The clustering of massive Primordial Black Holes as Dark Matter: Measuring their mass distribution with advanced LIGO," Physics of the Dark Universe, vol. 15, pp. 142–147, Mar. 2017. [Online]. Available: https://ui.adsabs.harvard.edu/abs/2017PDU....15..142C

[12] M. Sasaki, T. Suyama, T. Tanaka, and S. Yokoyama, "Primordial Black Hole Scenario for the Gravitational-Wave Event GW150914," Physical Review Letters, vol. 117, no. 6, p. 061101, Aug. 2016. [Online]. Available: https://ui.adsabs.harvard.edu/abs/2016PhRvL.117f1101S

[13] B. J. Carr, "Primordial Black Holes: Do They Exist and Are They Useful?" arXiv e-prints, pp. astro–ph/0 511 743, Nov 2005. [Online]. Available: https://ui.adsabs.harvard.edu/abs/2005astro.ph.11743C

[14] E. Bañados, B. P. Venemans, C. Mazzucchelli, E. P. Farina, F. Walter, F. Wang, R. Decarli, D. Stern, X. Fan, F. B. Davies, J. F. Hennawi, R. A. Simcoe, M. L. Turner, H.-W. Rix, J. Yang, D. D. Kelson, G. C. Rudie, and J. M. Winters,

"An 800-million-solar-mass black hole in a significantly neutral Universe at a redshift of 7.5," , vol. 553, pp. 473–476, Jan. 2018. [Online]. Available: https://ui.adsabs.harvard.edu/abs/2018Natur.553..473B

[15] C. J. Hailey, K. Mori, F. E. Bauer, M. E. Berkowitz, J. Hong, and B. J. Hord, "A density cusp of quiescent X-ray binaries in the central parsec of the Galaxy," , vol. 556, pp. 70–73, Apr. 2018. [Online]. Available: https://ui.adsabs.harvard.edu/abs/2018Natur.556...70H

[16] S. Weinberg, The first three minutes, 2nd ed. Basic Books, 1993. [Online]. Available: http://gen.lib.rus.ec/book/index.php?md5=FDA85C18F72C192339A06CB50CD4F73B

[17] C. W. Misner, K. S. Thorne, and J. A. Wheeler, Gravitation, 2nd ed. W H Freeman and Company, 1973. [Online]. Available: http://www.bibsonomy.org/bibtex/2bbb9312522215e479defd15c269f8efc/dhruvbansal

[18] S. Carroll and S. Carroll, Spacetime and Geometry: An Introduction to General Relativity. Addison Wesley, 2004. [Online]. Available: https://books.google.fi/books?id=1SKFQgAACAAJ

[19] R. D'Inverno, Introducing Einstein's Relativity. Clarendon Press, 1992. [Online]. Available: https://books.google.fi/books?id=isdsCAAAQBAJ

[20] D. Baumann, "Cosmology(lecture notes)." [Online]. Available: http://www.damtp.cam.ac.uk/user/db275/Cosmology/Lectures.pdf

[21] W. Keel, The road to galaxy formation, 2nd ed., ser. Springer Praxis Books / Astronomy and Planetary Sciences. Springer, 2007. [Online]. Available: http://gen.lib.rus.ec/book/index.php?md5=024F96A52CDE7BDFB708F9C5FDD9DE89

[22] A. G. Riess, L. M. Macri, S. L. Hoffmann, D. Scolnic, S. Casertano, A. V. Filippenko, B. E. Tucker, M. J. Reid, D. O. Jones, and J. M. Silverman, "A 2.4% Determination of the Local Value of the Hubble Constant," , vol. 826, no. 1, p. 56, Jul 2016. [Online]. Available: https://ui.adsabs.harvard.edu/abs/2016ApJ...826...56R

[23] Planck Collaboration, "Planck 2018 results. VI. Cosmological parameters," arXiv e-prints, p. arXiv:1807.06209, Jul 2018. [Online]. Available: https://ui.adsabs.harvard.edu/abs/2018arXiv180706209P

[24] S. Weinberg, Gravitation and Cosmology: Principles and Applications of the General Theory of Relativity, Jul. 1972. [Online]. Available: https://ui.adsabs.harvard.edu/abs/1972gcpa.book.....W

[25] R. M. Wald, General relativity. Chicago, IL: Chicago Univ. Press, 1984. [Online]. Available: https://cds.cern.ch/record/106274

[26] J. K. Yadav, J. S. Bagla, and N. Khandai, "Fractal dimension as a measure of the scale of homogeneity," , vol. 405, pp. 2009–2015, Jul. 2010. [Online]. Available: http://adsabs.harvard.edu/abs/2010MNRAS.405.2009Y

[27] V. Mukhanov, Physical Foundations of Cosmology. Cambridge: Cambridge Univ. Press, 2005. [Online]. Available: https://cds.cern.ch/record/991646

[28] S. Weinberg, Cosmology, ser. Cosmology. OUP Oxford, 2008. [Online]. Available: https://books.google.fi/books?id=nqQZdg020fsC

[29] M. Maggiore, Gravitational Waves: Volume 2: Astrophysics and Cosmology. OUP Oxford, 2018. [Online]. Available: https://books.google.fi/books?id=FGdRDwAAQBAJ

[30] A. R. Liddle and D. H. Lyth, Cosmological Inflation and Large-Scale Structure. Cambridge: Cambridge Univ. Press, 2000. [Online]. Available: https://cds.cern.ch/record/452061

[31] A. G. Riess, A. V. Filippenko, P. Challis, A. Clocchiatti, A. Diercks, P. M. Garnavich, R. L. Gilliland, C. J. Hogan, S. Jha, and R. P. Kirshner, "Observational Evidence from Supernovae for an Accelerating Universe and a Cosmological Constant," , vol. 116, no. 3, pp. 1009–1038, Sep 1998. [Online]. Available: https://ui.adsabs.harvard.edu/abs/1998AJ....116.1009R

[32] Planck Collaboration, "Planck 2018 results. X. Constraints on inflation," arXiv e-prints, p. arXiv:1807.06211, Jul 2018. [Online]. Available: https://ui.adsabs.harvard.edu/abs/2018arXiv180706211P

[33] B. A. Bassett, S. Tsujikawa, and D. Wands, "Inflation dynamics and reheating," Reviews of Modern Physics, vol. 78, no. 2, pp. 537–589, Apr 2006. [Online]. Available: https://ui.adsabs.harvard.edu/abs/2006RvMP...78..537B

[34] M. Longair, Galaxy Formation, ser. Astronomy and Astrophysics Library. Springer Berlin Heidelberg, 2007. [Online]. Available: https://books.google.fi/books?id=e-wJHSBOuZAC

[35] E. Lifshitz, "Republication of: On the gravitational stability of the expanding universe," General Relativity and Gravitation, vol. 49, 2 2017. [Online]. Available: http://gen.lib.rus.ec/scimag/index.php?s=10.1007/s10714-016-2165-8

[36] J. M. Bardeen, "Gauge-invariant cosmological perturbations," , vol. 22, pp. 1882–1905, Oct. 1980. [Online]. Available: http://adsabs.harvard.edu/abs/1980PhRvD..22.1882B

[37] H. Kodama and M. Sasaki, "Cosmological perturbation theory," Progress of Theoretical Physics Supplement, vol. 78, pp. 1–166, 1984. [Online]. Available: http://dx.doi.org/10.1143/PTPS.78.1

[38] G. F. R. Ellis and M. Bruni, "Covariant and gauge-invariant approach to cosmological density fluctuations," , vol. 40, pp. 1804–1818, Sep. 1989. [Online]. Available: https://ui.adsabs.harvard.edu/abs/1989PhRvD..40.1804E

[39] V. F. Mukhanov, H. A. Feldman, and R. H. Brandenberger, "Theory of cosmological perturbations," , vol. 215, pp. 203–333, Jun. 1992. [Online]. Available: http://adsabs.harvard.edu/abs/1992PhR...215..203M

[40] H. Ohanian and R. Ruffini, Gravitation and Spacetime. Cambridge University Press, 2013. [Online]. Available: https://books.google.fi/books?id=5DtkqcET4b0C

[41] R. Durrer and N. Straumann, "Some applications of the 3+1 formalism of general relativity," Helvetica Physica Acta, vol. 61, no. 8, pp. 1027–1062, 1988, iD: unige:1018. [Online]. Available: https://archive-ouverte.unige.ch/unige:1018

[42] E. Bertschinger, "Cosmological dynamics," NASA STI/Recon Technical Report N, vol. 96, Jan. 1995. [Online]. Available: http://adsabs.harvard.edu/abs/1995STIN...9622249B

[43] M. Bruni, S. Matarrese, S. Mollerach, and S. Sonego, "Perturbations of spacetime: gauge transformations and gauge invariance at second order and beyond," Classical and Quantum Gravity, vol. 14, pp. 2585–2606, Sep. 1997. [Online]. Available: http://adsabs.harvard.edu/abs/1997CQGra..14.2585B

[44] H. Kurki-Suonio, "Cosmological perturbation theory, part 1(lecture notes)." [Online]. Available: http://www.helsinki.fi/~hkurkisu/CosPer.pdf

[45] P. Peter and J. Uzan, Primordial cosmology, ser. Oxford graduate texts. Oxford University Press, 2009. [Online]. Available: https://books.google.fi/books?id=FZXvAAAAMAAJ

[46] R. H. Brandenberger, "Lectures on the Theory of Cosmological Perturbations," in The Early Universe and Observational Cosmology, ser. Lecture Notes in Physics, Berlin Springer Verlag, N. Bretón, J. L. Cervantes-Cota, and M. Salgad, Eds., vol. 646, 2004, pp. 127–167. [Online]. Available: http://adsabs.harvard.edu/abs/2004LNP...646..127B

[47] N. Bartolo, S. Matarrese, and A. Riotto, "Adiabatic and isocurvature perturbations from inflation: Power spectra and consistency relations," , vol. 64, no. 12, p. 123504, Dec. 2001. [Online]. Available: http://adsabs.harvard.edu/abs/2001PhRvD..64l3504B

[48] V. Mukhanov, H. Feldman, and R. Brandenberger, "Theory of cosmological perturbations," Physics Reports, vol. 215, no. 5, pp. 203 – 333, 1992. [Online]. Available: http://www.sciencedirect.com/science/article/pii/037015739290044Z

[49] S. Dodelson, Modern cosmology, 1st ed. Academic Press, 2003. [Online]. Available: http://gen.lib.rus.ec/book/index.php?md5=A58CC844174B751D6BCFEEE415A948B2

[50] A. Riotto, "Inflation and the Theory of Cosmological Perturbations," ArXiv High Energy Physics - Phenomenology e-prints, Oct. 2002. [Online]. Available: http://adsabs.harvard.edu/abs/2002hep.ph...10162R

[51] D. Baumann, "TASI Lectures on Inflation," ArXiv e-prints, Jul. 2009. [Online]. Available: http://adsabs.harvard.edu/abs/2009arXiv0907.5424B

[52] Planck Collaboration, Y. Akrami, F. Arroja, M. Ashdown, J. Aumont, C. Baccigalupi, M. Ballardini, A. J. Banday, R. B. Barreiro, and N. Bartolo, "Planck 2018 results. I. Overview and the cosmological legacy of Planck," arXiv e-prints, p. arXiv:1807.06205, Jul 2018. [Online]. Available: https://ui.adsabs.harvard.edu/abs/2018arXiv180706205P

[53] D. H. Lyth and A. R. Liddle, The primordial density perturbation: Cosmology, inflation and the origin of structure, 2009. [Online]. Available: http://www.cambridge.org/uk/catalogue/catalogue.asp?isbn=9780521828499

[54] M. Longair, Galaxy Formation, ser. Astronomy and Astrophysics Library. Springer Berlin Heidelberg, 2007. [Online]. Available: https://books.google.fi/books?id=e-wJHSBOuZAC

[55] F. L. Peter Coles, Cosmology: the origin and evolution of cosmic structure, 2nd ed. Wiley, 2002. [Online]. Available: http://gen.lib.rus.ec/book/index.php?md5=13924A16272421E405C3DF83845FF392

[56] D. Wands, K. A. Malik, D. H. Lyth, and A. R. Liddle, "New approach to the evolution of cosmological perturbations on large scales," , vol. 62, no. 4, p. 043527, Aug. 2000. [Online]. Available: http://adsabs.harvard.edu/abs/2000PhRvD..62d3527W

[57] K. A. Malik and D. Wands, "Cosmological perturbations," , vol. 475, pp. 1–51, May 2009. [Online]. Available: http://adsabs.harvard.edu/abs/2009PhR...475....1M

[58] W. H. Kinney, "TASI Lectures on Inflation," arXiv e-prints, p. arXiv:0902.1529, Feb 2009. [Online]. Available: https://ui.adsabs.harvard.edu/abs/2009arXiv0902.1529K

[59] I. Lawrie, A Unified Grand Tour of Theoretical Physics,. Taylor & Francis, 1990. [Online]. Available: https://books.google.fi/books?id=OT7AejgZTgIC

[60] J. Peacock, Cosmological Physics, ser. Cambridge Astrophysics. Cambridge University Press, 1999. [Online]. Available: https://books.google.fi/books?id=t8O-yylU0j0C

[61] T. S. Bunch and P. C. W. Davies, "Quantum field theory in de Sitter space - Renormalization by point-splitting," Proceedings of the Royal Society of London Series A, vol. 360, pp. 117–134, Mar. 1978. [Online]. Available: https://ui.adsabs.harvard.edu/abs/1978RSPSA.360..117B

[62] R. B. G. I. Giovanni Montani, Marco Valerio Battisti, Primordial Cosmology. World Scientific Publishing Company, 2011. [Online]. Available: http://gen.lib.rus.ec/book/index.php?md5=8C5EB511CC55C5EC1B3B18530E2C00D5

[63] D. H. Lyth, "Large-scale energy-density perturbations and inflation," Phys. Rev. D, vol. 31, pp. 1792–1798, Apr 1985. [Online]. Available: https://link.aps.org/doi/10.1103/PhysRevD.31.1792

[64] A. Kosowsky and M. S. Turner, "CBR anisotropy and the running of the scalar spectral index," , vol. 52, no. 4, pp. R1739–R1743, Aug 1995. [Online]. Available: https://ui.adsabs.harvard.edu/abs/1995PhRvD..52.1739K

[65] A. R. Liddle and D. H. Lyth, "COBE, gravitational waves, inflation and extended inflation," Physics Letters B, vol. 291, no. 4, pp. 391–398, Oct 1992. [Online]. Available: https://ui.adsabs.harvard.edu/abs/1992PhLB..291..391L

[66] Y. Tanaka and M. Sasaki, "Gradient Expansion Approach to Nonlinear Superhorizon Perturbations," Progress of Theoretical Physics, vol. 117, no. 4, pp. 633–654, Apr 2007. [Online]. Available: https://ui.adsabs.harvard.edu/abs/2007PThPh.117..633T

[67] D. S. Salopek and J. R. Bond, "Nonlinear evolution of long-wavelength metric fluctuations in inflationary models," Phys. Rev. D, vol. 42, pp. 3936–3962, Dec 1990. [Online]. Available: https://link.aps.org/doi/10.1103/PhysRevD.42.3936

[68] G. I. Rigopoulos and E. P. Shellard, "Separate universe approach and the evolution of nonlinear superhorizon cosmological perturbations," , vol. 68, no. 12, p. 123518, Dec 2003. [Online]. Available: https://ui.adsabs.harvard.edu/abs/2003PhRvD..68l3518R

[69] D. Wands, K. A. Malik, D. H. Lyth, and A. R. Liddle, "New approach to the evolution of cosmological perturbations on large scales," , vol. 62, no. 4, p. 043527, Aug 2000. [Online]. Available: https://ui.adsabs.harvard.edu/abs/2000PhRvD..62d3527W

[70] N. S. Sugiyama, E. Komatsu, and T. Futamase, "δN formalism," , vol. 87, no. 2, p. 023530, Jan 2013. [Online]. Available: https://ui.adsabs.harvard.edu/abs/2013PhRvD..87b3530S

[71] D. H. Lyth, K. A. Malik, and M. Sasaki, "A general proof of the conservation of the curvature perturbation," Journal of Cosmology and Astro-Particle Physics, vol. 2005, no. 5, p. 004, May 2005. [Online]. Available: https://ui.adsabs.harvard.edu/abs/2005JCAP...05..004L

[72] J. R. Oppenheimer and G. M. Volkoff, "On Massive Neutron Cores," Physical Review, vol. 55, pp. 374–381, Feb. 1939. [Online]. Available: https://ui.adsabs.harvard.edu/abs/1939PhRv...55..374O

[73] B. J. Carr and S. W. Hawking, "Black holes in the early Universe," , vol. 168, pp. 399–416, Aug. 1974. [Online]. Available: http://adsabs.harvard.edu/abs/1974MNRAS.168..399C

[74] E. R. Harrison, "Fluctuations at the Threshold of Classical Cosmology," , vol. 1, pp. 2726–2730, May 1970. [Online]. Available: https://ui.adsabs.harvard.edu/abs/1970PhRvD...1.2726H

[75] B. J. Carr, "The primordial black hole mass spectrum," , vol. 201, pp. 1–19, Oct. 1975. [Online]. Available: http://adsabs.harvard.edu/abs/1975ApJ...201....1C

[76] B. J. Carr and T. Harada, "Separate universe problem: 40 years on," , vol. 91, no. 8, p. 084048, Apr. 2015. [Online]. Available: http://adsabs.harvard.edu/abs/2015PhRvD..91h4048C

[77] I. D. Novikov, A. G. Polnarev, A. A. Starobinskii, and I. B. Zeldovich, "Primordial black holes," , vol. 80, pp. 104–109, Nov. 1979. [Online]. Available: http://adsabs.harvard.edu/abs/1979A%26A....80..104N

[78] A. G. Polnarev and I. Musco, "Curvature profiles as initial conditions for primordial black hole formation," Classical and Quantum Gravity, vol. 24, no. 6, pp. 1405–1431, mar 2007. [Online]. Available: https://doi.org/10.1088%2F0264-9381%2F24%2F6%2F003

[79] M. Kopp, S. Hofmann, and J. Weller, "Separate universes do not constrain primordial black hole formation," , vol. 83, no. 12, p. 124025, Jun. 2011. [Online]. Available: http://adsabs.harvard.edu/abs/2011PhRvD..83l4025K

[80] T. Harada and B. J. Carr, "Upper limits on the size of a primordial black hole," , vol. 71, no. 10, p. 104009, May 2005. [Online]. Available: http://adsabs.harvard.edu/abs/2005PhRvD..71j4009H

[81] T. Harada, C.-M. Yoo, and K. Kohri, "Threshold of primordial black hole formation," , vol. 88, p. 084051, Oct. 2013. [Online]. Available: https://ui.adsabs.harvard.edu/#abs/2013PhRvD..88h4051H

[82] B. Carr, T. Tenkanen, and V. Vaskonen, "Primordial black holes from inflaton and spectator field perturbations in a matter-dominated era," , vol. 96, p. 063507, Sep. 2017. [Online]. Available: https://ui.adsabs.harvard.edu/#abs/2017PhRvD..96f3507C

[83] M. Sasaki, T. Suyama, T. Tanaka, and S. Yokoyama, "Primordial black holes-perspectives in gravitational wave astronomy," Classical and Quantum Gravity, vol. 35, no. 6, p. 063001, Mar. 2018. [Online]. Available: http://adsabs.harvard.edu/abs/2018CQGra..35f3001S

[84] T. Harada, C.-M. Yoo, T. Nakama, and Y. Koga, "Cosmological long-wavelength solutions and primordial black hole formation," , vol. 91, p. 084057, Apr. 2015. [Online]. Available: https://ui.adsabs.harvard.edu/#abs/2015PhRvD..91h4057H

[85] M. W. Choptuik, "Universality and scaling in gravitational collapse of a massless scalar field," Phys. Rev. Lett., vol. 70, pp. 9–12, Jan 1993. [Online]. Available: https://link.aps.org/doi/10.1103/PhysRevLett.70.9

[86] J. C. Niemeyer and K. Jedamzik, "Near-critical gravitational collapse and the initial mass function of primordial black holes," Phys. Rev. Lett., vol. 80, pp. 5481–5484, Jun 1998. [Online]. Available: https://link.aps.org/doi/10.1103/PhysRevLett.80.5481

[87] ——, "Dynamics of primordial black hole formation," Phys. Rev. D, vol. 59, p. 124013, May 1999. [Online]. Available: https://link.aps.org/doi/10.1103/PhysRevD.59.124013

[88] C. Gundlach, "Critical phenomena in gravitational collapse," Living Reviews in Relativity, vol. 2, no. 1, p. 4, Dec 1999. [Online]. Available: https://doi.org/10.12942/lrr-1999-4

[89] I. Musco, J. C. Miller, and L. Rezzolla, "Computations of primordial black-hole formation," Classical and Quantum Gravity, vol. 22, pp. 1405–1424, Apr 2005. [Online]. Available: https://ui.adsabs.harvard.edu/#abs/2005CQGra..22.1405M

[90] I. Musco and J. C. Miller, "Primordial black hole formation in the early universe: critical behaviour and self-similarity," Classical and Quantum Gravity, vol. 30, p. 145009, Jul 2013. [Online]. Available: https://ui.adsabs.harvard.edu/#abs/2013CQGra..30n5009M

[91] L. Landau and Lifshitz, The Classical Theory of Fields, ser. Course of theoretical physics. Butterworth-Heinemann, 1975. [Online]. Available: https://books.google.fi/books?id=X18PF4oKyrUC

[92] C. W. Misner and D. H. Sharp, "Relativistic Equations for Adiabatic, Spherically Symmetric Gravitational Collapse," Physical Review, vol. 136, pp. 571–576, Oct. 1964. [Online]. Available: http://adsabs.harvard.edu/abs/1964PhRv..136..571M

[93] W. C. Hernandez, Jr. and C. W. Misner, "Observer Time as a Coordinate in Relativistic Spherical Hydrodynamics," , vol. 143, p. 452, Feb. 1966. [Online]. Available: http://adsabs.harvard.edu/abs/1966ApJ...143..452H

[94] A. B. Nielsen and D.-H. Yeom, "Spherically Symmetric Trapping Horizons, the Misner-Sharp Mass and Black Hole Evaporation," International Journal of Modern Physics A, vol. 24, pp. 5261–5285, Jan. 2009. [Online]. Available: https://ui.adsabs.harvard.edu/#abs/2009IJMPA..24.5261N

[95] G. V. Bicknell and R. N. Henriksen, "Formation of primordial black holes," , vol. 232, pp. 670–682, Sep. 1979. [Online]. Available: http://adsabs.harvard.edu/abs/1979ApJ...232..670B

[96] D. K. Nadezhin, I. D. Novikov, and A. G. Polnarev, "The hydrodynamics of primordial black hole formation," , vol. 22, pp. 129–138, Apr. 1978. [Online]. Available: http://adsabs.harvard.edu/abs/1978SvA....22..129N

[97] M. Shibata and M. Sasaki, "Black hole formation in the Friedmann universe: Formulation and computation in numerical relativity," , vol. 60, p. 084002, Oct. 1999. [Online]. Available: https://ui.adsabs.harvard.edu/#abs/1999PhRvD..60h4002S

[98] D. W. Neilsen and M. W. Choptuik, "Ultrarelativistic fluid dynamics," Classical and Quantum Gravity, vol. 17, pp. 733–759, Feb. 2000. [Online]. Available: https://ui.adsabs.harvard.edu/#abs/2000CQGra..17..733N

[99] I. Musco, J. C. Miller, and A. G. Polnarev, "Primordial black hole formation in the radiative era: investigation of the critical nature of the collapse," Classical and Quantum Gravity, vol. 26, p. 235001, Dec. 2009. [Online].

Available: https://ui.adsabs.harvard.edu/#abs/2009CQGra..26w5001M

[100] I. Musco, "The threshold for primordial black holes: dependence on the shape of the cosmological perturbations," arXiv e-prints, p. arXiv:1809.02127, Sep. 2018. [Online]. Available: https://ui.adsabs.harvard.edu/#abs/2018arXiv180902127M

[101] C.-M. Yoo, T. Harada, J. Garriga, and K. Kohri, "PBH abundance from random Gaussian curvature perturbations and a local density threshold," arXiv e-prints, p. arXiv:1805.03946, May 2018. [Online]. Available: https://ui.adsabs.harvard.edu/#abs/2018arXiv180503946Y

[102] T. Nakama, T. Harada, A. G. Polnarev, and J. Yokoyama, "Identifying the most crucial parameters of the initial curvature profile for primordial black hole formation," Journal of Cosmology and Astro-Particle Physics, vol. 2014, p. 037, Jan 2014. [Online]. Available: https://ui.adsabs.harvard.edu/#abs/2014JCAP...01..037N

[103] K. Jedamzik, "Primordial black hole formation during the QCD epoch," , vol. 55, pp. R5871–R5875, May 1997. [Online]. Available: https://ui.adsabs.harvard.edu/#abs/1997PhRvD..55.5871J

[104] C. Y. Cardall and G. M. Fuller, "Semianalytic Analysis of Primordial Black Hole Formation During a First-order QCD Phase Transition," arXiv e-prints, pp. astro–ph/9 801 103, Jan 1998. [Online]. Available: https://ui.adsabs.harvard.edu/abs/1998astro.ph..1103C

[105] J. Sobrinho, "Phd thesis: The possibility of primordial black hole direct detection," 2011. [Online]. Available: http://hdl.handle.net/10400.13/235

[106] J. L. G. Sobrinho, P. Augusto, and A. L. Gonçalves, "New thresholds for primordial black hole formation during the QCD phase transition," , vol. 463, pp. 2348–2357, Dec 2016. [Online]. Available: https://ui.adsabs.harvard.edu/#abs/2016MNRAS.463.2348S

[107] C. T. Byrnes, M. Hindmarsh, S. Young, and M. R. S. Hawkins, "Primordial black holes with an accurate QCD equation of state," Journal of Cosmology and Astro-Particle Physics, vol. 2018, p. 041, Aug 2018. [Online]. Available: https://ui.adsabs.harvard.edu/#abs/2018JCAP...08..041B

[108] M. Nagasawa and J. Yokoyama, "On the Jeans Instability during the QCD Phase Transition," Progress of Theoretical Physics, vol. 97, pp. 173–178, Jan 1997. [Online]. Available: https://ui.adsabs.harvard.edu/#abs/1997PThPh..97..173N

[109] C. Schmid, D. J. Schwarz, and P. Widerin, "Deviations from the Harrison-Zel'dovich spectrum due to the quark-gluon to hadron transition." Helvetica Physica Acta, vol. 69, pp. 198–201, Jan 1996. [Online]. Available: https://ui.adsabs.harvard.edu/#abs/1996AcHPh..69..198S

[110] D. N. Crawford, Matt; Schramm, "Spontaneous generation of density perturbations in the early universe," Nature, vol. 298, pp. 538–540, 1982. [Online]. Available: http://gen.lib.rus.ec/scimag/10.1038%2F298538a0

[111] N. Venkatesan, "Master thesis: Semiclassical plasma dynamics in electroweak baryogenesis," 2018. [Online]. Available: http://urn.fi/URN:NBN:fi:jyu-201811154724

[112] J.-P. Blaizot and J.-Y. Ollitrault, "Equation of state and hydrodynamics of quark-gluon plasmas," Physics Letters B, vol. 191, no. 1, pp. 21 – 26, 1987. [Online]. Available: http://www.sciencedirect.com/science/article/pii/0370269387913141

[113] S. Borsanyi, Z. Fodor, K. H. Kampert, S. D. Katz, T. Kawanai, T. G. Kovacs, S. W. Mages, A. Pasztor, F. Pittler, J. Redondo, A. Ringwald, and K. K. Szabo, "Lattice QCD for Cosmology," arXiv e-prints, p. arXiv:1606.07494, Jun 2016. [Online]. Available: https://ui.adsabs.harvard.edu/#abs/2016arXiv160607494B

[114] R. K. Sheth, H. J. Mo, and G. Tormen, "Ellipsoidal collapse and an improved model for the number and spatial distribution of dark matter haloes," , vol. 323, pp. 1–12, May 2001. [Online]. Available: https://ui.adsabs.harvard.edu/#abs/2001MNRAS.323....1S

[115] F. Kühnel and M. Sandstad, "Ellipsoidal collapse and primordial black hole formation," , vol. 94, p. 063514, Sep 2016. [Online]. Available: https://ui.adsabs.harvard.edu/#abs/2016PhRvD..94f3514K

[116] J. R. Bond and S. T. Myers, "The Peak-Patch Picture of Cosmic Catalogs. I. Algorithms," , vol. 103, p. 1, Mar. 1996. [Online]. Available: http://adsabs.harvard.edu/abs/1996ApJS..103....1B

[117] M. Y. Khlopov, "Primordial black holes," Research in Astronomy and Astrophysics, vol. 10, pp. 495–528, Jun. 2010. [Online]. Available: https://ui.adsabs.harvard.edu/abs/2010RAA....10..495K

[118] C. T. Byrnes, E. J. Copeland, and A. M. Green, "Primordial black holes as a tool for constraining non-Gaussianity," , vol. 86, no. 4, p. 043512, Aug 2012. [Online]. Available: https://ui.adsabs.harvard.edu/abs/2012PhRvD..86d3512B

[119] A. M. Green, A. R. Liddle, K. A. Malik, and M. Sasaki, "New calculation of the mass fraction of primordial black holes," , vol. 70, p. 041502, Aug 2004. [Online]. Available: https://ui.adsabs.harvard.edu/#abs/2004PhRvD..70d1502G

[120] B. J. Carr, K. Kohri, Y. Sendouda, and J. Yokoyama, "New cosmological constraints on primordial black holes," Phys. Rev. D, vol. 81, p. 104019, May 2010. [Online]. Available: https://link.aps.org/doi/10.1103/PhysRevD.81.104019

[121] B. Carr, M. Raidal, T. Tenkanen, V. Vaskonen, and H. Veermäe, "Primordial black hole constraints for extended mass functions," , vol. 96, no. 2, p. 023514, Jul 2017. [Online]. Available: https://ui.adsabs.harvard.edu/abs/2017PhRvD..96b3514C

[122] W. H. Press and P. Schechter, "Formation of Galaxies and Clusters of Galaxies by Self-Similar Gravitational Condensation," , vol. 187, pp. 425–438, Feb. 1974. [Online]. Available: http://adsabs.harvard.edu/abs/1974ApJ...187..425P

[123] J. M. Bardeen, J. R. Bond, N. Kaiser, and A. S. Szalay, "The Statistics of Peaks of Gaussian Random Fields," , vol. 304, p. 15, May 1986. [Online]. Available: https://ui.adsabs.harvard.edu/abs/1986ApJ...304...15B

[124] A. M. Green and A. R. Liddle, "Critical collapse and the primordial black hole initial mass function," , vol. 60, no. 6, p. 063509, Sep 1999. [Online]. Available: https://ui.adsabs.harvard.edu/abs/1999PhRvD..60f3509G

[125] S. Young, C. T. Byrnes, and M. Sasaki, "Calculating the mass fraction of primordial black holes," Journal of Cosmology and Astroparticle Physics, vol. 2014, no. 07, pp. 045–045, jul 2014. [Online]. Available: https://doi.org/10.1088%2F1475-7516%2F2014%2F07%2F045

[126] K. Jedamzik, "The Cloud-in-Cloud Problem in the Press-Schechter Formalism of Hierarchical Structure Formation," , vol. 448, p. 1, Jul 1995. [Online]. Available: https://ui.adsabs.harvard.edu/#abs/1995ApJ...448....1J

[127] J. R. Bond, S. Cole, G. Efstathiou, and N. Kaiser, "Excursion set mass functions for hierarchical Gaussian fluctuations," , vol. 379, pp. 440–460, Oct. 1991. [Online]. Available: http://adsabs.harvard.edu/abs/1991ApJ...379..440B

[128] V. De Luca, G. Franciolini, A. Kehagias, M. Peloso, A. Riotto, and C. Ünal, "The Ineludible non-Gaussianity of the Primordial Black Hole Abundance," arXiv e-prints, p. arXiv:1904.00970, Apr 2019. [Online]. Available: https://ui.adsabs.harvard.edu/#abs/2019arXiv190400970D

[129] S. Clesse and J. García-Bellido, "Massive primordial black holes from hybrid inflation as dark matter and the seeds of galaxies," , vol. 92, p. 023524, Jul 2015. [Online]. Available: https://ui.adsabs.harvard.edu/abs/2015PhRvD..92b3524C

[130] B. Carr, F. Kühnel, and M. Sandstad, "Primordial black holes as dark matter," , vol. 94, p. 083504, Oct 2016. [Online]. Available: https://ui.adsabs.harvard.edu/#abs/2016PhRvD..94h3504C

[131] E. Kolb and M. Turner, The Early Universe, ser. Frontiers in physics. Avalon Publishing, 1994. [Online]. Available: https://books.google.fi/books?id=Qwijr-HsvMMC

[132] M. Drees and E. Erfani, "Running-mass inflation model and primordial black holes," Journal of Cosmology and Astro-Particle Physics, vol. 2011, p. 005, Apr 2011. [Online]. Available: https://ui.adsabs.harvard.edu/abs/2011JCAP...04..005D

[133] J. García-Bellido, M. Peloso, and C. Unal, "Gravitational waves at interferometer scales and primordial black holes in axion inflation," Journal of Cosmology and Astro-Particle Physics, vol. 2016, p. 031, Dec 2016. [Online]. Available: https://ui.adsabs.harvard.edu/abs/2016JCAP...12..031G

[134] T. Bringmann, P. Scott, and Y. Akrami, "Improved constraints on the primordial power spectrum at small scales from ultracompact minihalos," , vol. 85, p. 125027, Jun 2012. [Online]. Available: https://ui.adsabs.harvard.edu/abs/2012PhRvD..85l5027B

[135] V. Faraoni, Cosmological and Black Hole Apparent Horizons, ser. Lecture Notes in Physics. Springer International Publishing, 2015. [Online]. Available: https://books.google.nl/books?id=iK8YCgAAQBAJ

[136] P. Ivanov, P. Naselsky, and I. Novikov, "Inflation and primordial black holes as dark matter," Phys. Rev. D, vol. 50, pp. 7173–7178, Dec 1994. [Online]. Available: https://link.aps.org/doi/10.1103/PhysRevD.50.7173

[137] G. Ballesteros and M. Taoso, "Primordial black hole dark matter from single field inflation," , vol. 97, p. 023501, Jan 2018. [Online]. Available: https://ui.adsabs.harvard.edu/abs/2018PhRvD..97b3501B

[138] J. García-Bellido and E. Ruiz Morales, "Primordial black holes from single field models of inflation," Physics of the Dark Universe, vol. 18, pp. 47–54, Dec 2017. [Online]. Available: https://ui.adsabs.harvard.edu/abs/2017PDU....18...47G

[139] C. Germani and T. Prokopec, "On primordial black holes from an inflection point," Physics of the Dark Universe, vol. 18, pp. 6–10, Dec 2017. [Online]. Available: https://ui.adsabs.harvard.edu/abs/2017PDU....18....6G

[140] J. García-Bellido, A. Linde, and D. Wands, "Density perturbations and black hole formation in hybrid inflation," , vol. 54, pp. 6040–6058, Nov 1996. [Online]. Available: https://ui.adsabs.harvard.edu/#abs/1996PhRvD..54.6040G

[141] Y.-F. Cai, X. Tong, D.-G. Wang, and S.-F. Yan, "Primordial black holes from sound speed resonance during inflation," Phys. Rev. Lett., vol. 121, p. 081306, Aug 2018. [Online]. Available: https://link.aps.org/doi/10.1103/PhysRevLett.121.081306

[142] A. Taruya, "Parametric amplification of density perturbations in the oscillating inflation model," Phys. Rev. D, vol. 59, p. 103505, Apr 1999. [Online]. Available: https://link.aps.org/doi/10.1103/PhysRevD.59.103505

[143] D. N. Page, "Particle emission rates from a black hole: Massless particles from an uncharged, nonrotating hole," Phys. Rev. D, vol. 13, pp. 198–206, Jan 1976. [Online]. Available: https://link.aps.org/doi/10.1103/PhysRevD.13.198

[144] J. H. MacGibbon and B. R. Webber, "Quark- and gluon-jet emission from primordial black holes: The instantaneous spectra," Phys. Rev. D, vol. 41, pp. 3052–3079, May 1990. [Online]. Available: https://link.aps.org/doi/10.1103/PhysRevD.41.3052

[145] J. H. MacGibbon, "Quark- and gluon-jet emission from primordial black holes. II. The emission over the black-hole lifetime," , vol. 44, no. 2, pp. 376–392, Jul 1991. [Online]. Available: https://ui.adsabs.harvard.edu/abs/1991PhRvD..44..376M

[146] X. Calmet, B. Carr, and E. Winstanley, Quantum Black Holes, ser. SpringerBriefs in Physics. Springer Berlin Heidelberg, 2013. [Online]. Available: https://books.google.fi/books?id=LhiCnAEACAAJ

[147] K. Kohri and J. Yokoyama, "Primordial black holes and primordial nucleosynthesis: Effects of hadron injection from low mass holes," Phys. Rev. D, vol. 61, p. 023501, Dec 1999. [Online]. Available: https://link.aps.org/doi/10.1103/PhysRevD.61.023501

[148] I. B. Zeldovich, A. A. Starobinskii, M. I. Khlopov, and V. M. Chechetkin, "Primordial black holes and the deuterium problem," Soviet Astronomy Letters, vol. 3, pp. 110–112, Jun. 1977. [Online]. Available: http://adsabs.harvard.edu/abs/1977SvAL....3..110Z

[149] K. J. Mack and D. H. Wesley, "Primordial black holes in the Dark Ages: Observational prospects for future 21cm surveys," arXiv e-prints, p. arXiv:0805.1531, May 2008. [Online]. Available: https://ui.adsabs.harvard.edu/abs/2008arXiv0805.1531M

[150] J. D. Bowman, A. E. E. Rogers, R. A. Monsalve, T. J. Mozdzen, and N. Mahesh, "An absorption profile centred at 78 megahertz in the sky-averaged spectrum," , vol. 555, no. 7694, pp. 67–70, Mar 2018. [Online]. Available: https://ui.adsabs.harvard.edu/abs/2018Natur.555...67B

[151] A. Barnacka, J. F. Glicenstein, and R. Moderski, "New constraints on primordial black holes abundance from femtolensing of gamma-ray bursts," , vol. 86, no. 4, p. 043001, Aug 2012. [Online]. Available: https://ui.adsabs.harvard.edu/abs/2012PhRvD..86d3001B

[152] P. W. Graham, S. Rajendran, and J. Varela, "Dark matter triggers of supernovae," , vol. 92, no. 6, p. 063007, Sep 2015. [Online]. Available: https://ui.adsabs.harvard.edu/abs/2015PhRvD..92f3007G

[153] F. Capela, M. Pshirkov, and P. Tinyakov, "Constraints on primordial black holes as dark matter candidates from capture by neutron stars," , vol. 87, no. 12, p. 123524, Jun 2013. [Online]. Available: https://ui.adsabs.harvard.edu/abs/2013PhRvD..87l3524C

[154] ——, "Constraints on primordial black holes as dark matter candidates from capture by neutron stars," , vol. 87, no. 12, p. 123524, Jun 2013. [Online]. Available: https://ui.adsabs.harvard.edu/abs/2013PhRvD..87l3524C

[155] K. Griest, A. M. Cieplak, and M. J. Lehner, "Experimental Limits on Primordial Black Hole Dark Matter from the First 2 yr of Kepler Data," , vol. 786, no. 2, p. 158, May 2014. [Online]. Available: https://ui.adsabs.harvard.edu/abs/2014ApJ...786..158G

[156] H. Niikura, M. Takada, N. Yasuda, R. H. Lupton, T. Sumi, S. More, T. Kurita, S. Sugiyama, A. More, M. Oguri, and M. Chiba, "Microlensing constraints on primordial black holes with the Subaru/HSC Andromeda observation," arXiv e-prints, p. arXiv:1701.02151, Jan 2017. [Online]. Available: https://ui.adsabs.harvard.edu/abs/2017arXiv170102151N

[157] P. Tisserand, L. Le Guillou, C. Afonso, J. N. Albert, J. Andersen, R. Ansari, É. Aubourg, P. Bareyre, J. P. Beaulieu, X. Charlot, C. Coutures, R. Ferlet, P. Fouqué, J. F. Glicenstein, B. Goldman, A. Gould, D. Graff, M. Gros, J. Haissinski, C. Hamadache, J. de Kat, T. Lasserre, É. Lesquoy, C. Loup, C. Magneville, J. B. Marquette, É. Maurice, A. Maury, A. Milsztajn, M. Moniez, N. Palanque-Delabrouille, O. Perdereau, Y. R. Rahal, J. Rich, M. Spiro, A. Vidal-Madjar, L. Vigroux, S. Zylberajch, and EROS-2 Collaboration, "Limits on the Macho content of the Galactic Halo from the EROS-2 Survey of the Magellanic Clouds," , vol. 469, no. 2, pp. 387–404, Jul 2007. [Online]. Available: https://ui.adsabs.harvard.edu/abs/2007A&A...469..387T

[158] C. Alcock, R. A. Allsman, D. R. Alves, T. S. Axelrod, A. C. Becker, D. P. Bennett, K. H. Cook, N. Dalal, A. J. Drake, K. C. Freeman, M. Geha, K. Griest, M. J. Lehner, S. L. Marshall, D. Minniti, C. A. Nelson, B. A. Peterson, P. Popowski, M. R. Pratt, P. J. Quinn, C. W. Stubbs, W. Sutherland, A. B. Tomaney, T. Vandehei, and D. L. Welch, "MACHO Project Limits on Black Hole Dark Matter in the 1-30 M_{solar} Range," , vol. 550, no. 2, pp. L169–L172, Apr 2001. [Online]. Available: https://ui.adsabs.harvard.edu/abs/2001ApJ...550L.169A

[159] H. Niikura, M. Takada, S. Yokoyama, T. Sumi, and S. Masaki, "Constraints on Earth-mass primordial black holes from OGLE 5-year microlensing events," , vol. 99, no. 8, p. 083503, Apr 2019.

[Online]. Available: https://ui.adsabs.harvard.edu/abs/2019PhRvD..99h3503N

[160] M. Zumalacárregui and U. Seljak, "Limits on Stellar-Mass Compact Objects as Dark Matter from Gravitational Lensing of Type Ia Supernovae," , vol. 121, no. 14, p. 141101, Oct 2018. [Online]. Available: https://ui.adsabs.harvard.edu/abs/2018PhRvL.121n1101Z

[161] M. Oguri, J. M. Diego, N. Kaiser, P. L. Kelly, and T. Broadhurst, "Understanding caustic crossings in giant arcs: Characteristic scales, event rates, and constraints on compact dark matter," , vol. 97, no. 2, p. 023518, Jan 2018. [Online]. Available: https://ui.adsabs.harvard.edu/abs/2018PhRvD..97b3518O

[162] M. Ricotti, J. P. Ostriker, and K. J. Mack, "Effect of Primordial Black Holes on the Cosmic Microwave Background and Cosmological Parameter Estimates," , vol. 680, no. 2, pp. 829–845, Jun 2008. [Online]. Available: https://ui.adsabs.harvard.edu/abs/2008ApJ...680..829R

[163] V. Poulin, P. D. Serpico, F. Calore, S. Clesse, and K. Kohri, "CMB bounds on disk-accreting massive primordial black holes," , vol. 96, no. 8, p. 083524, Oct 2017. [Online]. Available: https://ui.adsabs.harvard.edu/abs/2017PhRvD..96h3524P

[164] B. J. Carr and M. Sakellariadou, "Dynamical Constraints on Dark Matter in Compact Objects," , vol. 516, pp. 195–220, May 1999. [Online]. Available: http://adsabs.harvard.edu/abs/1999ApJ...516..195C

[165] T. D. Brandt, "Constraints on MACHO Dark Matter from Compact Stellar Systems in Ultra-faint Dwarf Galaxies," , vol. 824, no. 2, p. L31, Jun 2016. [Online]. Available: https://ui.adsabs.harvard.edu/abs/2016ApJ...824L..31B

[166] S. M. Koushiappas and A. Loeb, "Dynamics of Dwarf Galaxies Disfavor Stellar-Mass Black Holes as Dark Matter," , vol. 119, no. 4, p. 041102, Jul 2017. [Online]. Available: https://ui.adsabs.harvard.edu/abs/2017PhRvL.119d1102K

[167] P. Meszaros, "Primeval black holes and galaxy formation," , vol. 38, pp. 5–13, Jan. 1975. [Online]. Available: http://adsabs.harvard.edu/abs/1975A%26A....38....5M

[168] N. Afshordi, P. McDonald, and D. N. Spergel, "Primordial Black Holes as Dark Matter: The Power Spectrum and Evaporation of Early Structures," , vol. 594, no. 2, pp. L71–L74, Sep 2003. [Online]. Available: https://ui.adsabs.harvard.edu/abs/2003ApJ...594L..71A

[169] R. Murgia, G. Scelfo, M. Viel, and A. Raccanelli, "Lyman-$$ forest constraints on Primordial Black Holes as Dark Matter," arXiv e-prints, p. arXiv:1903.10509, Mar 2019. [Online]. Available: https://ui.adsabs.harvard.edu/abs/2019arXiv190310509M

[170] D. P. Quinn, M. I. Wilkinson, M. J. Irwin, J. Marshall, A. Koch, and V. Belokurov, "On the reported death of the MACHO era," , vol. 396, no. 1, pp. L11–L15, Jun 2009. [Online]. Available: https://ui.adsabs.harvard.edu/abs/2009MNRAS.396L..11Q

[171] P. N. Wilkinson, D. R. Henstock, I. W. Browne, A. G. Polatidis, P. Augusto, A. C. Readhead, T. J. Pearson, W. Xu, G. B. Taylor, and R. C. Vermeulen, "Limits on the Cosmological Abundance of Supermassive Compact Objects from a Search for Multiple Imaging in Compact Radio Sources," , vol. 86, no. 4, pp. 584–587, Jan 2001. [Online]. Available: https://ui.adsabs.harvard.edu/abs/2001PhRvL..86..584W

[172] K. Belczynski, D. E. Holz, T. Bulik, and R. O'Shaughnessy, "The first gravitational-wave source from the isolated evolution of two stars in the 40-100 solar mass range," , vol. 534, pp. 512–515, Jun. 2016. [Online]. Available: http://adsabs.harvard.edu/abs/2016Natur.534..512B

[173] J. H. MacGibbon, "Can planck-mass relics of evaporating black holes close the universe?" Nature, vol. 329, no. 6137, pp. 308–309, sep 1987. [Online]. Available: https://doi.org/10.1038%2F329308a0

[174] Y. Akrami, F. Kuhnel, and M. Sandstad, "Uncertainties in primordial black-hole

constraints on the primordial power spectrum," Physics of the Dark Universe, vol. 19, pp. 124–128, Mar 2018. [Online]. Available: https://ui.adsabs.harvard.edu/abs/2018PDU....19..124A

[175] J. R. Chisholm, "Clustering of primordial black holes: Basic results," , vol. 73, no. 8, p. 083504, Apr 2006. [Online]. Available: https://ui.adsabs.harvard.edu/abs/2006PhRvD..73h3504C

[176] Y. Tada and S. Yokoyama, "Primordial black holes as biased tracers," , vol. 91, no. 12, p. 123534, Jun 2015. [Online]. Available: https://ui.adsabs.harvard.edu/abs/2015PhRvD..91l3534T

[177] T. Bringmann, P. F. Depta, V. Domcke, and K. Schmidt-Hoberg, "Towards closing the window of primordial black holes as dark matter: The case of large clustering," , vol. 99, no. 6, p. 063532, Mar 2019. [Online]. Available: https://ui.adsabs.harvard.edu/abs/2019PhRvD..99f3532B

[178] V. Desjacques and A. Riotto, "Spatial clustering of primordial black holes," , vol. 98, no. 12, p. 123533, Dec 2018. [Online]. Available: https://ui.adsabs.harvard.edu/abs/2018PhRvD..98l3533D

[179] E. Poisson, A Relativist's Toolkit: The Mathematics of Black-Hole Mechanics. Cambridge University Press, 2004. [Online]. Available: https://books.google.nl/books?id=bk2XEgz_ML4C

[180] G. F. R. E. Stephen W. Hawking, The large scale structure of space-time, ser. Cambridge Monographs on Mathematical Physics. Cambridge University Press, 1975. [Online]. Available: http://gen.lib.rus.ec/book/index.php?md5=3A956100B468FAC6C702F9D937242221

[181] T. Jacobson, "Introductory lectures in black hole thermodynamics." [Online]. Available: http://www2.montgomerycollege.edu/departments/planet/planet/Numerical_Relativity/SR_&_GR_QGR/GR_&_QM/ThermoBH.pdf

[182] N. D. Birrell and P. C. W. Davies, Quantum Fields in Curved Space, ser. Cambridge Monographs on Mathematical Physics. Cambridge, UK: Cambridge Univ. Press, 1984. [Online]. Available: http://www.cambridge.org/mw/academic/subjects/physics/theoretical-physics-and-mathematical-physics/quantum-fields-curved-space?format=PB

[183] R. M. Wald, Quantum field theory in curved spacetime and black hole thermodynamics, 1st ed., ser. Chicago lectures in physics. University of Chicago Press, 1994. [Online]. Available: http://gen.lib.rus.ec/book/index.php?md5=014EB721B7F5569B5F9E4E1E7E2DA4FE

[184] L. Parker and D. Toms, Quantum Field Theory in Curved Spacetime: Quantized Fields and Gravity, ser. Cambridge Monographs on Mathematical Physics. Cambridge University Press, 2009. [Online]. Available: https://books.google.fi/books?id=5nNuGMBBTjMC

[185] S. W. Hawking, "Black hole explosions?" , vol. 248, no. 5443, pp. 30–31, Mar 1974. [Online]. Available: https://ui.adsabs.harvard.edu/abs/1974Natur.248...30H

[186] T. Harada and B. J. Carr, "Super-horizon primordial black holes," , vol. 72, no. 4, p. 044021, Aug 2005. [Online]. Available: https://ui.adsabs.harvard.edu/abs/2005PhRvD..72d4021H

[187] S. A. Hayward, "Gravitational energy in spherical symmetry," , vol. 53, pp. 1938–1949, Feb. 1996. [Online]. Available: http://adsabs.harvard.edu/abs/1996PhRvD..53.1938H